THE HONG KONG POLYTECHNIC UNIVERSITY

Department of Civil and Structural Engineering

Oxidant-assisted Photocatalytic Reaction of o-ClA in TiO_2

By Wing-Ki, Choy

A thesis submitted in partial fulfillment of the requirements for the
Degree of Doctor of Philosophy

August 2006

DECLARATION

I hereby declare that this thesis entitled "Oxidant-assisted photocatalytic reaction of o-ClA in TiO_2" has not been, either in whole or in part, previously submitted to any other institution for a degree or other qualification, and contains no material previously published or written by another person, except where due reference is made in the text.

Wing-ki, CHOY

ACKNOWLEDGMENTS

The completion of this dissertation would not have been possible without the input and support of numerous parties. I would like to express my gratitude to my supervisor, Dr. W. Chu, for his support in my research. I also wish to extend my thanks to our laboratory technician, Mr. W.C. Lam, for his inevitable technical support. Suggestions and encouragements from my colleagues, Dr. Ada Chan, Ms. Catherine Lau and Dr. Joanna Kwan are gratefully acknowledged.

At the same time, I wish to express my appreciation to my parents and my dearest husband for their concerns and moral support, especially for their understanding throughout the period.

Finally, I would be thankful for the financial support from the Hong Kong Polytechnic University (RGE1).

ABSTRACT

The removal of organic matter through the illumination of UV light has proven to be effective in the fields of air and wastewater treatment. However, direct photolysis only causes little or slow decay with insignificant number of radicals while a higher reaction rate is always observed with photon-assisted catalysts. The application of heterogeneous photocatalysts has received great consent because of its effectiveness and the wide adaptability in organic destruction. Titanium dioxide, TiO_2 is considered one of the best catalysts for the photo-oxidation process. It could assist the degradation of organic without altering itself under the UV light illumination. Excited conduction-band electrons (e^-_{CB}) and valance-band holes (h^+_{VB}) induce large amount of hydroxyl radicals ($^\bullet OH$), or other radicals ($^\bullet O_2$).

However, fast recombination of conduction-band electrons and valence-band holes would limit the degradation rates. To tackle with the problem, the use of inorganic oxidants has been proposed to prevent the occurrence of recombination. The photocatalytic degradation of an anthropogenic organic, o-chloroaniline (o-ClA), has been extensively studied. Comparison indicated that oxhalogens (especially IO_3^-) were found to the most effective oxidant among various selections (i.e., H_2O_2, rose bengal and oxhalogens) in the UV/TiO_2 system. With the addition of oxygen sources provided by the oxidants, TiO_2 particles acted as an electron donor to form the superoxide radical ion ($O_2^{\bullet -}$) which could yield higher degradation rate. The use of oxidants in UV/TiO_2 has proven as a pH dependent process. The change of surface charges on the TiO_2 surface is one of the explanations.

In addition, the identification and quantification of photo-products (aromatic intermediates and ionic end-products) were conducted in UV/TiO_2 and UV/TiO_2/IO_3^- system. The degradation of o-ClA was mainly attributed to the $^{\bullet}OH$ attack. The existence of aromatic intermediates would not accumulate in the solution and degradation was observed. The generation of NH_4^+, Cl^- and NO_2^- has also been detected. With the inclusion of the photo-products, the degradation pathway of o-ClA has been proposed accordingly.

The photocatalytic process was brought into practice by immobilizing TiO_2 particles onto supported substrate via sol-gel process. Degradation of o-ClA by the TiO_2 film can be achieved but affected by the calcination temperature, layers of coating and the use of light intensities. Also, recycling performance of film was reported to have high percentage of repeatability after nine consecutive usages.

TABLE OF CONTENTS

CHAPTER 1: INTRODUCTION

CHAPTER 2: LITERAURE REVIEW

2.1 Basics of photochemical reaction

2.2 Application of titanium dioxide (TiO_2)

2.3 The photocatalytic mechanism of TiO_2

2.4 Immobilization of TiO_2 by sol-gel process

2.5 Description of o-chloroaniline (o-ClA)

CHAPTER 3: MATERIALS & METHODS

3.1 Materials

3.2 Experimental Set Up

3.3 Instrumental Analysis

3.4 Data Analysis

CHAPTER 4: RESULTS & DISCUSSIONS

4A The Photocatalytic Degradation of o-ClA in TiO_2 Suspension

4B Effect of Additional Oxidants in UV/TiO_2 System

4B.2 Effect of H_2O_2

4B.3 Effect of Rose Bengal (RB)

4B.4 Effect of oxyahlogens

4C The Study of Photoproducts

4C.1 UV/TiO_2

4C.2 UV/TiO_2/IO_3^-

4D The Study of Photocatalytic Degradation of o-ClA on Supported TiO_2

CHAPTER 5: CONCLUSION & RECOMMENDATIONS

LIST OF TABLES

LIST OF FIGURES

1 Introduction and Objectives

1.1 Photocatalysis of o-ClA: a study of oxidants and generation of photo-products

The removal of organic matter through a photolytic process has proven to be effective in the fields of air and wastewater treatment. Researchers have shown that the use of UV/TiO_2, UV/O_3, UV/H_2O_2 and UV/Fenton were efficient in the organic degradation than direct photolysis (Kwan and Chu, 2003, Neamtu et al., 2002, Sauleda and Brillas, 2001). A wide variety of organic pollutants including alkanes, alcohols, carboxylic acids, alkenes, phenols, dyes, PCBs and pesticides were treated by UV illumination (Cermola et al., 2004; Chen et al., 2001) and mineralization was reported in many cases (Ekaterina et al., 2001; Wen et al., 2002).

Titanium dioxide (TiO_2), being one of the popular photocatalysts, has extensively applied in the organic contamination treatments. Its benefits include low cost, chemically stable, and the generation of highly oxidizing electron holes (Fujishima et al., 2000), lead to the wide applications in degrading many organic contaminants (Carp et al., 2004). The photodecay of organic by TiO_2 is mainly achieved by the generation of hydroxyl radical ($^{\bullet}OH$) from the excited electro-hole pair. Ollis et al. (1984) suggested that the oxidation of organic compounds was initiated by $^{\bullet}OH$ in the aqueous solution, which are mainly induced by the electron-hole pairs at the photocatalyst surface. The adsorption property of TiO_2 could be another possible mechanism. The organic compound was firstly adsorbed on the photocatlyst surface and then reacted with excited superficial pairs or $^{\bullet}OH$ to form the final products.

However, the dosage of TiO_2 could not unlimitedly be increased to improve the efficiency of photodecay. Researchers have reported that beyond the optimal TiO_2 dosage, the photodecay rates would be retarded or slowdown due to the light scattering effect by the excess TiO_2 dispersion and the fast recombination process (Wang and Hong, 1999). As a result, the photooxidation of TiO_2 may not be efficient when the loading of contaminant is high.

The use of inorganic oxidants, for examples H_2O_2, ClO_3^-, BrO_3^- and $S_2O_8^{2-}$ in UV/TiO_2 system could increase the quantum efficiencies either by inhibiting electron-hole pair recombination through scavenging conduction-band electrons at the surface of TiO_2 or offering additional oxygen atom as an electron acceptor to form the superoxide radical ion ($^{\bullet}O_2^-$) or reactive radical intermediates (Watanabe et al., 2003; Wang and Hong, 1999). However, the influence of the additives must be accurately examined before application as some of them may affect the degradation adversely at specific conditions.

Beside the selection of catalysts and oxidants, most researches on photodegradation of organics generally emphasize on either the initial stage, by measuring the reacted substrate, or to the final stage of the overall reaction by measuring CO_2 formation. Although decay of target compound is possible to observe in most cases, the destination of compounds remains unanswered and it cannot be proposed as a trouble-free method without the knowledge of the photoproducts. The target compound is possibly transformed to other form of organics. Such transformation might result in the generation of more toxic to the parent compound after the treatment. To ensure the photodegradation is a clean process, the identification of degradation products could provide valuable evident. Organics are expected to breakdown into simpler structures, and subsequently, mineralization is the target of the process. The degradation pathway can be precisely proposed according to the information of photoproducts. However, the identification of photoproducts could be varied from researchers as the photoreaction is condition dependent. Sanchez et al. (2002) have conducted the degradation of p-chloroaniline by ionizing radiation and the formation of aminophenol, chlorophenol, anilne, phenol and formaldehyde were reported. Apart from those, the photodecay of p-chloroaniline by Mailhot et al. (2004) has generated chlorocataechol and chloronitrobenzene in the presence of Fe(III). Therefore, the examination of photoproducts in each process is necessary. Moreover, the novel process of combined photo-oxidation by UV/TiO_2/IO_3^- in our study is newly developed and the photoproducts of o-ClA have not been reported through this process.

1.2 Immobilization of TiO_2 on substrate

The immobilization of TiO_2 has supplement the deficiency of powdery TiO_2 suspended in the water where post-treatment is necessary. The use of sol-gel method has attracted high popularity because of its high homogeneity, easy composition control with high purity, low processing temperature, low equipment cost, and wide industrial applications (Singh, 2002; Young, 2002). However, this process is sensitive to several parameters. The ratio of sol mixture should be controlled as the rate of condensation and hydrolysis processes could affect the density or the quality of the film. Besides, the coating process should be handled with care as it could be easily affected by the atmospheric environment which could significantly deteriorate the performance of the film. Also, the annealing process for crystal growth is critical to the applied temperature.

1.3 Scope and Objectives

This study is basically constituted by four parts (A-D). The first part is mainly focus on the photo-kinetic study of an azo dye intermediate, o-chloroaniline (o-ClA), in TiO_2 suspensions; while second part is the effect on selected oxidants. The photoproducts and mechanistic pathway have been included in the third part and the final part is mainly about the immobilization of TiO_2 film at various conditions. The major objectives of this study were described as below.

Parameters affecting the kinetics of photodecay in TiO_2 have been studied in part A. Details include:

- to examine the dark adsorption of o-ClA onto TiO_2;
- to study the function of TiO_2 in different light intensities;
- to study the loading effect of TiO_2 to the o-ClA photodecay;
- to study the solution pH in the UV/TiO_2;

In part B, the function of three selected oxidants was studied in the UV/TiO_2 process.

- to observe the effect of additional oxidants (H_2O_2, rose bengal and oxyhalogens) in UV/TiO_2 system;
- to study the oxidant dosage effect;
- to examine the solution pH in selected oxidants; and
- to analyze the effect of second IO_3^- dosing.

The identification of photoproducts is the major component of part C.

- to quantify the organic intermediates and ionic end-products of o-ClA in UV/TiO_2 system.
- to identify the photoproducts in UV/TiO_2/IO_3^- process; and
- to propose degradation pathway of o-ClA in UV/TiO_2/IO_3^- process from the result of photoproducts.

In part D, the immobilization of TiO_2 onto substrate has been investigated. The major research areas are:

- to study the growth of TiO_2 at different annealing temperatures and its effect on photocatalytic activity;
- to enhance the photo-efficiency by increasing the coating cycles;
- to observe the light intensity effect to the film; and
- to extend the life of film by carrying out the reusability test of the TiO_2 film.

2 Literature Review

2.1 Basics of photochemical reaction

2.1.1 Law of photochemistry

All photochemical processes obey four photochemical laws which can be applied generally in photochemistry (Rabek, 1982):

1. A photochemical reaction may occur only if light of sufficient energy is absorbed by the system.
2. Each photon or quantum absorbed activates only one molecule in the primary excitation step of a photochemical sequence.
3. Each photon or quantum absorbed by a molecule has a certain probability of populating either the lowest excited singlet state (S_1) or the lowest triplet state (T_1).
4. The lowest excited signlet (S_1) and triplet (T_1) states are the starting levels (in solution) of most organic photochemical processes.

Photochemical processes usually occur in two stages which have been discussed in 2.1.2 and 2.1.3 respectively.

2.1.2 Absorption of photons

The primary photochemical reaction is the reaction which is directly due to the absorbed photon or quantum involving electronically excited states (Kalyanasundaram and Gratzel, 1993). This is process has been found to be independent of temperature.

$A + h\upsilon \rightarrow {}^{*}A$ (2-1)

Eqn. 2-1 has expressed the excitation process which is a high energy, unstable and must undergo some types of deactivation. The illustration in Figure 2-1 has described the excited state deactivation can occur through:

1. disappearance of the original molecule and formation of products (photochemical reaction);
2. emission of light (radioactive deactivation);
3. degradation of excess energy into heat (non-radiactive deactivation) and
4. some types of interaction with other species present in the solution (quenching process).

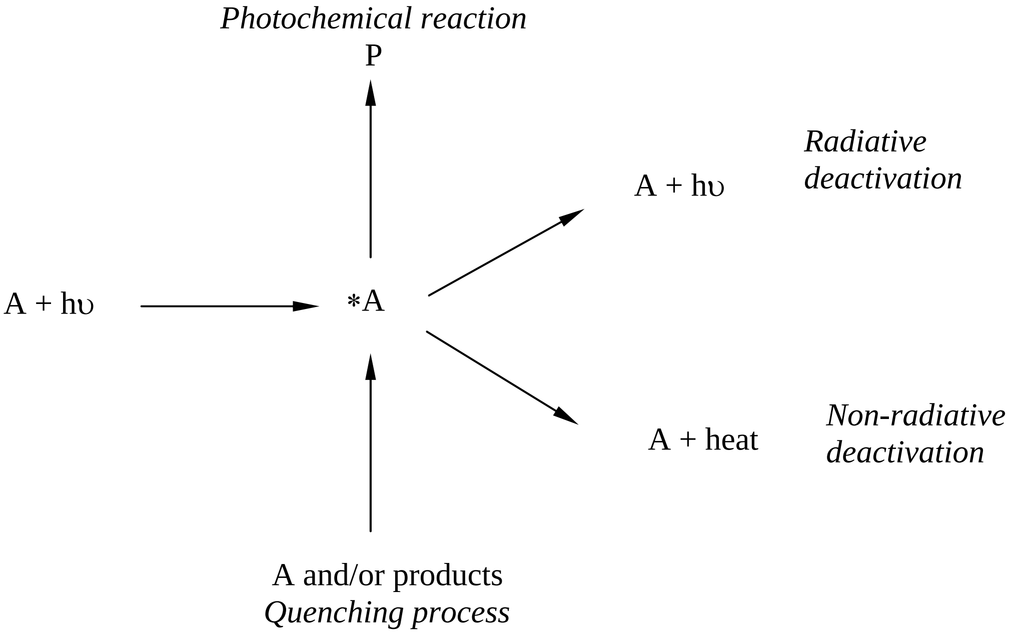

Figure 2-1: Unimolecular and bimolecular deactivation processes of an excited state (Kalyansundaram and Gratzel, 1993).

As indicated in Eqn. 2-2, an electronically excited state has a distinctive feature which is possible to transfer energy to another species:

$$^{*}A + B \rightarrow A + {}^{*}B \qquad (2\text{-}2)$$

The simultaneous deactivation of the originally excited molecule to its ground state and the promotion of the acceptor molecule to an electronically excited state are called electronic energy transfer.

2.1.3 The role of radical and scavenger

The secondary photochemical reactions (also called dark reactions) are reactions of radicals, radical ions, ions and electrons which were produced by the primary photochemical reaction. A free radical is defined as an atom, a group of atoms or a molecule containing at least one unpaired electron which occupies an outer orbital, e.g. the hydrogen radical ($^{\bullet}H$), hydroxyl radical ($^{\bullet}OH$), or methyl radical ($^{\bullet}CH_3$). Superoxide ($^{\bullet}O_2$) and perhydroxyl ($^{\bullet}OH_2$) radicals are other radicals formed from the reactions of electrons with adsorbed oxygen. The generated radicals can then oxidize organic pollutants at the solid-liquid interface. The formation of $^{\bullet}OH$ has been observed when TiO_2 is irradiated with ultraviolet light. It is believed that such radicals are the most powerful oxidizing species after fluorine which could oxidize most organic compounds at almost diffusion controlled rates. Dorfman and Adams (1973) have reported the second-order reaction rates are commonly on the order of 10^8 to 10^9 $M^{-1}s^{-1}$; the reaction rate of $^{\bullet}OH$ with the enzyme catalase is 2.6×10^{11} $M^{-1}s^{-1}$. In the UV/TiO_2 process, if organic compounds are rich in electrons, hydroxylation will proceed. Hydrogen abstraction usually occurs in reaction with unsaturated organic compounds. $^{\bullet}OH_2$ can be produced by the reaction between the organic radicals and the molecular oxygen.

Scavengers of radical are compounds that react with radicals as rapidly as or even more rapidly than other compounds, and which thus, when added to a model system or biological system in high enough concentrations, prevent other $^{\bullet}OH$ mediated reactions from occurring. To be suitable for this purpose, compounds must not be especially reactive with substances other than the $^{\bullet}OH$; furthermore, the products of their reaction with $^{\bullet}OH$ must not be particularly damaging in themselves.

2.1.4 Quantum yields

The efficiency of a photocatalytic reaction is usually expressed by quantum yield. It is a number of molecules converted relative to the total number of quanta absorbed by the photocatalyst surface. Or alternatively, Serpone (1997) has defined it is equal to the number of the molecules changed in a particular way to the number of the photons absorbed (Eqn. 2-3).

$$\phi = \frac{\text{rate of reaction}}{\text{rate of photons absortion}} \tag{2-3}$$

Since not all photons are absorbed productively, the typical quantum yield will be less than 1 or practically lies between 10^{-2} and 70%. It is possible to be greater than 1 for photo-induced or radiation-induced chain reactions, in which a single photon may trigger a long chain of transformations. Herrmann (1999) has listed out several parameters that could affect the value of quantum yield. They include the mass of photocatalyst, wavelength of the light, reactant concentration, operation temperature and the light intensity.

2.2 Application of titanium dioxide (TiO_2)

2.2.1 Background of TiO_2

Boreskov (1973) has formulated the definition of catalysis and catalyst: Catalysis is a change in the rate of chemical reactions in the presence of substances or catalysts which come into intermediate chemical interactions with the reactants, but restore their chemical composition after each cycle of the intermediate interactions. Reactions with the participation of the catalysts are called catalytic. TiO_2 belongs to one of the types. It classified as the transition metal oxides (Greenwood and Earnshaw, 1997) and has received a great deal of attention due to its chemical stability, non-toxicity, low cost and other advantageous properties. These benefits have made it becomes a popular additive in many industries. Its widespread application includes white pigment in paints, pharmaceuticals as UV absorber in sunscreen product, anti-reflection coating and biomaterial for bone reinforcing mechanical supports.

2.2.2 Synthetic process

Depending on the structure desires, TiO_2 could be synthesized by various methods of which sulfate method and vapor-phase oxidation of $TiCl_4$ are the two common preparation techniques for the anatase TiO_2. The preparation of TiO_2 has been studied to enhance its photocatalytic properties. Scalfani et al. (1990) has found that the fastest photocatalytic degradation rates exist for anatase samples that have been prepared by precipitation of titanium isoperoxide at 350°C. Anatase samples that have been heated to 700°C will transform to rutile TiO_2 (Bickley et al., 1991) which will be discussed in more detail in 2.4.

2.2.3 TiO_2 as a photocatalyst

TiO_2 was initially produced industrially in the late 1910 as a white pigment with a high opacifying property due to its high refractive index. Not until 1960s, TiO_2 was first classified as photocatalyst when Fujishima and Honda (1972) used a single crystal of TiO_2 as an anode and connected this to a platinum cathode in water in the presence of UV irradiation. Both current flow and hydrogen evolution from the anode were observed while the TiO_2 anode did not change during the reaction. Besides, Formenti et al (1971) studied the anatase TiO_2 supported on a porous cellulose acetate film for heterogeneous catalytic reaction in the presence of light. The partial oxidations of paraffins were facilitated oxygenated species on TiO_2. Since then, TiO_2 has been widely used as a photocatalyst in many industrials. Selected applications were outlined in Table 2-1.

Most of the applications are aimed to convert toxic and biologically persistent compounds into CO_2, H_2O, NO_3, or other oxides, halides, phosphates, etc. Extensive works with UV/TiO_2 have shown that many organic wastes can be completely mineralized with irradiated TiO_2 in both water and air contaminations. Pollutants commonly present in industrial wastewaters, such as phenols, chlorinated aromatic compounds, colored organic compounds, pesticides, surfactants and nitroaromatic have been readily photodegradaed by UV/TiO_2. Also, the process is promising for groundwater contaminants. They usually include unsaturated or saturated chlorinated aliphatic compounds and some aromatic compounds existing in ppm levels. Numerous reports of complete mineralization of a wide range of contaminants have been reported. In the air purification, gaseous pollutants present in air emissions from various chemical plants are primarily inorganic compound, such as nitrogen and sulfur oxides and odor-causing compounds such as sulfides and various sulfur-containing compounds can be degraded by TiO_2 photodegradation.

Table 2-1: Selected applications of photocatalyst of TiO_2 (Fujishima et al., 2000).

Property	Category	Applications
Self-cleaning	- Materials for residential and office buildings	- Exterior tiles, kitchen and bathroom components, interior finishings, plastic surfaces, aluminum sideing, building, stone and curtains, paper window blinds
	- Indoor and outdoor lamps and related systems	- Tanslucent paper for indoor lamps covers, coatings on fluorescent lamps and highway tunnel lamp cover glass
	- Materials for roads	- Tunnel wall, sound proof wall, traffic signs and reflector
	- Others	- Tent material, cloth for hospital garments and uniforms and spray coatings for cars
Air cleaning	- Indoor air cleaners	- Room air cleaners, photocatalyst-equipped air conditioners and interior air cleaner for factories
	- Outdoor air purfiers	- Concrete for highways, roadways and footpaths, tunnel walls, soundproof walls and building walls
Water purification	- Drinking water	- Rive water, ground water, lakes and water storage tanks
Antitumor activity	- Cancer therapy	- Endoscopic-like instruments
Self-sterilizing	- Hospital	- Tile to cover floor and walls of operating rooms, silicone rubber for medical catheters and hospital garments and uniforms
	- Others	- Public restrooms, bathrooms and rat breeding rooms

2.2.4 Various forms of TiO_2

Although the existence of TiO_2 could be occurred in four various forms (Ilmenite, Rutile, Brookite and Anatase), the photocatalytic activities of each are significantly different. Anatase and rutile of TiO_2 are the two common forms adopted in the photoreaction. Researchers have discussed (D'Oliveira et al., 1993; Ollis et al., 1984) the different behavior of rutile and anatase having the same specific surface area may be attributed to the more positive conduction band of rutile and the higher recombination rate of electro-hole pair photoproduced in rutile. Also, higher adsorption of O_2 occurs on anatase than on rutile is important for photocatalytic oxidation on titania surfaces (Ollis and Ekabi, 1993).

2.2.5 Surface adsorption and the Langmuir-Hinshelwood (LH) model

Photocatalytic oxidation is a surface-catalysed reaction; pre-adsorption should play a prominent role in the whole process. It may undergo a two-step process: organics are pre-adsorbed on the surface of the photocatalyst followed by the photoactivation. A strong correlation between the adsorptive capacity of thiocarbamates and the extent of photocatalytic oxidation has been demonstrated by Sturini et al. (1996). The reaction rate of thiocarbamate has been found to be governed by its adsorption kinetics. In addition, thiocarbamates are not soluble in water and were observed to be adsorbed onto the TiO_2 surface. Besides, Richard and Benagana (1996) have reported that the degradation of fenuron is affected by the solution pH which could be explained by the point of zero charge (pzc) of TiO_2. The surface charge is neutral in neutral medium. While pH is lower than the pzc, the surface is positively charged and molecules are attracted to the surface by their electronegative component.

The Langmuir-Hinshelwood (LH) kinetics are widely used to quantitatively delineate substrate preadsorption in both solid-gas and solid-liquid reaction (Tang, 2004). Photodegradation reactions in aqueous solutions and the gas phase have generally been observed to follow such kind of kinetics (Fox & Dulay, 1993).

The LH model assumes:

1. The number of surface adsorption sites is fixed at equilibrium.
2. Only one substrate may bind at each surface site.
3. The heat of adsorption by the substrate is identical for each site and is independent of surface coverage.
4. No interaction occurs between adjacent adsorbed molecules.
5. The rate of surface adsorption of the substrate is greater than the rate of any subsequent chemical reaction.
6. No irreversible blocking of active sites by binding to product occurs.

Under these assumptions, the relationship of surface coverage, θ, initial substrate concentration, C_0 and adsorption equilibrium constant, K, can be expressed by Eqn. 2-4 (Hinshelwood, 1926):

$$\theta = \frac{\mathrm{KC_0}}{1+\mathrm{KC_0}} \qquad (2\text{-}4)$$

The initial degradation rate of a substrate can also be represented in terms of initial concentration and adsorption characteristics (Eqn. 2-5):

$$R = -\frac{dC_o}{dt} = \frac{kKC_0}{1+KC_0} \qquad (2\text{-}5)$$

where k is the rate constant, and t is the reaction time. Oxidation rate constants and adsorption equilibrium constants can be obtained from the slope (1/kK) and intercept (1/k) of the straight line. The order of the reaction changes from first at low pollutant concentration to zero at high. This expression is adequate to explain the basic initial kinetics of disappearance of the target compound for the individual system.

2.3 The photocataly tic mechanism of TiO$_2$

2.3.1 Working Principal

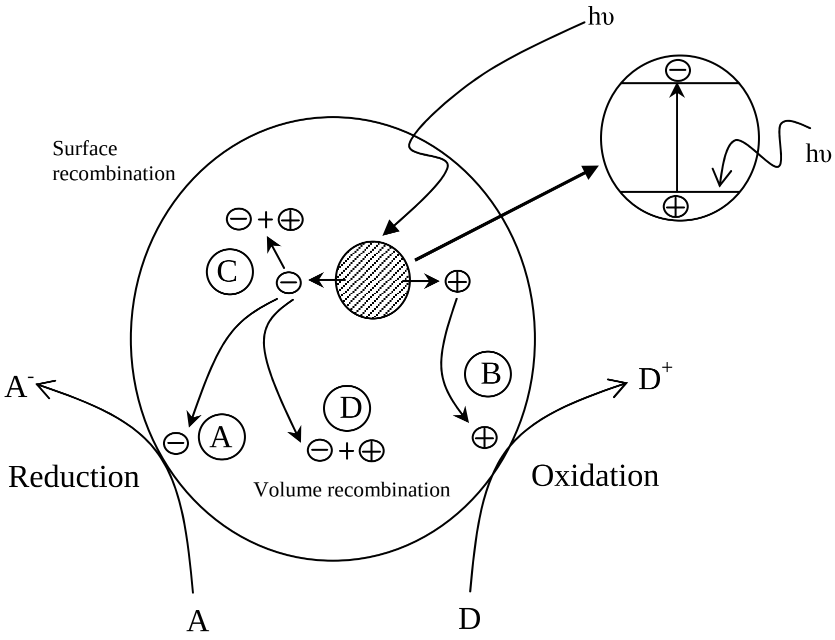

Figure 2-2: Schematic representations of photoexcitation in a solid semiconductor followed by de-excitation events (Linsebigler et al., 1995)

The photoinduced transfer of an electron to an adsorbed organic or inorganic species or to a solvent in the system results from diffusion or migration of electrons and holes to the surface of the semiconductor. This diffusion or migration is driven by the space charge gradient. While at the surface, the electron can be donated to a surface species, thereby reducing an electron acceptor (pathway A). On the other hand, holes can combine with electrons from an electron donor to oxidize the donor species (pathway B). Hole trapping generates a cation radical, $^{\bullet}D^{+}$, while electron trapping generates an anion radical, $^{\bullet}A^{-}$.

The bandgap energy of TiO_2 is between 3.0 and 3.2 eV. The electrons and holes could only be initiated when UV radiation with wavelength at or smaller than 380 nm. However, Serpone et al. (1994) have pointed out that only 3% of the solar spectrum falls into this range of UV radiation by the use of solar energy. Therefore, the use of monochromatic UV lamps is a common practice in the photocatalytic reactions. Photocatalytic oxidation by UV/TiO_2 involves the excitation of TiO_2 particles by UV light from the valance band of the solid to the conduction band. When TiO_2 is illuminated with the light of energy greater than its band-gap energy, an electron (e^-) is transferred to the conduction band leaving a vacancy in the valence band. A positive hole (h^+) is a highly localized electron vacancy in the lattice of the irradiated TiO_2 particle (Eqn. 2-6). These holes could react with OH^- or H_2O to produce $^{\bullet}OH$ (Eqns. 2-7 and 8) which are considered as the major oxidizing species during the mineralization process in TiO_2 photocatalysis. The electron and hole can migrate to the surface of the TiO_2. At the interface, electron transfer can occur either from the conduction band (CB) to an acceptor or a donor to the valence band (VB). In addition, the photoinduced electrons (e^-) could also react with electron acceptors such as O_2 dissolved in water to produce superoxide radical anion ($^{\bullet}O_2^-$) (Eqn. 2-9). (Tang, 2004).

$$TiO_2 + h\upsilon \rightarrow e^-{}_{CB} + h^+{}_{VB} \qquad (2\text{-}6)$$

$$h^+{}_{VB} + OH^- \rightarrow {}^\bullet OH \qquad (2\text{-}7)$$

$$h^+ + H_2O \rightarrow {}^\bullet OH + H^+ \qquad (2\text{-}8)$$

$$e^-{}_{CB} + O_2 \rightarrow {}^\bullet O_2{}^- \qquad (2\text{-}9)$$

In competition with charge transfer to an adsorbed species, recombination of electrons and holes take place. Recombination of the separated electrons and holes can occur either on the surface (pathway C), or in the bulk volume of the semiconductor (pathway D) with attendant dissipation of heat. It is possible that the donation of charge from an adsorbed species back to the semiconductor surface which is named as the charge recombination process.

2.3.2 Charge recombination process

Excited state conduction-band electrons (e^-_{CB}) and valence-band holes (h^+_{VB}) can recombine and dissipate the input energy as heat, get trapped in stable surface states, or react with electron donors or electron acceptors on the surface of the semiconductor. In the absence of suitable electrons and hole scavengers, the stored energy is dissipated within a few nanoseconds by recombination. In order to promote an efficient photocatalysis, it is necessary to prevent the accumulation of e^-_{CB} and h^+_{VB} on the surface as such an accumulation could increase the recombination rate and lower the quantum yield. Irmak et al. (2004) have pointed out that an increase in the number of trapped electrons could prevent the recombination from occurring.

Rothenberger et al. (1985) have found that trapping of conduction band electrons occurs within 30 picoseconds in the photolysis while a much slower trapping is required for valence band holes requiring an average time of 250 nanoseconds. The time for recombination of trapped electrons with free or trapped holes ranges from 10 picoseconds to 1 microsecond.

2.3.3 Photodegradation of organics

The photocatalytic degradation of organic compounds occurs on the surface of TiO_2, primarily in trapped holes. The production and reactivity of the radical intermediates are the main factors limiting the entire oxidation reaction rate. Hydroxyl radical ($^{\bullet}OH$) and superoxyl radical ($^{\bullet}O_2^{2-}$) are considered as primary reactive species and O_2 and H_2O are necessary for photocatalytic degradation. Oxygen adsorbed on the TiO_2 surface prevents the recombination of electron–hole pairs by trapping electrons while $^{\bullet}OH$ radicals are formed from holes reacting with either H_2O or OH^- adsorbed on the TiO_2 surface.

Many researchers have proven that $^{\bullet}OH$ is the most reactive oxidation species to initiate the degradation reaction in the photocatalysis of various organic substrates (Turchi and Ollis, 1990; Ceresa et al., 1983; Jaeger and Bard, 1979). It is strong enough to break bonds of the toxic organic compounds adsorbed on the surface of the TiO_2 leading to the formation of non-toxic CO_2 and inorganic ions. When the intensity of light was constant, the number of $^{\bullet}OH$ and $^{\bullet}O_2^{2-}$ radicals increase with increasing irradiation period, resulting in the complete photodegradation of organic molecules to smaller fragments like CO_2 and H_2O while the other elements bonded to the organic compounds are converted to anions such as nitrate sulfate or chloride.

2.3.4 Photocatalysis by oxidants

Although the organics degradation has proven to be effective in the presence of UV/TiO_2, Tang (2003) has pointed out this process is not economically effective owing to substantial irradiation times are required for mineralization of organics and this process is unlikely to be used in the treatment of high-strength industrial wastewater. Inorganic oxidants have also been proposed to increase quantum efficiencies of TiO_2/UV treatments partially by inhibiting electron–hole pair recombination through scavenging conduction-band electrons at the surface of TiO_2 and partially by augmenting the TiO_2/UV process through thermal and photochemical oxidations in the bulk solution (Martin et al., 1995). The use of inorganic oxidants, for examples H_2O_2, ClO_3^-, BrO_3^- and $S_2O_8^{2-}$ in UV/TiO_2 system could possibility be one of the solutions to increase the quantum efficiencies (Watanabe et al., 2003). The advantages of additional oxidants have been discussed by Carp et al. (2004).

1. The provision of oxidants can increase the trapped electrons which could prevent or slowdown the recombination process.
2. The low oxygen concentration could be avoided whenever aeration is unavailable.
3. The generation of more $^{\bullet}OH$ or other strongly oxidizing radicals which could enhance the photocatalytic degradation of organics as below (Eqns. 2-10 and 11):

$$H_2O_2 + e^-{}_{CB} \rightarrow {}^\bullet OH + OH^- \quad (2\text{-}10)$$

$$S_2O_8{}^{2-} + e^-{}_{CB} \rightarrow SO_4{}^{2-} + SO^\bullet{}_4{}^- \quad (2\text{-}11)$$

According to the investigation of H_2O_2 by Aceituno et al. (2002), low dose of H_2O_2 could lead to a faster degradation on organic compounds in the original UV/TiO_2 photocatalytic system. However, the dosage of H_2O_2 is critical to the UV/TiO_2 process. Zhang et al. (1998) have elevated H_2O_2 concentration could scavenge the photogenerated holes and the radicals that originally generated in the solution yielding the less-reactive $HO_2{}^\bullet$ instead. (Eqns. 2-12-14).

$$H_2O_2 + {}^\bullet OH \rightarrow HO^\bullet{}_2 + H_2O \quad (2\text{-}12)$$

$$HO^\bullet{}_2 + OH \rightarrow H_2O + O_2 \quad (2\text{-}13)$$

$$H_2O_2 + h^+{}_{VB} \rightarrow HO^\bullet{}_2 + H^+ H_2O_2 \quad (2\text{-}14)$$

Pelizetti et al. (1990) have reported a rate enchantment of using several inorganic oxidants on the TiO_2 catalyzed photodegradation of organophosphorus compounds. The observed degradations were mainly attributed to the increased electron scavenging from the extra oxidant sources. Also, Wagner and Strehlow (1982) have proposed a mechanism of periodate ($IO_4{}^-$) during UV illumination, where the involvement of several reactive radicals and non-radical intermediates such as $IO_3{}^\bullet$, ${}^\bullet OH$, $IO_3{}^-$ and $IO_4{}^\bullet$ in assisting the photo-oxidation process was suggested.

Wang and Hong (1999) have worked on the photodecay of 2-chlorobiphenyl in periodate solution. They claimed that the photolytic decomposition of periodate involves the formation of a number of highly reactive radical and non-radical intermediates such as $IO^{\bullet}_3$, $^{\bullet}OH$, IO_3^- and $IO^{\bullet}_4$. The photolytic reduction pathways for periodate was also proposed by Weavers et al. (1997).

However, Abdullah et al. (1990) have observed the presence of perchlorate and nitrate anions have little effect on the kinetics of the TiO_2 photocatalysis, whereas sulphate, chloride and phosphate anions can reduce the rate by 20-70% due to competitive adsorption at the photoactivated reaction sites.

2.4 Immobilization of TiO_2 by sol-gel process

2.4.1 Introduction

Although TiO_2 is believed to be one of the best catalysts in the market, powder dispersion always requires pose-filtration treatment which complicates the treatment procedures. Researchers have tried to develop alternatives to anchor particles onto substrates. The most common methods include chemical vapor deposition (Kavan and Gratzel, 1995), chemical spray pyrolysis (Kavan et al. 1993), electrodeposition (Natarajan and Ogami, 1996.), and sol-gel method (Yasumori, et al. 2001).

2.4.2 Background and applications

Sol-gel technique is a simple and convenient method for the fabrication of a thin-film materials, such as optical, ferroelectric, dielectric, and other materials. A wide range of parameters can be used to tailor the product because it is typical of chemical synthesis routes. Sol-gel technology is developed in the early 60's to aid in the production of nuclear fuel, but it has been used in many other applications.

The recent great interest in utilizing sol-gel derived thin and thick films for the application to telecommunications, automotive, information storage devices and others. The easiness and cost-effectiveness for the thin and thick film fabrication of sol-gel techniques are leading to its use in many novel applications. Advantages of sol-gel method are listed below (Woolfrey and Bartlett, 1998):

1. Mixing of multi-component systems is intimate and uniform (homogeneous) because of the interactions of the reactants at the molecular level.
2. Processed materials can be very reactive and hence the sintering temperatures are much lower than those employed for conventionally prepared powders. This is mainly due to the high surface energy of the sol-gel derived colloidal particles.
3. If the process is free from contamination, the final product is expected to be highly pure with respect to the high purity of the raw materials.
4. Because of the low calcinations and sintering temperatures needed for the sol-gel derived materials, the size and crystallinity of the resulting particles can be controlled.
5. Various shapes and configuration of materials such as fibers, uniform particles, thin and thick film coatings and solid dense or porous bodies can be developed by altering the sol condition (e.g., pH, viscosity)

2.4.3 Definition of sol-gel

Pierre (1998) has given a detail definition of sol and gel. The term “sol” is applied to a colloidal suspension of solid particles in a liquid. And, the colloid is a suspension in which the dispersed phase is so small (~1μm) that gravitational forces are negligible. “Gel” delicates to a suspension in which the solid part of the suspension reaches from one end of the container to the other.

2.4.4 Chemistry of sol-gel

The preparation of sol-gel solution usually consists of four major steps (Brinker and Sherrer, 1990):

1. The desired colloidal particles once dispersed in a liquid to form a sol.
2. The deposition of sol solution produces the coatings on the substrates by spraying, dipping or spinning.
3. The particles in sol are polymerized through the removal of the stabilizing components and produce a gel in a state of a continuous network.
4. The final heat treatments hydrolyze the remaining organic or inorganic components and form an amorphous or crystalline coating

The process is sensitive to several parameters, such as the control of hydrolysis and condensation, the annealing temperature, and the use of acid/alkaline catalyze (Yu et al., 2003; Singh et al., 2002). In the common practice, the preparation of TiO_2 sol-gel is conducted via the hydrolysis and condensation process of highly reactive alkoxide titanium precursor to yield the Ti-O-Ti network. Though this process could be exceptionally fast, it would lead to precipitation of amorphous particles with uncontrolled structure. Careful control on this process could be achieved by acid or base addition.

2.4.5 Preparation by metal alkoxide

Synethsis of sol can either be made through the non-alkoxide or the alkoxide route. Inorganic salts (Bach et al., 1998; Sivakumar et al., 2002) (such as nitrates, chlorides, acetates, carbonates, acetylacetonates, etc.) were used in the non-alkoxide route which requires an additional removal of the inorganic anion. The alkoxide route required metal alkoxides as starting material (Watson et al., 2003). This method involves the formation of a TiO_2 sol or gel or precipitation by hydrolysis and condensation (with polymer formation) of titanium alkoxides. The use of metal alkoxide as precursor is the commonest method for sol-gel preparation (Ian, 1988). It gives a general formula as:

$$M(OR)_X$$

where M is the metal, R is an alkyl group, and x is the valence state of the metal.

Because of its highly electronegative OR group, metal alkoxides are very active which are rapidly hydrolyzed to the corresponding hydroxide or oxide. The method of hydrolysis can be varied and many times depends on the final use of the product. The overall reaction can be represented in Eqns. 2-15 and 16 while the by-product ROH is an aliphatic alcohol and readily removed by volatilization.

$$M(OR)_x + xH_2O \rightarrow M(OH)_x + xROH \qquad (2\text{-}15)$$

$$2M(OH)_x \rightarrow M_2O_x + xH_2O \qquad (2\text{-}16)$$

Transition metals alkoxides (e.g., $Ti(OR)_4$) are much more reactive toward mucleophilic reagents than other metal alkoxides (e.g., $Si(OR)_4$). As such, they must be handled in dry condition and stabilized via chemical modification (Livage et al., 1988). As titanium sources, Ti(*O*-E)$_4$ (Okudera and Yokogawa, 2003), Ti(OR)$_4$ (Stir et al., 2003), and Ti(O-*n*Bu)$_4$ (Yang et al., 2002) are most commonly used. Taking Ti(OR)$_4$ as an example, Eqn. 2-17 represents the hydrolysis reaction occurring upon the addition of water or alcohol solution.

$$Ti(OR)_4 + H_2O \underset{Reesterification}{\overset{Hydrolysis}{\rightleftharpoons}} Ti(OH)(OR)_3 + ROH \tag{2-17}$$

The polycondensation has indicated in Eqn. 2-18

$$Ti(OH)(OR)_3 + Ti(OH)(OR)_3 \underset{Hydrolysis}{\overset{Condensation}{\rightleftharpoons}} Ti_2O(OR)_6 + H_2O \tag{2-18}$$

Owing to the high reactivity of transition metal alkoxides with water, precipitation is usually observed rather than gelation, where homogeneity cannot be observed. This problem can be solved by introducing additives such as solvents and acidic or basic catalyst stabilizing agents. In most cases, these additives introduce nucleophilic molecules that react with the alkoixde resulting in a new molecular precursor. The new molecular precursor reacts differently with the nucleophilic agent. More electronegative ligands are removed during the condensation reactions, while the less electronegative ones are quickly removed at the initial stages of hydrolysis. As a result, instead of a fast precipitation, a controlled formation of polymeric gels is expected (Dunuwila et al., 1994).

2.4.6 Acid and base catalysis

The hydrolysis reaction replaces alkoxide groups (OR) with hydroxyl groups (OH) through the addition of water. Under normal conditions, the hydrolysis reaction is very slow. It is most rapid and complete when catalysts (acid and base) are employed. The choice of acid or base catalysis has a substantial influence on the nature of the gel (Wright and Sommerdijk, 2001).

Employing acid catalysis increases hydrolysis rates and ultimately crystalline powders are formed from fully hydrolyzed precursors. It leads to gels with a finer, denser structure instead of particulate and consists of comparatively linear, lightly cross linked polymeric clusters. The first step of acid catalysed hydrolysis is the fastest and the product of this first step also undergoes the fastest condensation. Hence an open network structure results initially, followed by further hydrolysis and cross-condensation reactions.

Base catalysis is aimed to promote condensation with the result that amorphous powders are obtained containing unhydrolyzed alkoxide ligands. This process could produce gels that are granular in texture and retain less organic material. In the basic conditions, the negatively charged transition state becomes more stable as more hydroxyl groups replace the electron donating alkoxyl groups. Thus successive hydrolysis steps occur increasingly rapidly, and the fully hydrolyzed species undergoes the fastest condensation reactions. As a consequence, in base catalysed reactions highly cross-linked large sol particles are initially obtained which eventually link to form gels with large pores between the inter connected particles.

2.4.7 Dip coating

Many coating methods are available for the substrate deposition. It includes spin-coating, dip coating, spraying, elecrophoresis, thermoporesis and settling. Among them, dip coating is the most common and easiest technique to deposit sol-gel film with controlled thickness for various substrates. The substrate is immersed in the solution and extracted by withdrawing or by lowering the solution batch. In this process, a liquid layer remains on the substrate with a thickness profile that is determined by the effect of different forces (mainly viscous force, gravity, and surface tension) on its flow. By this method, one or both sides of the flat substrates can be coated by dipping the substrate into the solution and withdrawing vertically or at an angle from the solution at a constant speed. Normally, the process can divided into five stages (Scriven, 1988): (1) immersion; (2) start up; (3) deposition; (4) drainage; (5) evaporation.

The coating thickness is mainly defined by the withdrawal speed, by the solid content and the viscosity of the liquid. If the withdrawal speed is chosen such that the sheer rates keep the system in the Newtonian regime, the coating thickness (h) can be calculated by the Landau and Levich (1942) in Eqn. 2-19.

$$h = 0.94\frac{(\eta v)^{2/3}}{\gamma_{LV}{}^{1/6}(\rho g)^{1/2}} \qquad (2\text{-}19)$$

where $\eta$is the liquid viscosity, v is the substrate speed, γ_{LV} is the liquid-vapor surface tension, ρ is the fluid density and g is gravity.

2.4.8 Drying process

The process of drying of a porous material can be divided into several stages (Brinker and Scherer, 1990):

1. The body shrinks by an amount equal to the volume of liquid that evaporates, and the liquid-vapor interface remains at the exterior surface of the body.
2. It begins when the body becomes too stiff to shrink and the liquid recedes into the interior, leaving air-filled pores near the surface. Even as air invades the pores, a continuous liquid film supports flow to the exterior, so evaporation continues to occur from the surface of the body.
3. The liquid becomes isolated into pockets and drying can proceed only by evaporation of the liquid within the body and diffusion of the vapor to the outside.

Defects of film may arise where the drying process or environment is inappropriate. The most common problem is the observation of warping and cracking. This is due to the high amount of solvent to be removed from the interior parts. With careful control on the rate of drying, this could be avoided. Besides, owing to the physical driving forces or the chemical forces incurred in the process, volume shrinkage is possible to occur.

2.4.9 Sintering

Sintering is a heat-assisted treatment for the improvement of mechanical strength of the material through the formation of a solid bond between the particles. In this stage, porosity could also be eliminated through densification. Most of ceramic particles, including oxides, need the high temperatures to be sintered to high levels of densification. Free energy of surfaces should be reduced by bonding individual particles together by the driving force. This could be done by the elimination of pores and reduction of grain boundaries via grain growth. Temperature, time, and the primary particle size of the material are the most important factors which can influence the sintering process and the resulting microstructure.

2.5 Description of o-Chloroaniline (o-ClA)

2.5.1 Introduction

Chlorinated anilines are anthropogenic organic compounds and are used as intermediates in the manufacture of azo dyes, drugs, and agricultural agents. o-Chloroaniline (o-ClA) is synthesized by the reduction of 1-chloro-2-nitrobenzene (The Merck Index, 1983)

2.5.2 Sources of pollution

o-ClA belongs to the anilines family which is frequently used as starting substances for chemical synthesis in the manufacture of petroleum solvents, rubber, and fungicides (Jen et al., 2001; Voyksner et al., 1993; IARC, 1987 & 1982). The Toxic Substances Control Act Chemical Substances Inventory reported in 1977 that between 100,000 and 1,000,000 pounds were produced in the United States and approximately 200,000 pound were imported (CICIS, 1977).

2.5.3 Environmental hazard

ClA maybe released into the environment from process/waste emissions involved in their production or use and may also enter the environment as degradation products of various pesticides (Hargesheimer et al., 1981.) or from residues in food (HSDB, 1995). The Environmental Agency of Japan (2000) reported that there was a maximum of 0.56 mg L^{-1} o-ClA in the country's coastal waters in 1990. According to IAWR (1998), industrial processes generated 6.1 tonnes of ClAs in 1985 were estimated to be released to the river Rhine. USEPA (1987) has proven that it could retain in the environment as degradation products of various pesticides and it would undergo a more persistence chemical bonding with humic materials when released to soil (Lyman et al., 1982). Since it is a suspected carcinogen and is highly toxic to aquatic life (Laha and Luthy, 1990), developing strategies for pollution prevention and minimization is necessary.

2.5.4 Human exposure

Occupational exposure to o- and m-ClA occurs primarily by dermal contact or inhalation. NIOSH surveys showed that approximately 18,138 workers were exposed to o-ClA in the U.S. between 1972 and 1974 (NIOSH, 1990). Long-term exposure of o-ClA may cause damage of spleen, liver and kidney (Kuhn et al., 1989).

2.5.5 The necessity for treatment

Owing to the toxicity mentioned, o-ClA has been included in the List II of European Union (EU, 1976) while o, m-ClA have also been designated as hazardous wastes by the USEPA (40 CFR, Part 61, 1985). The possibility of o-ClA decayed by UV has been proposed by USEPA (1987) on both soil and water surfaces. However, only limited researchers have provided information on the photoreaction of ClA. Although BUA report (1995) has been pointed out direct photolysis of o-ClA was possible under sunlight, the degradation product of chloronitrobenzene was still stable over the irradiation period of 20 hours (Miller and Crosby, 1983). Hommel (1985) has reported that the use of strong oxidants could assist the mineralization of ClA. Therefore, a detail examination on the photochemistry of o-ClA is thus valuable and of our great interest.

3 Materials and Methods

3.1 Materials

3.1.1 Chemicals and reagents used

All the chemicals used in this study were tabulated in Table 3-1. All the chemicals were used without further purification. The water used in the preparation of all the solutions was obtained from a Barnstead Nonopure water purification system with conductivity above 18 Ωm. o-chloroaniline (o-ClA) has been chosen as the target pollutant. Selected physical properties of o-ClA were listed in Table 3-2 and its MSDS was shown in Appendix I.

Powdary TiO_2 was purchased from Degussa P25 (70% anatase and 30% rutile) with a BET surface area of 50-55 m^2g^{-1} and a density of 3.85 gcm^{-3}. It is formed by the hydrolysis of $TiCl_4$ in a hot flame (Wold, 1993) and the relatively short residence time required for the conversion to TiO_2 gives a product that has high surface area. It has an average aggregate size of 200 nm and is made up of 30 nm primary particles (Beydoun et al., 2002; Goutailler et al. 2001). Linsebigler et al. (1995) stated that a high percentage of the anatase phase in P25 TiO_2 is more photoactive than in the brocktile or rutile phases.

Table 3-1: List of chemicals used in this study.

Chemicals	Molecular weight, g mol^{-1}	Formula	Purchased from
o-chloroaniline (99.5%)	127.57	C_6H_6ClN	Fluka AG
Titanium dioxide (P25)	79.87	TiO_2	Degussa
Titanium isopropoxide (99%)	284.22	$C_{12}H_{28}O_4Ti$	Aldrich
<u>Oxidants</u>			
Hydrogen Peroxide (30%)	34.00	H_2O_2	Aldrich
Rose Bengal	1017.64	$C_{20}H_2Cl_4I_4Na_2O_5$	Aldrich
Potassium Chlorate	122.55	$KClO_3$	International Lab.
Potassium Bromate	167.00	$KBrO_3$	International Lab.
Potassium Iodate	214.00	KIO_3	International Lab.
<u>Intermediates</u>			
1,4-benzoquinone (98%)	108.09	$C_6H_4O_2$	Acro
2-chlorophenol	128.56	C_6H_4OHCl	Riedel-de Haen
2-chloro-1,4-benzoquinone (95%)	142.54	$C_6H_3ClO_2$	Acro
2-chloronitrobenzene	157.55	$C_6H_4ClNO_2$	International Lab.
2-iodoaniline (98%)	219.02	C_6H_6IN	Aldrich

(Cont’d Table 3-1)

Solvents			
Acetonitrile (HPLC grade)	41.05	C_2H_3N	Tedia
Acetone (AR grade)	58.08	C_3H_6O	Tedia
Methanol	32.04	CH_4O	Tedia
Isopropanol (99%)	60.10	C_3H_8O	Tedia
Ethyl acetate (99.8%)	88.11	$C_4H_8O_2$	Lab-scan
Hexane (99.9%)	86.18	C_6H_{14}	Lab-scan
Others			
Sodium Carbonate (99.7%)	105.99	$NaCO_3$	AnalaR
Sodium Bicarbonate (99.9%)	84.01	$NaHCO_3$	AnalaR
Sodium Chloride (99.99%)	58.44	NaCl	Fisher
Sodium Nitrite (99.5%)	69.00	$NaNO_2$	AnalaR
Nitric Acid	63.01	HNO_3	Tedia
Sulfuric Acid	98.08	H_2SO_4	Tedia
Sodium Hydroxide (96%)	40.00	NaOH	Uni-Chem
Ammonium Chloride (99.5%)	53.49	NH_4Cl	Uni-Chem
Potassium Iodide	166.00	KI	Aldrich

Table 3-2: Physical Properties of o-Chloroaniline (The Merck Index, 1983).

Formula	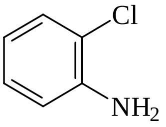 C_6H_6ClN
Molecular mass	127.57
Physical state	Clear amber liquid
Melting point (°C)	-1.94
Boiling point (°C)	208.84
Density	d_4^{22} 1.2114
Vapor pressure	0.17 mm Hg
Water solubility	Insoluble
Solvent solubility	Soluble in most organic solvents also in acids
pKa	2.6
Maxima of absorption spectrum	232 and 289 nm

3.1.2 Preparation of sol

The preparation of film was fabricated by sol-gel method and was illustrated by the flow chart in Figure 3-1. Acid-catalyzed sol-gel formation was used for the synthesis of TiO_2 sol. Titanium isopropoxide (TTIP) was used as the precursor. The molar ratio of TTIP:iPrO:H_2O:HNO_3 was fixed at 1:63.4:0.06:0.51. The HNO_3 solution (at 50%) was first diluted by water and mixed with the iso-propanol. The required TTIP was slowly added into the solution under magnetic stirring. After stirring for two hours, 0.75 g of commercial TiO_2 (P25) was introduced to the sol solution and the mixture was sonciated for another 15 mins. The mixture was then stabilized for 24 hours before coating.

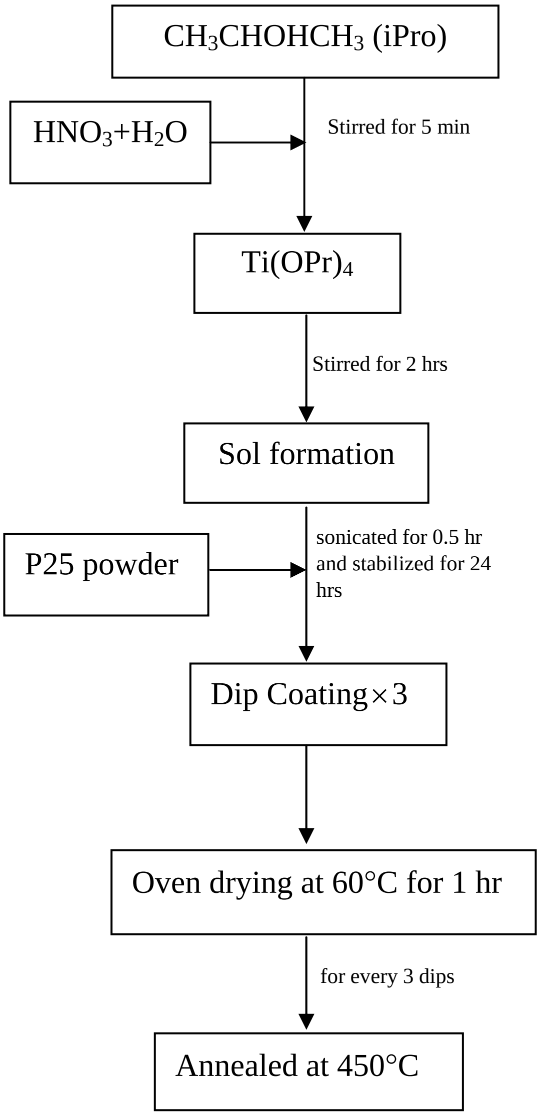

Figure 3-1: TiO_2 film preparation procedures.

3.1.3 Dip Coating

Quartz and glass slides in the dimensions of 24×50 mm^2 were selected as the substrate. Thorough cleaning is necessary to ensure film surface was free from dust and grease. The slides were first sonicated with distilled water and acetone. They were rinsed with doubly-ionized water and dried in the oven at 500°C prior coating. The substrate was mounted by the telfon tube and was carefully dipped into the sol for 5 mins. Afterward, it was slowly lifted by a mechanical motor at a rate of 10 mms^{-1}. This procedure was repeated to obtain thicker samples of titania. Drying of alcohol was allowed for one hour in the oven at 60°C. Films were then annealed at 450°C (unless specify) to undergo crystallization for every three dips. The weight increment of film was recorded in Table 4D-2.

3.2 Experimental Set Up

3.2.1 Dark adsorption test

The adsorption isotherm of o-ClA was determined in the dark environment. Exact 75 mL of solution at different o-ClA concentrations were stirred in the presence of 0.1 gL^{-1} TiO_2. Magnetic stirring was maintained for 20 hours to establish the equilibrium of o-ClA between TiO_2 particles and the aqueous phase. Each set of test was repeated by different solution pHs at a constant temperature at 24°C throughout the experiment. The remaining o-ClA in the aqueous phase was passed through a 0.45 µm-pore filter membrane before quantification.

3.2.2 Photochemical reaction

All the photochemical experiments were conducted in a Rayonet^{TM} RPR-200 photoreactor surrounded by pre-installed UV lamps at selected wavelengths (as in Figure 3-2). A cooling fan was installed at the reactor base such that a constant experimental temperature of 23°C could be kept in an air-conditioned laboratory. To ensure a thorough mixing, 150 mL of solution (containing o-ClA, TiO_2 or oxidants in some cases) were dispensed into a 300 mL quartz cylinder with mechanical stirring before and during the illumination. For the study of TiO_2 film, the coated substrate was hanged in the reactor as shown in Figure 3-2. Phosphor-coated low-pressure mercury lamps were installed in the photoreactor. The pH level of the solution was adjusted by H_2SO_4 and NaOH, respectively. Samples were withdrawn at pre-determined time and filtered through a 0.45μm pore size membrane before quantification. Methanol (Arnold et al., 1995) and sodium nitride were used as the quencher for the oxidants H_2O_2, Rose Bengal (RB) and oxyhalogens (Cermola et al., 2004) to prevent subsequent oxidation. Control experiments without a photocatalyst and UV illumination were also performed for comparison. The experimental conditions of each run have been listed in Appendix II.

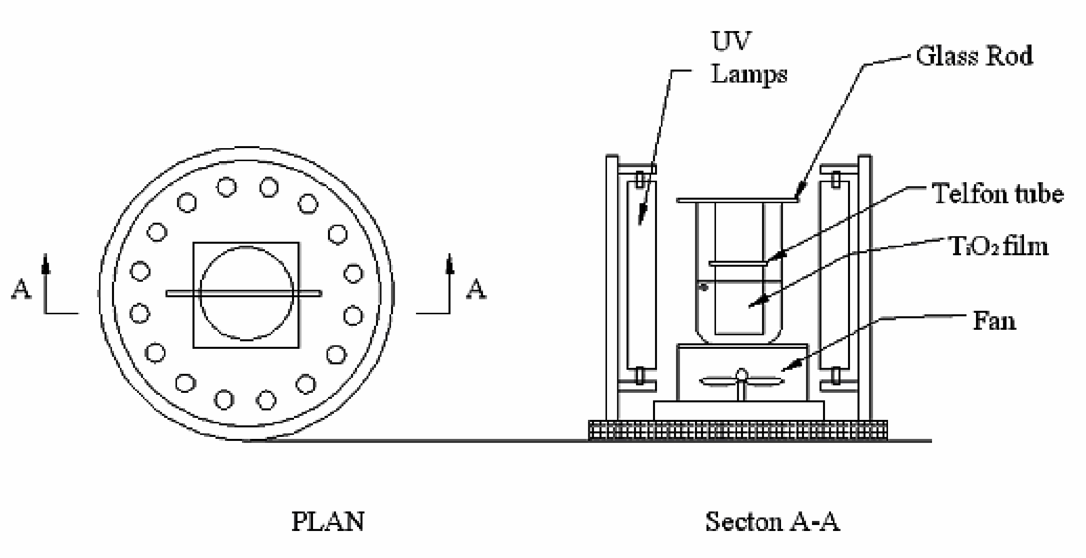

Figure 3-2: The top view and sectional view of the photoreactor.

3.3 Instrumental Analysis

3.3.1 Analysis by high performance liquid chromatography (HPLC)

Remaining o-ClA after photoreaction was quantified by HPLC, in which a silica packed column (Restek pinnacle octyl amine) in 5 μm × 0.46 cm × 25 cm dimension was used as the stationary phase. The system also included a high pressurized pump (Finnigan MAT SCM 1000), an UV detector (UV 6000LP), an autosampler and a UV/VIS (WATERS 486) detector. The selective absorbance of o-ClA were set at 289 nm according to the strongest signal from UV-Vis spectrophotometer (spectrum was shown in Appendix IV). The elution solvent was a mixture of acetonitrile-water at 60:40 (v/v) with a flow of 1 $mLmin^{-1}$. Four-point calibration was conducted for every batch of analysis.

3.3.2 Analysis by ion chromatography (IC)

The generation of ions was believed as the end-products in the organic photodegradation. Therefore, the presence of chloride and nitrite were quantified by the ion chromatography (Dionex Series 4500i) composed of an anion column (Dionex Ionpac AS11 (4×250 mm) and AG11 (4×50 mm), and a suppressor (ASRS-II) in auto suppression recycling mode. A mixture of 0.8 mM of $NaHCO_3$ and 0.8 mM of $NaCO_3$ was used as the mobile phase eluting at 1 $mLmin^{-1}$.

3.3.3 Analysis by gas chromatography (GC/MS)

The identification of intermediates was conducted by a GC/MS with a Hewlett-Packard system composed of a HP 3800 gas chromatograph connected with Varian factor four capillary column (VF-5ms 30m×0.25mm), coupled with a Varian 1200L quadrupole MS/MS operating in EI mode at 900V. Helium gas in the constant flow of 1 mLmin^{-1} was used as the carrier gas. An autosampler was installed and 1 μL of sample was injected from the injector port (280°C) in the splitless mode. Extraction solvent was 1 mL mixture of 50% ether and 50% hexane with 0.2 g of sodium chloride. 1 mL of sample was added to the eluent and was then shaken by the mixer (Barnstead Thermolyne Type 37600) for 1 min. Top layer of extracts were collected for analysis. Separation of intermediates were ramped by a temperature program with an initial temperature at 50°C for 1 min, rising to 200°C at 5°C per min for another 3 min, then it finally reached to 260°C at the same rate for 2 min. The peaks observed for the reaction intermediates were referenced with the appropriate external standards. While those compounds were not commercially available, their relative abundance was predicted by their corresponding ion intensity with the probe compound, o-ClA, from the MS analysis. Details of intermediates were shown in Table 3-4 and their MS spectrums were indicated in Appendix III.

Table 3-4: Information on organic intermediates. (Linstrom and Mallard, 2005)

Identified Intermediates (Nomenclature)	Molecular Weight	Structural formula	MS spectrum (abundance > 50%)	Toxicity (MSDS, 2007)
Aniline (AL)	93.13	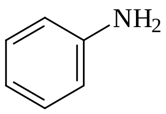	93	LD_{50}(rat) = 250 mg/kg LC_{50}(man) = 175 in 7hr
1,4-benzoquinone (BQ)	108.09	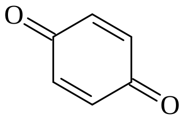	108, 54, 26	LD_{50} = 100 mg/kg
2-chlorophenol (CP)	128.56	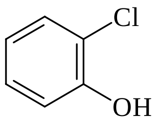	128	LD_{50}(rat) = 670 mg/kg
2-chloro-1,4-benzoquinone (CBQ)	142.54	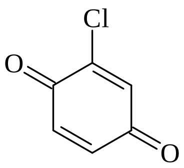	142, 54, 26, 82, 53, 60	LD_{50}(rat) = 219 mg/kg
2-chloronitrobenzene (CNB)	157.55	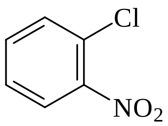	75, 111, 157, 99	n/a
2-iodoaniline (IA)	219.02	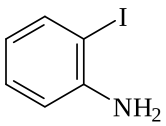	219, 65, 127, 92	LD_{50}(man) = 2900 mg/kg
2-iodophenol (IP)	220.01	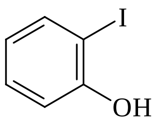	220	n/a
bis(2-chlorophenyl)-diazene (BCD)	251.11	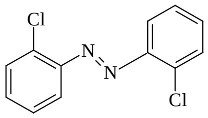	111, 139	n/a

3.3.4 Analysis by ammonia electrode

Ammonium ion was measured by the ammonia gas-sensing electrode (Cole-Parmer). Samples were measured immediately after collection. 10 M NaOH was added to each sample to promote the pH between 11 and 14 where the ammonium species were able to convert to ammonia. The solution was stirred and data was recorded when it reached a stable value. The amount of ammonia was compared to the standard of ammonium chloride.

3.3.5 TOC measurement

The total organic carbon (TOC) concentration was analyzed by a Shimadzu TOC-5000A analyzer equipped with an ASI-5000A autosampler to determine the total mineralization degree of the organic pollutants during the advanced oxidation process.

3.3.6 pH measurement

Solution pH was adjusted by the addition of diluted H_2SO_4 or NaOH. Measurement was carried out by the pH meter (Cole Parmer) and thorough mixing was ensured by magnetic stirrer.

3.3.7 Analysis by X-ray diffraction

X-ray diffraction (XRD) was employed to investigate the phase homogeneity of the titanium dioxide. Also, this method was used to derive information about the (average) size of the nanoparticles in the film. Philips MPD 18801 X-ray diffractometer using Cu Kα irradiation (wavelength = 0.154 nm) at a scan rate of

0.05° was used to determine the crystalline phase and the crystallite size. Diffraction patterns were taken over the 2θ range from 10-70°. The accelerating voltage and the applied current were 35 kV and 20 mA, respectively.

3.3.8 Analysis by scanning electron micrographs (SEM)

The morphology of the films was examined by the scanning electron micrographs (SEM) (a Leica Stereoscan 440) with a tungsten filament.

3.4 Data Analysis

3.4.1 Pseudo first-order decay

Pseudo first-order reaction has been widely and successfully used for the description of organic decay in photoreaction (Naomi et al., 2000; Pruden and Ollis, 1983). The initial decay rates of the o-ClA is therefore expressed as (Eqn. 3-1):

$$d[C]/dt = -k[C] \quad \text{or} \quad [C_t] = [C_0]\exp^{-kt} \tag{3-1}$$

where $[C_0]$ is the initial concentration of o-ClA and $[C_t]$ is the concentration at time t, and k (min^{-1}) is the pseudo-first-order decay rate constant which can be estimated from the slope of $\ln(C/C_0)$ against t.

3.4.2 Quantum yield

Quantum yield is a useful parameter to indicate the efficiency of a photochemical reaction which is defined as the number of probe molecules undergoing a specific chemical reaction divided by the number of photons absorbed (Klessinger and Michel, 1995). The quantum yield of o-ClA decay can be calculated from the observed first-order decay rate constant as proposed by Choudhry and Webster (1987), where a specific form of quantum yield, ϕ based on first order kinetics was indicated in Eqn. 3-2:

$$\phi = \frac{k}{2.303 I_{0,\lambda} \varepsilon_{D,\lambda} \ell} \tag{3-2}$$

where $I_{0,\lambda}$ is the incident light intensity at specific wavelength (Einstein $l^{-1}s^{-1}$), the intensities of three different wavelengths used in this study were reported in Table 3-5, $\varepsilon_{D,\lambda}$ is the molar absorptivity ($M^{-1}cm^{-1}$) of probe, and ℓ is the length of the light-path in the quartz cell (cm). The molar absorptivity, $\varepsilon_{D,\lambda}$, was calculated by the Beer-Lambert Law from the measurement of absorbance at different o-ClA concentrations (Kagan, 1993).

Table 3-5: Light intensities of selective wavelength (Data provided by the Southern New England Ultraviolet Company).

Wavelength, nm	Light intensity per lamp, $El^{-1}s^{-1}$
254	1.5×10^{-6}
300	0.7×10^{-6}
350	3.11×10^{-6}

3.4.3 Particle size of TiO_2

Without BET measurement, the crystallite size of TiO_2 films can be deduced from XRD lines broadening using the Scherrer equation (Eqn. 3-3) (Cullity, 1978; Langford and Wilson, 1978; Klug and Alexander, 1954):

$$D = \frac{0.94\lambda}{\beta \cos\theta} \qquad (3\text{-}3)$$

where *D* is the crystallites size, *λ* is the X-ray wavelength used, *β* is the broadening of diffraction line measured as half of its maximum intensity (FWHM) and *θ* is the corresponding angle.

3.4.4 Phase content estimation

Hague and Mayo (1993) have suggested the calculation of phase content for anatase and rutile fraction determination by (Eqn. 3-4):

$$f = (1 + 1.26\frac{I_R}{I_A})^{-1} \qquad (3\text{-}4)$$

where f is the weight fraction of anatase phase, I_A and I_R are the strongest intensities of x-ray with respect to anatase and rutile phase.

4A The Photocatalytic Degradation of o-ClA in TiO_2 Suspension

4A.1 Dark Adsorption of TiO_2 at different initial pH levels

Dark adsorption test was carried out according to method described in 3.2.1. The adsorption behavior was characterized by the empirical Langmuir equation which has been used by various researchers for the sorption of variety of compounds. The model assumes uniform energies of adsorption onto the surface, no transmigration of adsorbate in the plane of the surface, and no interaction between the adsorption sites (Bouzaida et al., 2004).

The Langmuir adsorption isotherm is given by Eqn. 4A-1:

$$\theta = Q_{ads} / Q_{max} = KC_{eq} /(1 + KC_{eq}) \qquad (4A\text{-}1)$$

where Q_{ads} (mmol/g) is the number of adsorbed molecules at the adsorption equilibrium, Q_{max} (mmol/g) is the maximum adsorbable quantity, K (L mmol^{-1}) is the Langmuir adsorption constant of o-ClA on TiO_2 and C_{eq} is the concentration of o-ClA at the adsorption equilibrium.

Eqn. 4A-1 could be further transformed into linear form as in Eqn. 4A-2 for data analysis:

$$1/Q_{ads} = 1/Q_{max} + 1/(Q_{max}KC_{eq}) \qquad (4A\text{-}2)$$

A set of isotherm at different initial pH values was shown in Figure 4A-1. In this plot, the ordinate at the y-intercept is equal to the reciprocal of Q_{max}, whereas K can be calculated from the slope (slope=1/$Q_{max}K$). The figure presents a good correlation of the model with r^2 above 0.99 for all the tested pH. The adsorption behaviors of TiO_2 were quite similar from neutral to basic pH levels except at extremely low pH level of 2, where a distinctive trend was observed.

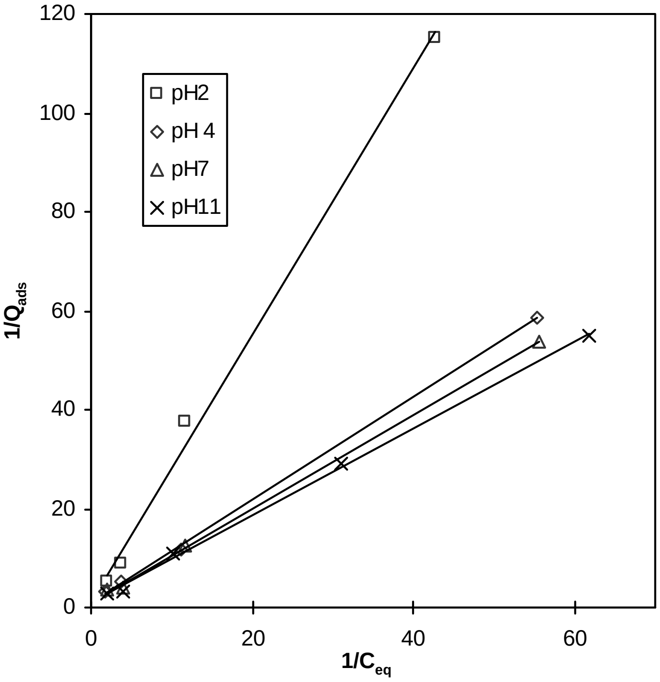

Figure 4A-1: Langmuir isotherm transformation on TiO_2 at different pH solutions. (1/Q_{ads} vs 1/C_{eq})

Table 4A-1: Adsorption parameters of o-ClA onto TiO_2 at different initial pH levels.

Initial pH	Slope	Intercept	r^2	Q_{max}, mmol g^{-1}	K, L $mmol^{-1}$
2	2.690	1.374	0.9955	0.728	0.511
4	1.041	1.067	0.9995	0.937	1.026
7	0.944	1.168	0.9996	0.856	1.237
11	0.929	0.593	0.9989	1.076	1.566

Judging from the calculated Q_{max} in Table 4A-1, in general, the Q_{max} decreased from high to low pH suggesting the maximum active adsorption sites of TiO_2 are reduced as solution pH decreased. Therefore, o-ClA molecules have lower affinity to be adsorbed by TiO_2 in strong acidic condition.

4A.2 Effect of Wavelength and Light Intensity

The photodecay of o-ClA was illuminated at three selected wavelengths (254, 300 and 350 nm) and their corresponding reaction rates were shown in Figure 4A-2.

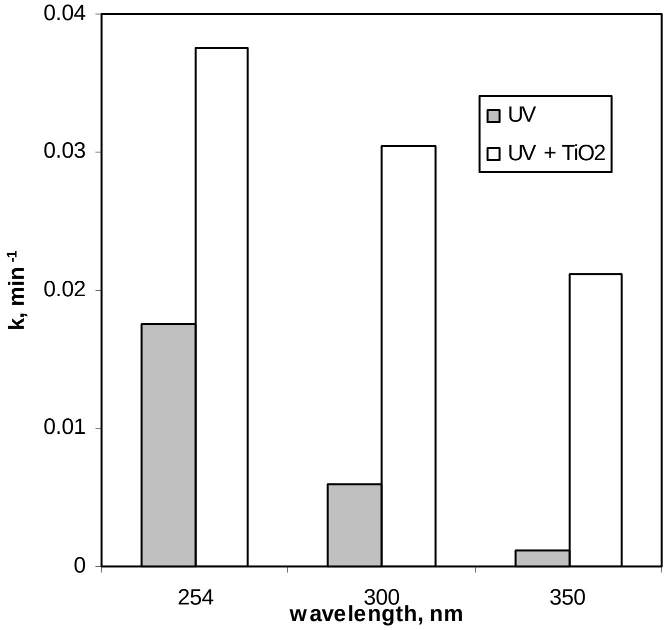

Figure 4A-2: First-Order Kinetic Constants of o-ClA at various wavelengths. (Notes: $[o\text{-}ClA]_0 = 0.095$ mM; $[TiO_2] = 0.1\ gL^{-1}$).

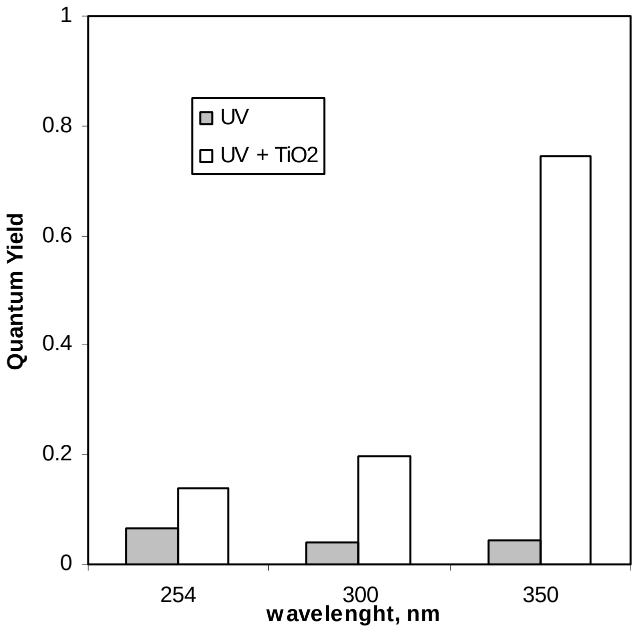

Figure 4A-3: Quantum yield of o-ClA (Notes: $[o\text{-}ClA]_0$ = 0.095 mM; $[TiO_2]$ = 0.1 gL^{-1}).

Using the same number of UV lamps of eight, the difference in reaction rates showed that photodecay of o-ClA was most effective at 254 nm while longer wavelength caused a slower decay in both sole UV and UV/TiO_2 systems. Since the amount of photons in each specific wavelength are different (see Table 3-5); quantum yield would be a better and more precise parameter to describe and compare the photolytic efficiency.

The decay quantum yield at different wavelengths could be manipulated by Eqn. 3-2 with the inclusion of rate constants, molar absorptivity, and light intensities, and the results were summarized in Figure 4A-3. It was found that the difference as well as the level of quantum yields through direct photolysis (by sole UV) was generally trivial comparing to that of catalytic photolysis (by UV/TiO_2). The highest quantum yield of direct photolysis of o-ClA was found at 254 nm and followed by 350 and 300 nm, but all the yields are less than 0.1. However, as TiO_2 was introduced into the system the quantum yield could significantly increased above 0.7, besides, a dramatic change of the quantum efficiency was observed in the order of 350 nm, 300 nm, and 254 nm. This result has concurred with the study conducted by Chen et al. (2002), where higher quantum efficiency were observed at 300 or 350 nm implying the excitation of electron-hole in TiO_2 is more sensitive at these wavelengths.

4A.3 Dosage effect on o-ClA and TiO_2

Fixing $[\text{o-ClA}]_0$ at 0.095 mM, different [TiO_2] doses were added to the sample with continuous stirring under UV illumination, and the remaining o-ClA is shown in Figure 4A-4.

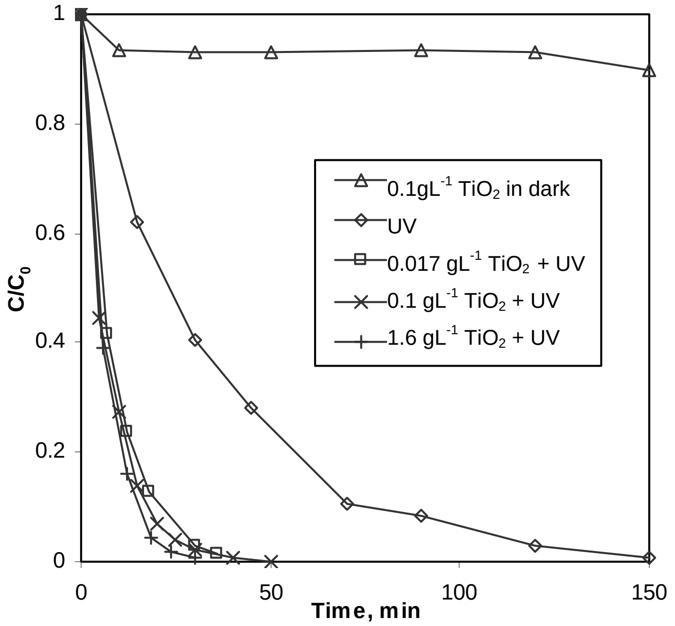

Figure 4A-4: Comparison of photodecay rate of o-ClA at various TiO_2 dosages. (Note: $[\text{o-ClA}]_0$ = 0.095 mM; no. of lamps = 8; wavelength =300 nm)

The o-ClA decay at different conditions was indicated in Figure 4A-4. A dark reaction with sole TiO_2 was also included for comparison. No obvious degradation in a dark TiO_2 system was observed, implying that an external light source is necessary to initiate the process. There was a loss of o-ClA of less than 10% solely due to adsorption on the TiO_2 surface, and no further adsorption was observed after 24 hours. The adsorption effect is regarded as minimal when compared with the TiO_2/UV system, which reached a rate of removal of above 90% within 30 minutes in most of our tests. It is therefore reasonable to believe that the photocatalytic process with TiO_2 is the dominant reaction pathway contributing to the removal of o-ClA.

Compared to the direct photolysis (i.e., in the absence of TiO_2), an improvement in the reaction rate of about three times was observed with the minimum addition of 0.017 gL^{-1} TiO_2. This increase in the reaction rate should be the result of the increase in activated oxidants in the system by the introduction of TiO_2 particles. More surface active sites are available for photon absorption, and therefore more $^{\bullet}OH$ and/or h^+_{VB} was generated in the system.

The study of dosage effect was extended in various TiO_2 and o-ClA concentrations and the corresponding o-ClA decay rates were summarized in Figure 4A-5.

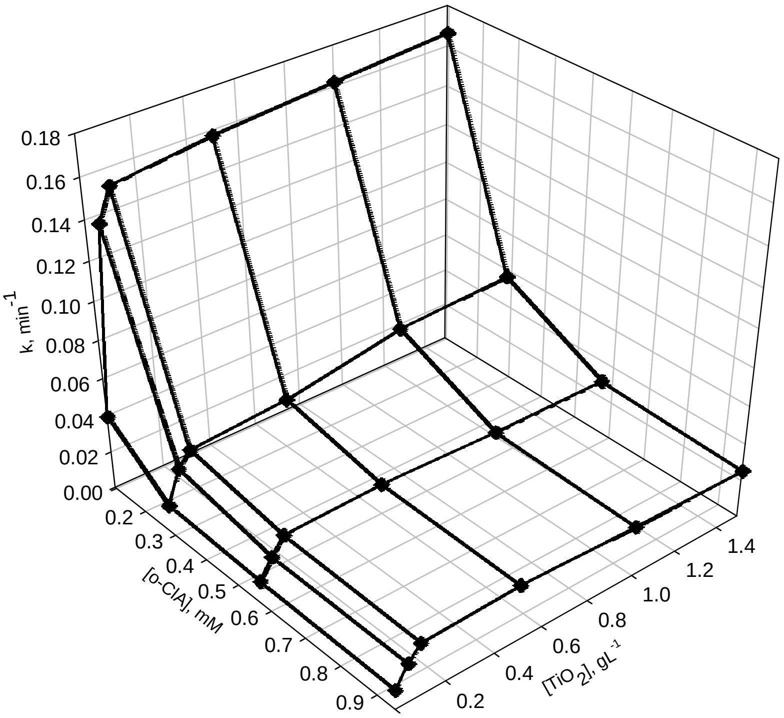

Figure 4A-5: Profile of first order rate constant at various o-ClA and TiO_2 dosages under irradiation at 300 nm.

All of the degradations follow the pseudo first-order decay with an r^2 of above 0.98. The photo-catalytic degradation of o-ClA was not a simple linear correlation with the [TiO_2] doses. At lower TiO_2 dosage, the pseudo first-order rate constants increased significantly (and linearly) with the increment of TiO_2 doses. As the TiO_2 doses increased above 0.1 gL^{-1}, however, another linear correlation was observed at a much lower rate of improvement, indicating that the process was gradually retarded. This is possibly due to the increase in the opacity of the solution with an excessive amount of TiO_2 in the reaction, causing a reduction in the penetration of light and a slowdown in further rate increments (Inel and Okte, 1996). Besides the dosage effect has extensively been discussed by Carp et al. (2004). They explained the surface of the solid photocatalyst is the main steps in the photocatalytic process and the adsorption capacity should be associated with the rate of reaction. Since the active sites are occupied at high organic concentration, a further increase of the concentration does not affect the actual catalyst surface concentration, and therefore, this may result in a decrease of the observed first-order rate constant. Secondly, the generation and migration of photogenerated electron-hole pairs and their reaction with organic compounds occur in series. Therefore, each step may become rate-determining for the overall process. At low concentrations, the later dominates the process and, therefore, the degradation rate increases linearly with concentration. However, at high concentrations, the former would become the governing step, and the degradation rate increases slowly with concentration, and for a given illumination intensity, even a constant degradation rate may be observed as a function of concentration. Also, they believed the generation of intermediates during the photocatalytic process also affect the rate constant of its parent compound. A higher initial concentration could yield a higher concentration of adsorbed intermediates, which affect the overall rate. To sum up, an unlimited increase in photocatalyst does not always guarantee a beneficial effect to the photoreaction. An optimum dose of photocatalyst is surely one of the critical design parameters for such a slurry system in any practical application.

4A.3.1 Langmuir–Hinshelwood (LH) kinetic

The photodecay of o-ClA ranging from 0.095 to 0.570 mM in the presence of 0.1 gL^{-1} TiO_2 under a 300 nm UV irradiation is shown in Figure 4A-6. For a 30-min illumination, it was observed that 96% of the o-ClA was removed as the initial [o-

ClA] was low (0.095 mM), while the performance was significantly reduced to about 50% as the initial [o-ClA] was increased to 0.570 mM. Generally speaking, a higher initial o-ClA yielded a lower removal rate under the same reaction conditions. The organic dependent phenomenon has been observed by Wei and Wan (1992) in the investigation of photodegradability of phenol. Mills et al. (1993) and Fox et al. (1990) have described pre-adsorption process by TiO_2 is feasible before the degradation proceeded. The adsorption is not limited to the target organics; Leng et al. (1992) have claimed that the photo-generated intermediates and OH^- are also the adsorbates onto TiO_2. At high initial o-ClA concentration, the amount of intermediates formed from the degradation is relatively high thereby reducing the number of available active sites on TiO_2 for adsorption of H_2O/OH^- and o-ClA, causing a decrease in the reaction rate constant of o-ClA itself.

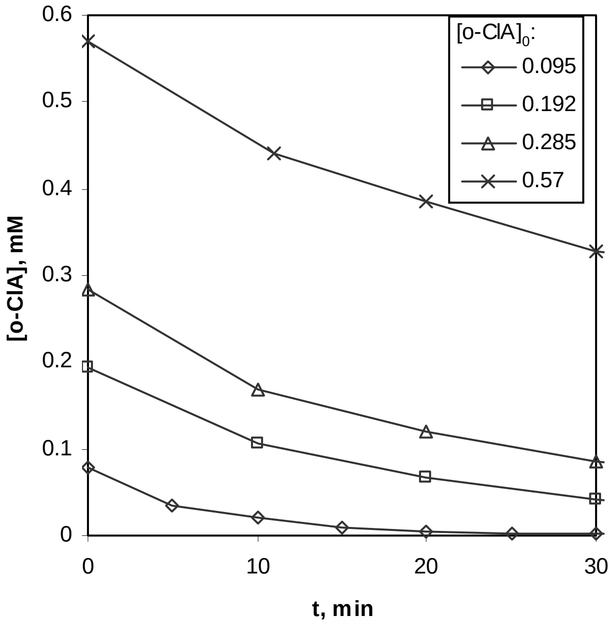

Figure 4A-6: Effect of o-ClA concentrations at fixed TiO_2 dosage (Note: $[TiO_2]$ = 0.1 gL^{-1}; initial pH = 7).

Since the conventional pseudo first-order method is not capable to incorporate the variation of [o-ClA]$_0$ concentrations to the corresponding rate constants, an alternative approach was used in this study for further analysis. The LH kinetic was used to quantitatively delineate substrate pre-adsorption in both solid-gas and solid-liquid reactions (Turchi and Ollis, 1990). It is also possible to use the LH kinetic in heterogeneous photocatalysis systems only when homogeneous reaction is assumed to be insignificant (Augugliaro et al. 2000; Fox and Dulay, 1993) The initial rate for the first 30-min, R (mM min^{-1}) can be expressed as:

$$R = -\frac{d[ClA]_0}{dt} = \frac{kK[ClA]_0}{1 + K[ClA]_0}, \qquad (4A\text{-}3)$$

where K is the equilibrium absorption constant of o-ClA on the surface (mM^{-1}) of the catalyst (i.e., TiO_2) and *k* represents the limiting reaction rate at maximum coverage (mM min^{-1}). In a pseudo first-order kinetic, the incorporation of –d[C]/dt = k_1[C] (Eqn. 3-1) into Eqn (4A-3) gives

$$k_1[ClA]_0 = \frac{kK[ClA]_0}{1 + K[ClA]_0}. \qquad (4A\text{-}4)$$

The above equation can be linearized by taking the reciprocal on both sides. After rearranging, the equation becomes

$$\frac{1}{k_1} = \frac{1}{k}[ClA]_0 + \frac{1}{kK}. \qquad (4A\text{-}5)$$

The plot of 1/k_1 versus [ClA]$_0$ resolves 1/*k* and 1/*k*K from the slope and intercept, respectively, and the results were shown in Figure 4A-7.

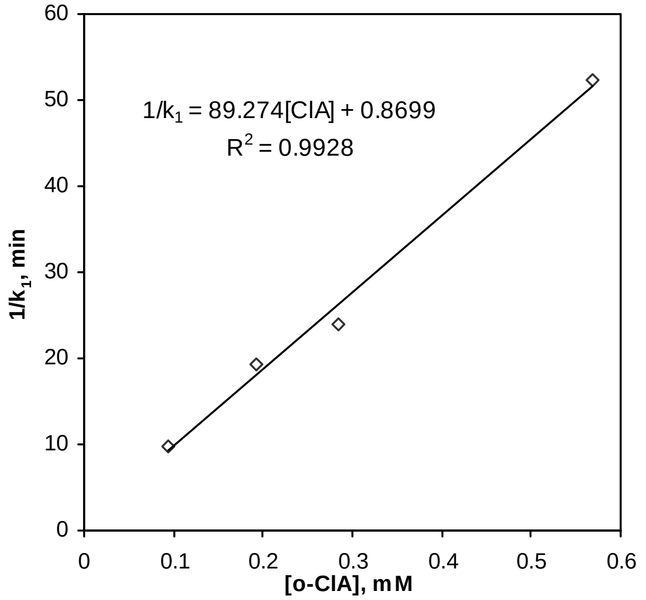

Figure 4A-7: A plot of LH model for o-ClA photodecay.

The degradation of o-ClA at different initial concentrations fits well to the LH model with a linear regression (r^2) of 0.993. The two constants, *k* and K, were calculated to be 0.0112 mM min^{-1} and 102.6 mM^{-1} from the slope and intercept, respectively. The good correlation reveals that the adsorption of o-ClA to the surface of TiO_2 is likely one of the major mechanisms governing the decay of o-ClA in such a photocatalytic process.

4A.4 Effect on solution pH

The pH levels of the solution could be another critical factor affecting the UV-catalytic process. A study of initial pH levels was therefore conducted at a range of 2 to 11, where the extension of the study to very low pH levels was due to the consideration of the possible effect of the pK_a of o-ClA. Winarno and Getoff (2002) have reported the pK_a of o-ClA was 2.6 (Eqn. 4A-6).

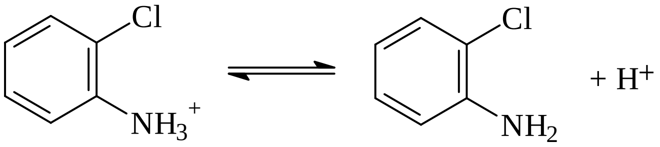

(4A-6)

The distribution of the two species could be calculated by the relationship of dissociation constant, K_a.

$$K_a = \frac{[H^+][C]}{[C^+]} \tag{4A-7}$$

Taking logarithm on both sides,

$$\log K_a = -\log[H^+] - \log[C] + \log[C^+] \tag{4A-8}$$

Since $-\log K_a = pK_a$, $-\log[H^+] = pH$ and o-ClA$^+$ could be expressed in terms of $[C_{tot}]$-[C], Eqn. 4A-8 could be rearranged into

$$pK_a - pH = \log\frac{[C_{tot}] - [C]}{[C]} \tag{4A-9}$$

The concentration of molecular o-ClA could be estimated by

$$[C] = \frac{C_{tot}}{(1 + 10^{pKa-pH})} \tag{4A-10}$$

According to the value of pK_a, the distribution of cationic and molecular form can be manipulated in Figure 4A-8.

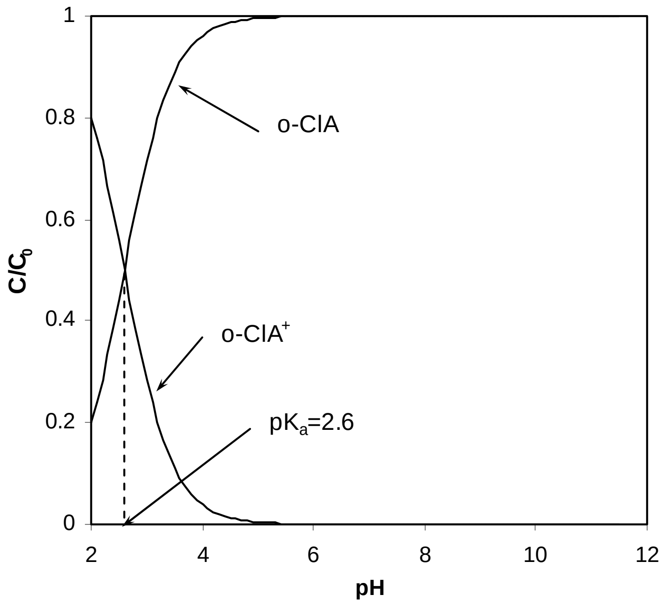

Figure 4A-8: The distribution of o-ClA speciations.

The 30-minute photodecay at various initial pH levels was plotted in Figure 4A-9. It is noted that the initial decay rates were found to increase generally from a low to a high pH, but the trend leveled off to about 0.1 min^{-1} when the pH was greater than 7.

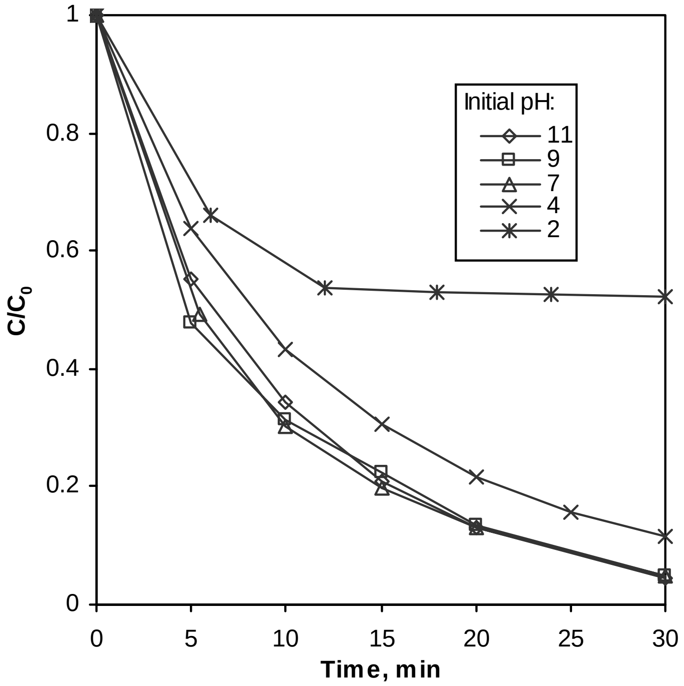

Figure 4A-9: Effect of initial pH on o-ClA photodecay (Notes: $[o\text{-ClA}]_0 = 0.095$ mM; $[TiO_2] = 0.1$ gL^{-1}).

All of the data followed the pseudo first-order reaction except the one at a very low pH level. At a pH level of 2, the slowest initial decay was observed and only 48% of the o-ClA was removed at the end of the reaction. This is compared to the situation at other pH levels, where a removal rate of more than 90% can be obtained. In fact, the decay was severely hindered and the reaction ceased after 10 minutes of illumination. This is likely due to the change in the molecular and particle structure of o-ClA and TiO_2, respectively, under high concentrations of proton, which would be discussed later in detail.

By comparing the initial reaction rates among various initial pH levels as shown in Figure 4A-10, the initial decay rates were generally found to increase from a low to a high pH, but to level off to about 0.1 min^{-1} when the pH became greater than 7.

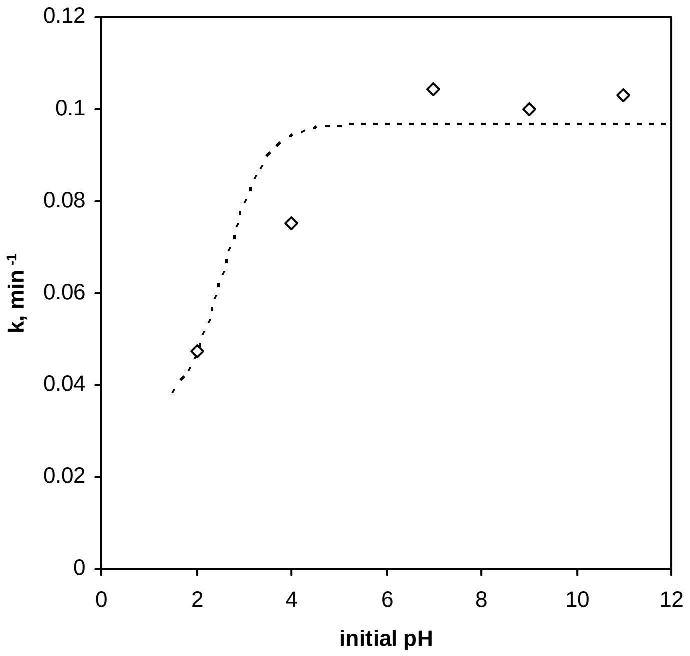

Figure 4A-10: A plot of first order decay rates at different initial pH levels (dashed line is the model curve).

This feature is likely due to the surface charge of TiO_2. Poulios and Tsachpinis (1999) have reported the point of the zero charge (pzc) of TiO_2 is reported to be pH 6.8, implying TiO_2 carries a positive charge below that value (in an acidic medium) while it is negatively charged above pH 6.8 (in alkaline). Positive charges on the surface (pH < 6.8) favor the migration of photo-produced electrons and suppress electron–hole recombination, but produce comparatively fewer oxygenate radicals. On the contrary, negative charges on the surface (pH > 6.8) enhance the transportation of holes to the surface, which react with OH^- and H_2O and generate $^\bullet OH$; hence, the rate of photo oxidation increases. The effect is magnified when pKa is taken into account in the process at an extremely acidic medium. Recall that the cationic o-ClA is dominant at pH 2 (about 80% are $[\text{o-ClA}]^+$, as shown in Figure 4A-7. The repulsive force is well established between the charged $[\text{o-ClA}]^+$ molecules and $[TiO_2]^+$ particles, which dramatically hinders the photodegradibility of the probe at extremely acidic conditions.

4A.4.1 Prediction model

Boreen et al. (2004) has suggested that the overall first-order rate constant (k_{tot}) could be contributed and calculated by the speciation (i.e., two components in our case) (Eqn. 4A-11)

$$(\chi_{C^+})(k_{C^+}) + (\chi_C)(k_C) = k_{tot} \qquad (4A\text{-}11)$$

where χ_{C^+}, χ_C are the fraction of the fully protonated (o-ClA^+) and neutral (o-ClA), respectively. For pH ranged from 2 to 11, Eqn. 4A-11 could be expanded into matrix form to solve the component values:

$$\begin{matrix} \text{pH11} \\ \\ \text{pH2} \end{matrix}\begin{pmatrix} \chi_{C^+} & \chi_C \\ \cdots & \cdots \end{pmatrix}\begin{pmatrix} k_{C^+} \\ k_C \end{pmatrix} = \begin{matrix} \text{pH11} \\ \\ \text{pH2} \end{matrix}\begin{pmatrix} k_{tot} \\ \cdots \end{pmatrix} \qquad (4A\text{-}12)$$

Eqn. 4A-12 is in the form of Aa = b. As the A and b are known, the components of (χ_{C^+}, χ_C) were determined using the least-square method by employing the pseudo-inverse of A showing in Eqn.4A-13:

$$a = (A^T A)^{-1} A^T b \qquad (4A\text{-}13)$$

By solving the above equation, $k_{[C^+]}$ and $k_{[C]}$ are determined to be 0.0338 and 0.0965 min^{-1}, respectively. The calculated values can be incorporated into the matrix form and the predicted k_{tot} at different pHs is illustrated as dashed line in Figure 4A-10. The curve fits well to the experimental data and the prediction of rate constants corresponding to the two species have provided information on their reactivity involving in the photoreaction. Judging from the results, the decay rate by molecular species is found to be about 3 times faster than that of cationic species. Being dominated by large amount of cationic species at lower pH levels, this explained the slower degradation obtained at acidic conditions. The higher degradation rate was quite stable at higher pH which is obviously due to the existence of 100% molecular o-ClA in the solution, thus the species effect becomes independent to the pH.

4B Effect of Additional Oxidants in UV/TiO_2 System

4B.1 Comparison among selected oxidants

According to the above study, limitations of UV/TiO_2 reaction have been observed such that the quantity of $^{\bullet}OH$ radicals cannot increase infinitely in UV/TiO_2 system as over-dosing of TiO_2 would scatter the light in the solution. To further improve the degradation efficiency, searching for better oxidants to increase the generation of radicals or to optimize the photo-oxidation process. In this part, the photo-oxidizing capability of three selected oxidants has been focused. The photodegradation performances of hydrogen peroxide (H_2O_2), rose bengal (RB) and oxyhalogens (IO_3^-) were depicted in Figure 4B-1.

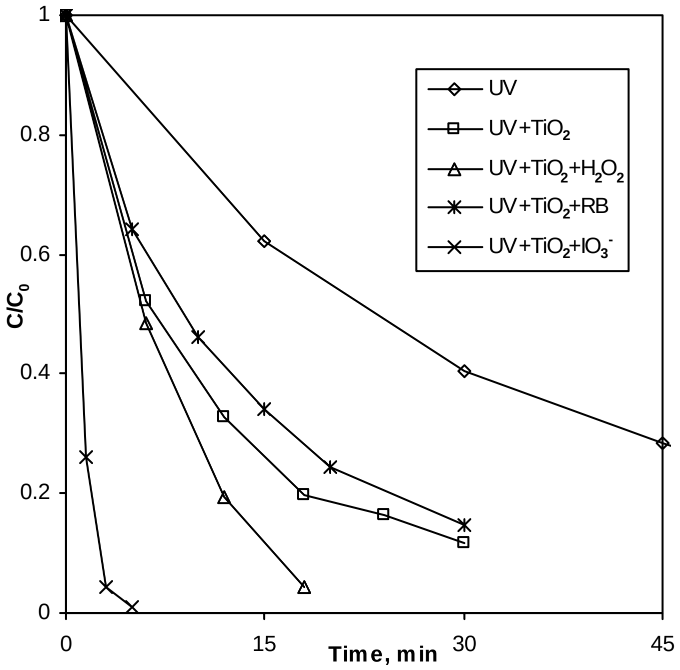

Figure 4B-1: Decay of o-ClA at various conditions (Notes: [o-ClA]$_0$ = 0.095 mM; [TiO_2] = 0.1 gL^{-1}; [H_2O_2] =10 mM; [IO_3^-] = 0.195 mM; [RB] = 0.5 mgL^{-1}; initial pH = 7).

With the applied wavelength at 300 nm and 0.1 gL^{-1} TiO_2 in the system, additional H_2O_2 and IO_3^- could assist the photodegradation efficiently. Moreover, the use of IO_3^- obviously caused a much faster decay of o-ClA than H_2O_2 although optimum H_2O_2 (10 mM) has already shown in the plot. Researchers have proven the deferment of the charge recombination rate is the major advantage of oxidant in UV/TiO_2 system (Schindler and Kunst, 1990). However, the use of RB gave different results. It could not speed up the process, but retard the reaction of o-ClA decay. The effects of each oxidant to the degradation of o-ClA have been discussed in the following sections.

4B.2 Effect of H_2O_2

4B.2.1 Dosage of H_2O_2

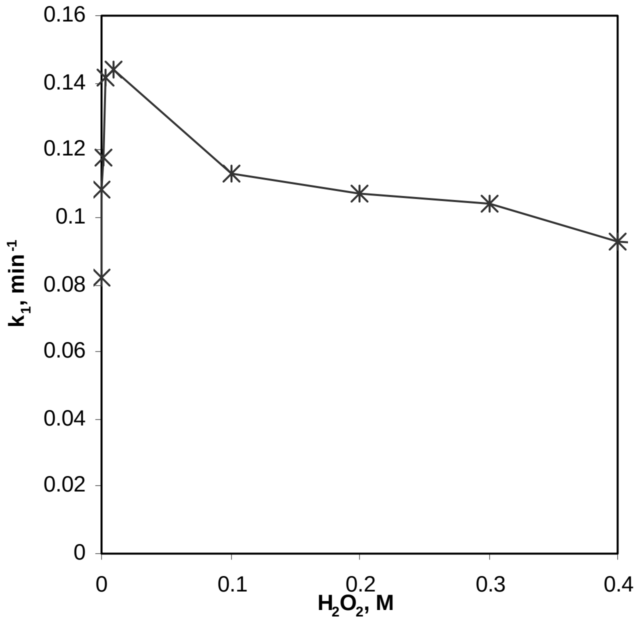

Figure 4B-2: Reaction rates of o-ClA at various H_2O_2 dosages at fixed UV/TiO_2 system. (Notes: $[o\text{-}ClA]_0$ = 0.095 mM; $[TiO_2]$ = 0.1 gL^{-1}; initial pH = 7)

The degradation rate of o-ClA tends to increase at low dosages of H_2O_2 and a maximum enhancement of 1.8 times was observed at 10 mM in Figure 4B-2. Gao et al., (2002) have suggested that the enhancement is mainly brought by the additional free radicals generated from the cleavage of O-O bond of photoexcited H_2O_2. Also, being an electron acceptor, H_2O_2 has a higher activity and efficiency in this role than oxygen for the titania-excited electrons. This would reduce the chances of an electron-holes recombination, which is an undesirable process in the photocatalytic process. In addition, the presence of oxygen in the water (i.e., dissolved oxygen) may induce the formation of H_2O_2 and subsequently give rise to $^{\bullet}OH$ concentration. Therefore, the addition of H_2O_2 may shorten the sub-reactions and accelerate the process directly. Eqns. 4B-1 to 4 show the formation of $^{\bullet}OH$, of which Eqns. 4B-3 to 4 represent both generated and additional H_2O_2 (San et al., 2001).

$$e^{-}{}_{CB} + O_2 \rightarrow {}^{\bullet}O_2{}^{-} \tag{4B-1}$$

$$^{\bullet}O_2{}^{-} + 2H^{+} + e^{-} \rightarrow H_2O_2 \tag{4B-2}$$

$$H_2O_2 + h\upsilon \rightarrow 2{}^{\bullet}OH \tag{4B-3}$$

$$H_2O_2 + e_{CB}{}^{-} \rightarrow {}^{\bullet}OH + OH^{-} \tag{4B-4}$$

However, the further addition of H_2O_2 (above 10 mM) to the solution inhibits the reaction rate. As the [H_2O_2] dose was increased gradually, retardation of the process was observed simultaneously. The pseudo first-order decay constant of o-ClA at 0.4 M H_2O_2 drops back to almost the same level as that of sole UV/TiO_2 system. This is because the H_2O_2 presenting in excess amount could consume the valuable $^{\bullet}OH$ (like a scavenger) that previously formed in the solution and subsequently generate less-reactive $HO_2^{\bullet}$. Similar results were described by Wong and Chu (2003) in Eqns. 4B-5 to 7:

$$H_2O_2 + {}^{\bullet}OH \rightarrow HO_2^{\bullet} + H_2O \qquad (4B\text{-}5)$$

$$HO_2^{\bullet} + {}^{\bullet}OH \rightarrow H_2O + O_2 \qquad (4B\text{-}6)$$

$$H_2O_2 + 2h^{+}{}_{VB} \rightarrow HO_2^{\bullet} + 2H^{+} \qquad (4B\text{-}7)$$

In addition, Zhang et al. (1998) have revealed that H_2O_2 may react with the photogenerated holes at elevated dosages, which partly contributes to the rate retardation at higher [H_2O_2] levels.

4B.2.2 Change of solution pHs

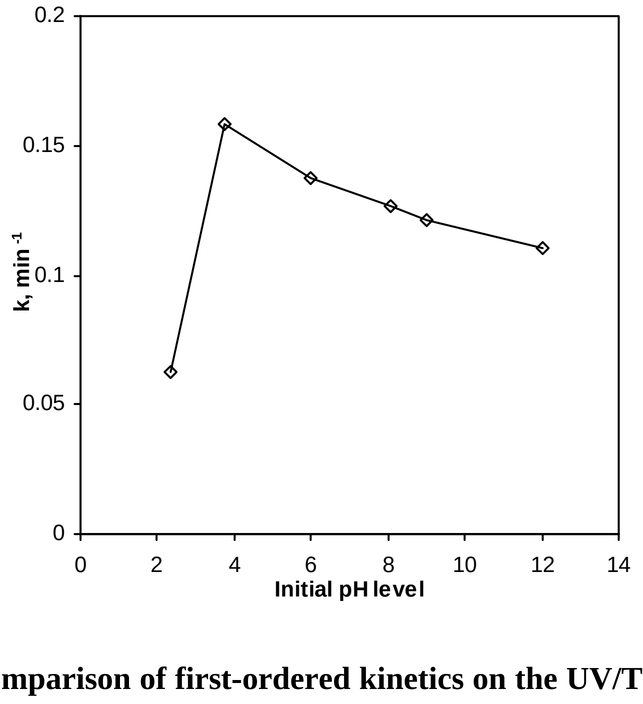

Figure 4B-3: Comparison of first-ordered kinetics on the UV/TiO_2/H_2O_2 system (Notes: [o-ClA]$_0$ = 0.095 mM; [TiO_2]= 0.1 gL^{-1}; [H_2O_2] = 0.01mM; [RB] = 0.5 mgL^{-1}).

The pH effect in UV/TiO_2/H_2O_2 system was studied. The dosage of TiO_2 and H_2O_2 were fixed at 0.1 gL^{-1} and 0.01 mM, respectively. Recall the pH effect of UV/TiO_2 process in 4A.4, photodecay rate generally increased from low to high pH. It was interesting to note that this pattern has been changed after incorporating H_2O_2 to the UV/TiO_2.

The highest decay rate was observed at about pH 4 in Figure 4B-3, while increase of pH further lower the degradation rates. The lowest photodecay rate in UV/TiO_2/H_2O_2 process was found again at extremely low pH level around 2 due to the surface charge of TiO_2 and o-ClA discussed in 4A.4. The reason for lower performance of the UV/TiO_2/H_2O_2 at higher pH levels is likely because the special property of H_2O_2. In alkaline medium, the H_2O_2 becomes highly unstable and self-decomposition of H_2O_2 occurs, which is strongly dependent on pH (Chan et al., 2004). The self-decomposition could rapidly breakdown the H_2O_2 molecules into water and oxygen (Eqn. 4B-8) and makes the molecule losses its characteristics as oxidant and most importantly the source of $^{\bullet}OH$.

$$2H_2O_2 \rightarrow H_2O + O_2 \qquad (4B\text{-}8)$$

The reaction rate of o-ClA in UV/TiO_2/H_2O_2 process was therefore reduced significantly at higher pH levels.

4B.3 Effect of Rose Bengal (RB)

4B.3.1 Dosage of RB

Rose Bengal (RB) is one of the most popular anionic sensitizers used in water solutions. Wilkinson et al. (1993) have pointed out its excited triplet state is efficiently quenched by oxygen showing a high quantum yield of singlet oxygen formation. However, it was unusual to see the occurrence of rate retardation as the dose of [RB] was increased, as shown in Figure 4B-4.

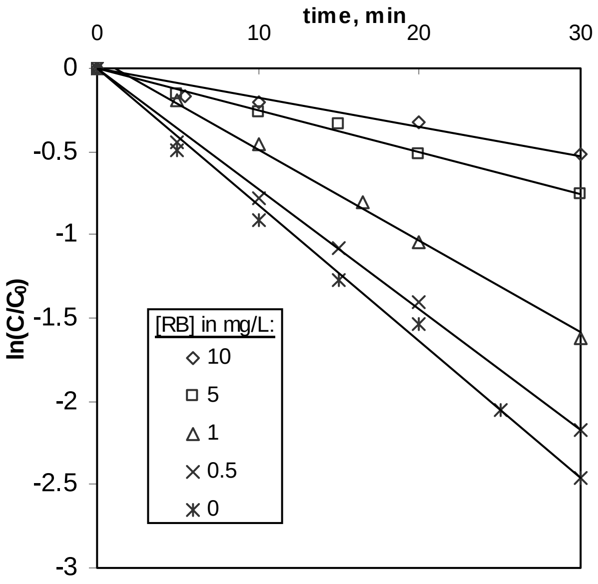

Figure 4B-4: The first-order decay of o-ClA in UV/TiO_2/RB (Notes: $[o\text{-}ClA]_0$ = 0.095 mM; $[TiO_2]$ = 0.1 gL^{-1}; initial pH = 7).

For example, with 10 mg L^{-1} RB in the UV/TiO_2 solution, the reaction was reduced by about 4.7 times compared to the situation in the absence of an RB sensitizer. This was partly due to the poor light absorption character of RB in the solution. The UV absorptivity of RB is high at 450-550 nm and below 270 nm (Appendix IV), while the sensitivity of absorbance was quite low at 300 nm. The proposed singlet oxygen production by RB was possibly suppressed under the light with 300 nm, which significantly reduced the sensitization ability. Unfortunately, the 300 nm is the best wavelength for UV/TiO_2 applications. In addition, the decrease in the number of TiO_2 active sites could retard the degradation process as well. RB, being an organic sensitizer, can become a competitor with o-ClA for free radicals and for the active site on the TiO_2 surface (which reduces the adsorption probability of the probe compound onto the TiO_2 surface). Therefore, it is believed that both the low sensitivity of RB at 300 nm and the competition for the active site are the dominant mechanisms to inhibit the photocatalytic process.

4B.4 Effect of oxyahlogens

4B.4.1 UV/oxyhalogens

The potential to use oxyhalogens in improving the sole UV process for o-ClA decay was investigated. The selected oxyhalogens, XO_3^- (X = Cl, Br and I) exhibited negligible dark reaction (i.e. not exposed to UV) at our tested concentrations. The decay of o-ClA by the photo-oxidation in the assist of oxyhalogens was presented in Figure 4B-5.

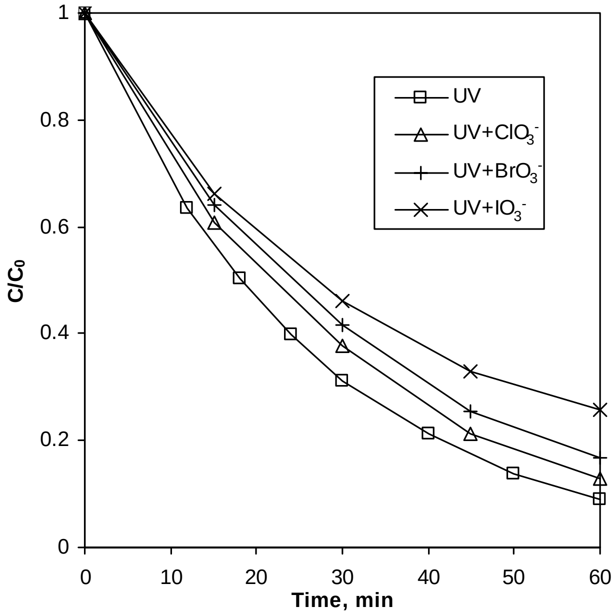

Figure 4B-5: Photodegradation of o-ClA at different oxyhalogens (Notes: [o-ClA]$_0$ = 0.095 mM; [XO_3^-] = 0.195 mM; initial pH = 7).

Different from UV/H_2O_2 discussed by (Wong and Chu, 2003), the addition of oxyhalogens surprisingly showed no enhancement to the process at all; instead the processes are slightly retarded comparing to that of sole UV. This is likely due to the light attenuation effect.

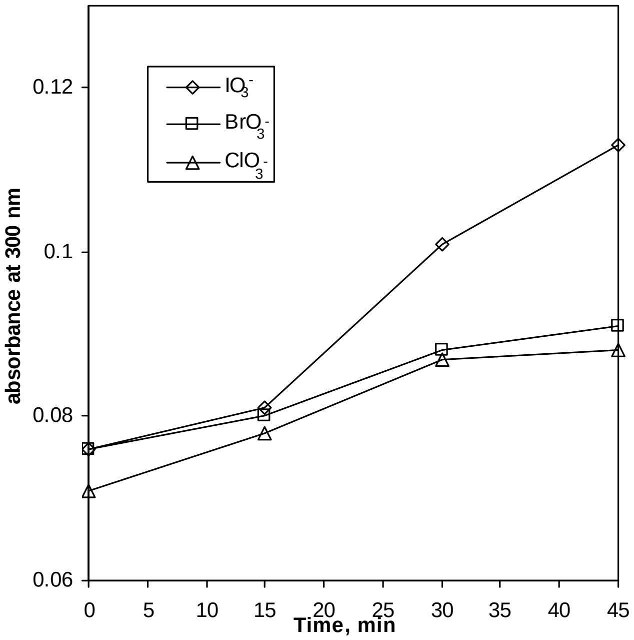

Figure 4B-6: Change of absorbance at 300 nm in the presence of oxyhalogens during photoreaction.

The change of absorbance at our selected wavelength 300 nm was given in Figure 4B-6, where an increasing absorption was recorded during reaction when same amount of oxyhalogens were introduced in the solution. During the photoreaction, photo-absorptive species were generated from either degradation of o-ClA (intermediates) or the reduction of XO_3^-. Weaver et al. (1997) have pointed out that IO_3^- could undergo subsequent reduction steps in the presence of UV light. As a result, available photons were reduced for o-ClA degradation and thus the observed decay rate was decreased. In addition, the absorbance increment was ranked from IO_3^- (highest), BrO_3^-, to ClO_3^- (lowest), which agreed with the descending retardation effect in Figure 4B-5.

4B.4.2 UV/TiO_2/oxyhalogen

Because a negative effect was found when oxyhalogen is used with UV exclusively, the use of oxyhalogens in photocatalytic process as an alternative was examined via the UV/TiO_2/oxyhalogens process.

Totally different from the UV/oxyhalogens system; the use of oxyhalogens can significantly improve the o-ClA decay in the UV/TiO_2/oxyhalogens process as indicated by the pseudo first-order decay curves in Figure 4B-7.

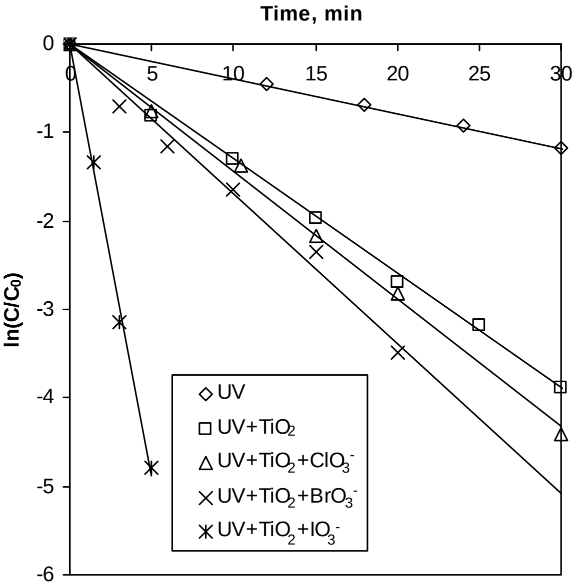

Figure 4B-7: Pseudo first-order reaction of o-ClA in UV/TiO_2/oxyhalogens (Notes: $[o\text{-}ClA]_0$ = 0.095 mM; $[TiO_2]$ = 0.1 gL^{-1}; initial pH = 7).

Faster decay of o-ClA was observed for any oxyhalogen addition in the order of IO_3^- > BrO_3^- > ClO_3^-. In addition, as noted in Figure 4B-7, the performance of IO_3^- is exceptionally fast. With the use of 0.195 mM IO_3^- in the solution, 0.095 mM of o-ClA could be disappeared within 7 minutes from the LC analysis.

The rate improvement is likely resulted several reasons. Firstly, the involvement of oxyhalogen may defer the recombination of e^- and h_{VB}^+ through the capture of electrons ejected from TiO_2 surface. The number of available h_{VB}^+ in solution is therefore increased and their longer lifetime would be beneficial to the degradation of the organics. The electrons abstraction ability is believed to be contributed by the polarization effect on the inorganic anion (oxyhalogen) itself. With one halogen atom holding three oxygen atoms at one side, this structure induces a high polarity in the molecule and creates a high electropositive environment nearby the halogen atom, which induces a strong attraction for electrons. Moreover, the polarizing difference could also account for the difference of degradation rate with different halogen atoms. The degradation of o-ClA was found in the order of IO_3^- > BrO_3^- > ClO_3^-. The electronegativity is decreased down the periodic table from Cl to Br than I. The chloride atom, being the strongest electronegative species among the three, would yield the lowest oxidizing efficiency in the reaction. On the contrary, the less electronegative halogen (i.e., the iodide atom) is a stronger electron scavenger which could achieve a faster degradation through the increase of h_{VB}^+ and the generation of $^{\bullet}OH$ in the system.

Secondly, the atomic radius of the halogens could also be another influencing factor. All the selected halogens held by the same numbers of oxygen atom, the smallest atomic radius of Cl is less accessible (or more hindrance) by the counter components in the solution comparing to that of Br and I. Therefore, the interaction or the ability to trap electrons on TiO_2 surface would be significantly decreased.

Finally, other than the nonselective $^{\bullet}OH$ that reacts with o-ClA and its reaction intermediates, additional reactive radical species (e.g. $IO^{\bullet}_3$) that generated during the application of oxyhalogens (San et al., 2001; Wang and Hong, 1999) could offer extra pathways to improve the degradation of o-ClA.

4B.4.3 Dosage effect of IO_3^- in UV/TiO_2

Different dosages of IO_3^- were used together with the UV/TiO_2 process and the results of o-ClA decay were illustrated in Figure 4B-8.

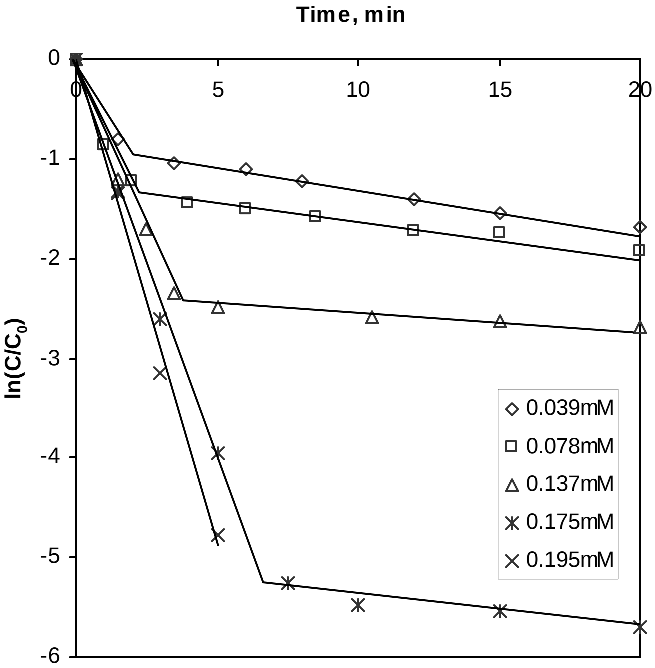

Figure 4B-8: Pseudo first-order decay of o-ClA at different IO_3^- dosages in UV/TiO_2 system (Notes: $[o\text{-}ClA]_0 = 0.095$ mM; $[TiO_2] = 0.1$ gL^{-1}; initial pH = 7).

It is clear to see that the pseudo first-order decay rate could be generally divided into two stages except the one at the highest IO_3^- dosage. The decay is started by a fast initial decay and then followed by a much slower retardation stage. A break point is clearly observed to separate the two stages, where the time to reach the break point is shorter when the applied $[IO_3^-]$ decreased. The second (or retardation) stage could be vanished providing $[IO_3^-]$ is adequate (0.195 mM in this case) in the solution, in which the o-ClA was fully degraded before the second stage can be observed or initiated. In general, the higher the initial $[IO_3^-]_0$ in the solution, the higher the first stage decay rate (k_1), but it is surprisingly to see that the decay rate of second stage (k_2) was slightly decreased with the amount of $[IO_3^-]_0$ applied. At the beginning of the process, all the reaction pathways involving the UV/TiO_2/IO_3^-, sole UV, and UV/TiO_2 are available, which results in a faster initial stage. As IO_3^- would gradually be consumed in the solution, photocatalytic reaction (UV/TiO_2) and sole UV become the remaining pathways for the further decay of o-ClA (retardation stage). In the first stage, higher the $[IO_3^-]_0$ gives a higher k_1 and a longer time to reach the break point, which results in a lower remaining [o-ClA] and higher levels of intermediates in solution. Under these circumstances, the k_2 of o-ClA decay in second stage is slightly lowered because the probability for remaining o-ClA molecules to react (or collide) with the active reagent (e.g. free radicals) is reduced due to its lower concentration and the competition form higher level of intermediates.

Unlike the conventional oxidant H_2O_2, the use of higher dosages of $[IO_3^-]$ does not cause a negative result (i.e. overdosed effect) to the decay of o-ClA (the 100% disappearance of o-ClA could be achieved in less than a minute when UV/TiO_2

system contained 0.78 mM of IO_3^-), while the lower dose of IO_3^- makes the process reach the slower second stage quickly.

4B.4.4 Predication model of IO_3^- dosage in UV/TiO_2 system

From the design point of view, to select a reasonable IO_3^- dosage and to determine a proper retention time for the second stage is necessary to ensure a cost-effective process. A mathematical model is therefore proposed and derived for the prediction of o-ClA decay in UV/TiO_2 system at different IO_3^- dosages.

From the data presenting in Figure 4B-8, higher IO_3^- dosage would generally postpone the commencement of second stage. It is obvious that the time of phase change is dependent on the amount of IO_3^- used in the process. Therefore, the time of break point, t′ (in min), at a given iodate concentration, $[IO_3^-]$ (in mM), could be expressed in a linear form (see also Figure 4B-9) as:

$$1/t' = -2.692[IO_3^-] + 0.622 \qquad (4B\text{-}8)$$

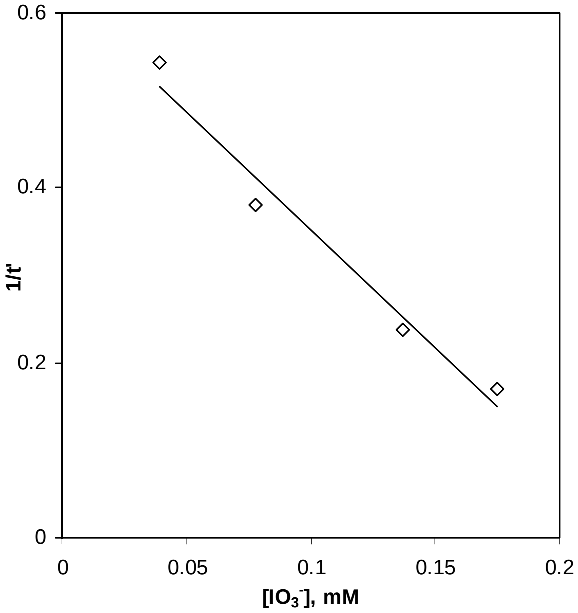

Figure 4B-9: A plot of 1/t' against [IO$_3^-$].

Mathematically, we can find two boundary points at 0 and 0.231 mM for the applicable range of [IO$_3^-$] concentration as indicated in Eqn. 4B-8, but the physical meanings of these two points are lot more interesting: when [IO$_3^-$] is at very low concentration (i.e. approaching zero), the second stage would be initiated at a time no earlier than 1.6 min; when [IO$_3^-$] is higher or equal to 0.231 mM, the second stage is vanished, and all the o-ClA could be degraded within the first stage.

During the reaction, as the reaction time t is shorter than the time of break point calculated from Eqn. 4B-8 (i.e., $t \le t'$), the pseudo first-order kinetic constants of the first stage (k_1) of reaction could be correlated to [IO$_3^-$] concentration by:

$$k_1 = 2.791[IO_3^-] + 0.3338 \qquad (4B\text{-}9)$$

A good correlation was indicated in the plot of Figure 4B-10.

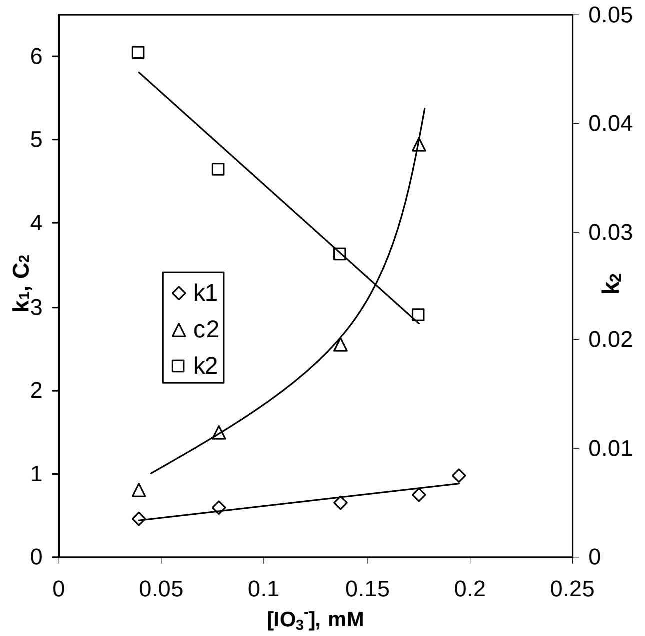

Figure 4B-10: A plot of k_1, k_2 and c_2 against $[IO_3^-]$.

Because there is no decay of o-ClA in dark reaction (i.e., $C/C_0 = 1$ at t=0), the first stage of o-ClA decay in the presence of $UV/TiO_2/IO_3^-$ could be predicted by:

$$\frac{C}{C_0} = \exp(-2.791[IO_3^-] + 0.3338)t \qquad (4B\text{-}10)$$

When the reaction time is longer than the time of break point (i.e., $t > t'$), on the other hand, the second stage of reaction rate (k_2, min^{-1}) and their relevant intercepts (c_2) are also analyzed in Figure 4B-10. Taking the reciprocal of c_2, a high correlation greater than 0.9 was obtained in Figure 4B-11.

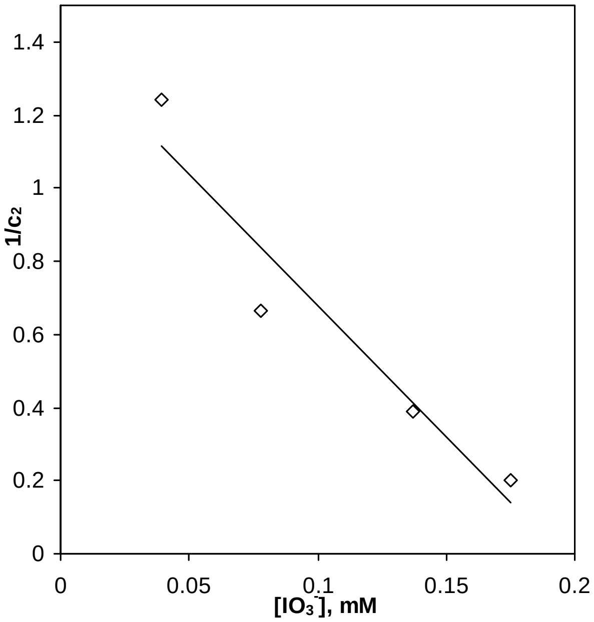

Figure 4B-11: A plot of $1/c_2$ against $[IO_3^-]$.

In the form of equations, they are expressed in:

$$k_2 = -0.171[IO_3^-] + 0.051 \tag{4B-11}$$

$$1/c_2 = -7.178[IO_3^-] + 1.395 \tag{4B-12}$$

Combining Eqns. 4B-11 and 4B-12, the second stage of o-ClA could be estimated in terms of reaction time t (min) and $[IO_3^-]$ (mM):

$$\frac{C}{C_0} = \exp[(0.171t - 7.178)[IO_3^-] + (0.051t - 1.395)] \tag{4B-13}$$

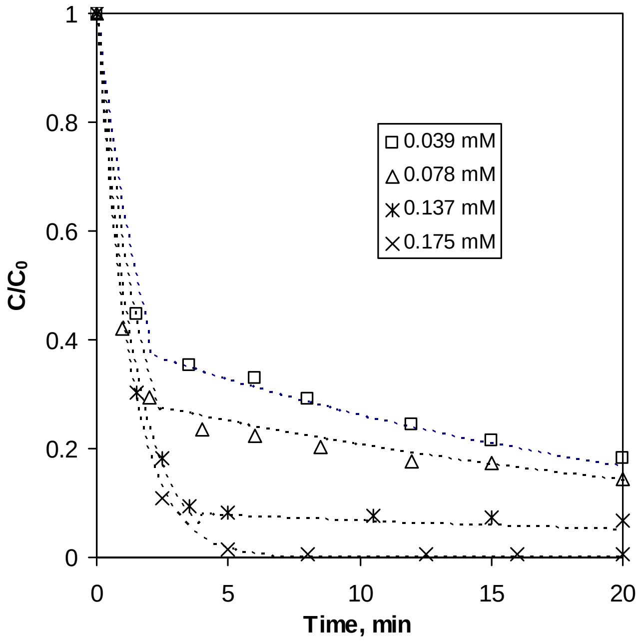

Figure 4B-12: Comparison of modeling and experimental data at different [IO_3^-] dosages (dashed lines are generated from the model).

After incorporating the original data and modeled data into Figure 4B-12, the modeled curves fit quite well to the real data, indicating this approach provides an efficient method to have a quick prediction of o-ClA decay in UV/TiO_2 with various IO_3^- dosages.

4B.4.5 Effect on initial pH in UV/TiO_2/IO_3^-

From Figure 4B-13, it is observed that the presence of IO_3^- in UV/TiO_2 system is also a pH dependent process. At relative lower pH, the degradation of o-ClA was generally found to be faster. It was also observed that a two-stage decay was established: an instantaneous and fast initial decay followed by a slower second stage. The two-stage kinetics was however vanished in alkaline condition (i.e., pH 9 and 11) in which the initial decay rate was obviously slower in this range. The application of IO_3^- in the UV/TiO_2 dose not only delays the charge recombination process of TiO_2, it could also assist the oxidation of organics in the presence of UV light generating distinct iodide radical species.

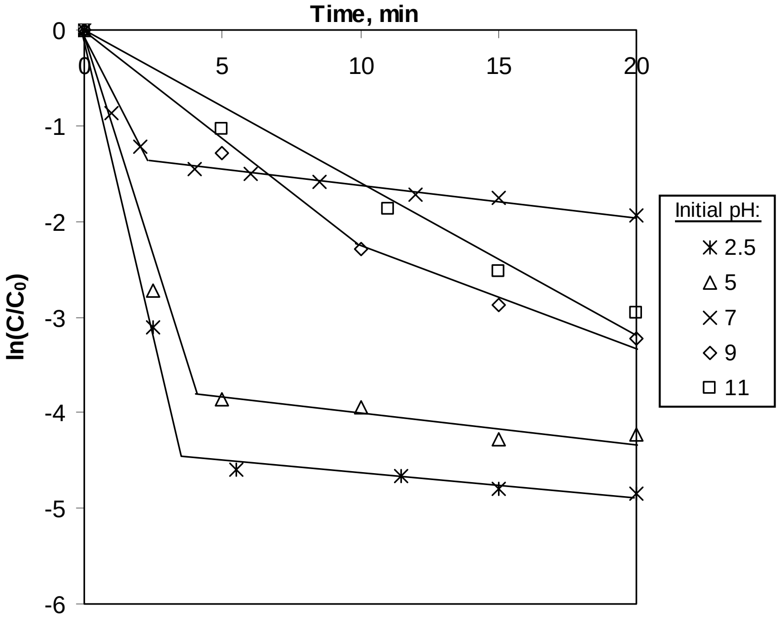

Figure 4B-13: Effect of initial pH in UV/TiO_2/IO_3^-. (Note: [o-ClA] = 0.095 mM; [TiO_2] = 0.1 g/L; [IO_3^-] = 0.078 mM)

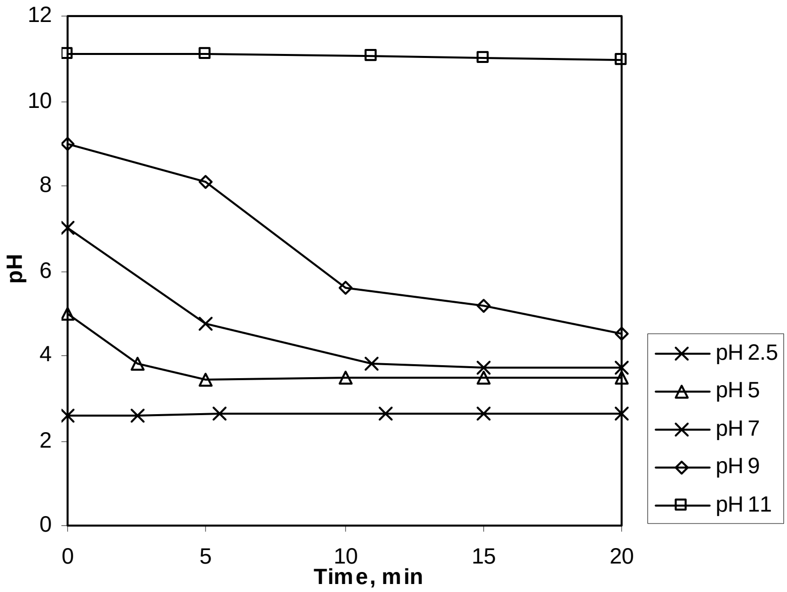

Figure 4B-14: Change of pH during photodegradation. (Note: $[o\text{-ClA}]_0 = 0.095$ mM; $[TiO_2] = 0.1$ g/L; $[IO_3^-] = 0.078$ mM)

Cotton et al. (1995) have suggested the overall reaction of iodate reduction yielding iodide as the end product (Eqn. 4B-14).

$$IO_3^- + 6H^+ + 6e^- \rightleftharpoons [IO_2^-, HOI] \rightleftharpoons I^- + 3H_2O \qquad (4B\text{-}14)$$

The equation explained the faster degradation at lower pH. Since a surge of H^+ available in acidic solution favors the forward reaction, the reduction of IO_3^- is thus vigorous and is more powerful to oxidize organics. When IO_3^- has been used up or is deficient to remove all the o-ClA in the system, a much slower second stage becomes dominant. On the contrary, the OH^- at high pH has significantly slowed down the reduction of IO_3^- by neutralizing the limited H^+ in the solution. The change of pH during the reaction was also recorded in Figure 4B-14, where a drop of pH is generally observed. Except the highest pH at 11, the profiles of pH were all dropped below 7 (acidic). Referring to initial pH at 9 in Figure 4B-13, the degradation showed a transition character between pseudo first-order and two-stage kinetics due to the transformation of solution pH from alkaline to acidic condition. Besides, the generation of intermediates species or radicals reduced from IO_3^- could also affect the degradation rate of o-ClA. Mezyk and Elliot (1994) suggested that the radical species generated was very much depends on the presence of ions at different solution pHs. In acidic solution, $IO^{\bullet}{}_3^{2-}$ was formed as the primary species from the presence of IO_3^- and the excited e- by TiO_2. Large amount of H^+ at low pH can then react with $IO^{\bullet}{}_3^{2-}$ giving $HOIO^{\bullet}{}_2^-$ as described in Eqns. 4B-15 to 16:

$$IO_3^- + e^- \rightarrow IO^{\bullet}{}_3^{2-} \qquad (4B\text{-}15)$$

$$IO^{\bullet}{}_3^{2-} + H^+ \rightleftharpoons HOIO^{\bullet}{}_2^- \qquad (4B\text{-}16)$$

Nevertheless, the relative slower reaction at high pH could arise from the consumption of powerful hydroxyl radicals to the formation of less reactive species. The reduction of IO_3^- would process differently via Eqns. 4B-17 to 18):

$${}^{\bullet}OH + OH^- \rightleftharpoons O^{\bullet -} + H_2O \qquad (4B\text{-}17)$$

$$O^{\bullet -} - + IO_{3-} \rightarrow IO^{\bullet}{}_4^{2-} \qquad (4B\text{-}18)$$

As the generation of different radicals could affect the rate of degradation, this effect was further verified by the change of dosages at extreme solution pH (2.5 and 11) in this study. The usage of iodate at pH 2.5 has enhanced the degradation significantly as indicated in Figure 4B-15. More than 99% of o-ClA could be removed within 3 mins of reaction. Yet, the effect of iodate dosage is very limited at pH 11, where the increase of iodate for 5 times (from 0.039 mM to 0.195 mM) only resulted in an improvement of 10%. Judging from the different radical species with the dosage effect of iodate, the reactivity of $HOIO^{\bullet}{}_2^-$ generated at lower pH is verified to be more powerful than that of $IO^{\bullet}{}_4^{2-}$ at high pH.

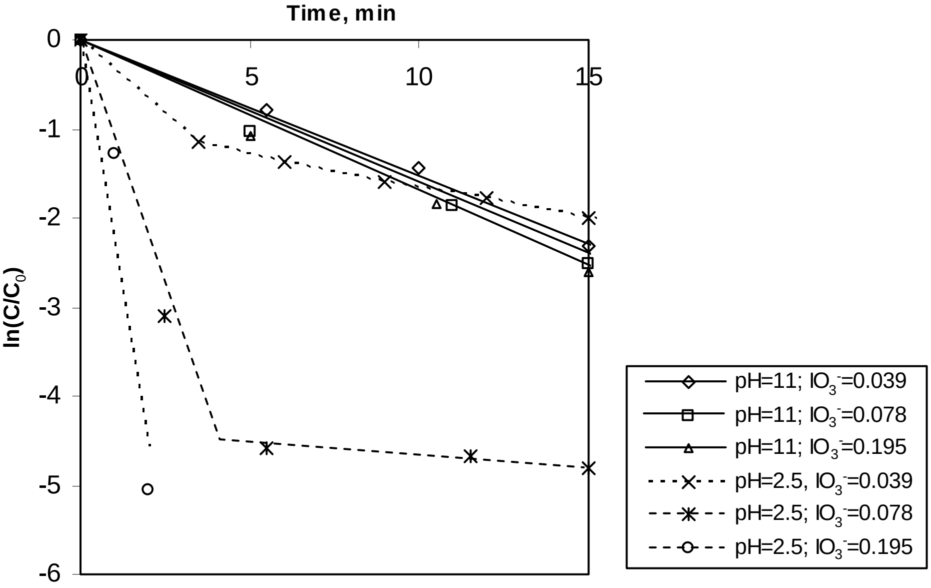

Figure 4B-15: The first order decay of o-ClA in UV/TiO$_2$/IO$_3^-$ at selected pH and IO$_3^-$ dosages.

4B.4.6 Second IO_3^- dosing

In previous section, it has proven that IO_3^- is a very powerful oxidant when working with UV/TiO$_2$. In the meantime, the measurement of IO_3^-, showing in the photoproduct study (Figure 4C-3b), has indicated the consumption was extremely fast. Within 5 min of reaction time, about 96% of IO_3^- was utilized in the solution. Therefore, the possibility of second IO_3^- dosing was proposed to improve the process performance. Solution of o-ClA containing 0.1 gL^{-1} of TiO$_2$ and 0.158 mM of IO_3^- was mixed and was irradiated at the same condition as indicated before. An additional 0.158 mM of IO_3^- was dosed at pre-selected time intervals to the solution. The performance of o-ClA by second iodate dose was depicted in Figure 4B-16.

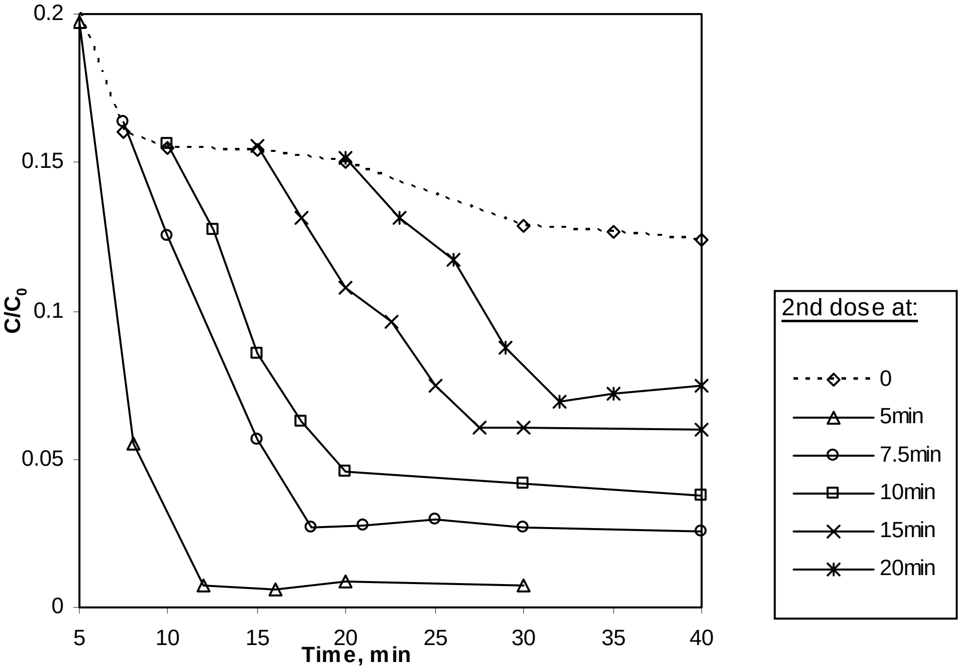

Figure 4B-16: Effect of second iodate dosing. (Note: Each dose of IO_3^- was controlled at 0.156 mM; [o-ClA]$_0$ = 0.285 mM; solution pH = 7; [TiO_2] = 0.1 gL^{-1})

With the inclusion of single IO_3^- dose, it can be compared that the overall o-ClA removal was enhanced by the second IO_3^- dose. Fast degradation of o-ClA could be observed at the beginning of second dosing, but the decay was slow down at a later stage. In addition, it was observed that the removal efficiency of o-ClA depended on the time of second dosing: the earlier the second dosing, the faster and higher the degradation. When the second dose was applied at 20 min, additional 11% of o-ClA was removed in 11 min, while 19% more of o-ClA was removed in 7 min when the dosing time was shorten to 5 min. Such observation is possibly attributed to the intermediates effect. In the presence of IO_3^- in the UV/TiO_2 system, the fast initial decay of o-ClA has led to formation of intermediates. The increase amount of intermediates would compete for further decay with the o-ClA resides in the solution implying the chance to oxidize o-ClA is thus reduced. The monitoring of its organic intermediates has been reported in 4C.2.

4C The Study of Photoproducts

4C.1 UV/TiO_2

4C.1.1 Organic intermediates

The investigation of degraded intermediates is valuable to verify the photochemical process does not generate more toxic substances in the effluent. In order to identify the degradation products, the initial concentration of o-ClA was increased to the level of 10^{-3} M. The extract of the solvent after reaction was analyzed by GC/MS. In the UV/TiO_2 process, two major intermediates (2-chlorophenol and 1,4-benzoquinone) were identified and their peak areas were compared with the original standards. Their profiles in the process were displayed with the decay of o-ClA in Figure 4C-1. About 80% of o-ClA was quickly disappeared in 120 mins of reaction time, but such an effective rate was retarded afterward likely due to the competition of active sites between o-ClA and intermediates on the TiO_2 surface (Irmak et al., 2004).

As observed in Figure 4C-1, 2-chlorophenol (CP) at about 10^{-5} mM was generated as the primary product reaching its maximum at 60 mins of reaction time. When it is gradually decayed, the secondary intermediate, 1,4-benzoquinone (BQ), was formed. The amount of BQ was about an order less than that of CP, and its degradation was also observed after 420 mins. The level of intermediates detected was far less than that of o-ClA applied implying the organic intermediates could undergo further decay and would not accumulate in the system.

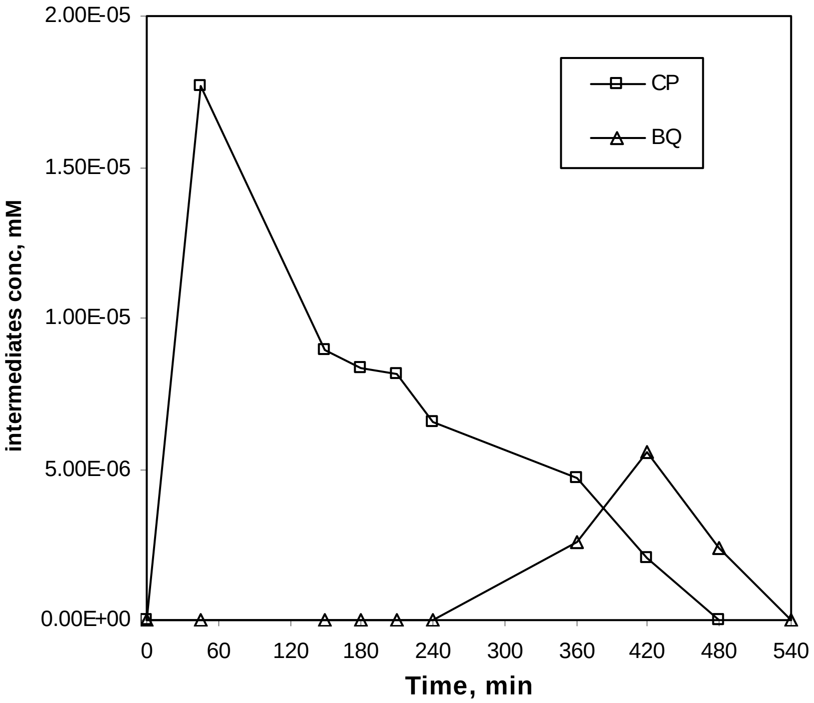

Figure 4C-1: The generation of o-ClA intermediates in the UV/TiO$_2$ process (Note: [o-ClA]$_0$ = 0.95 mM; [TiO$_2$] = 0.1 gL^{-1}; initial pH = 7).

4C.1.2 End-products

The identification of fast decayed intermediates has already proven UV/TiO$_2$ process is successful to convert o-ClA to low level organics in aqueous phase. An increase of ionic products was quantified during the mineralization process, simultaneously. The accumulation profiles of chloride, nitrite and ammonium ions were also recorded in Figure 4C-2.

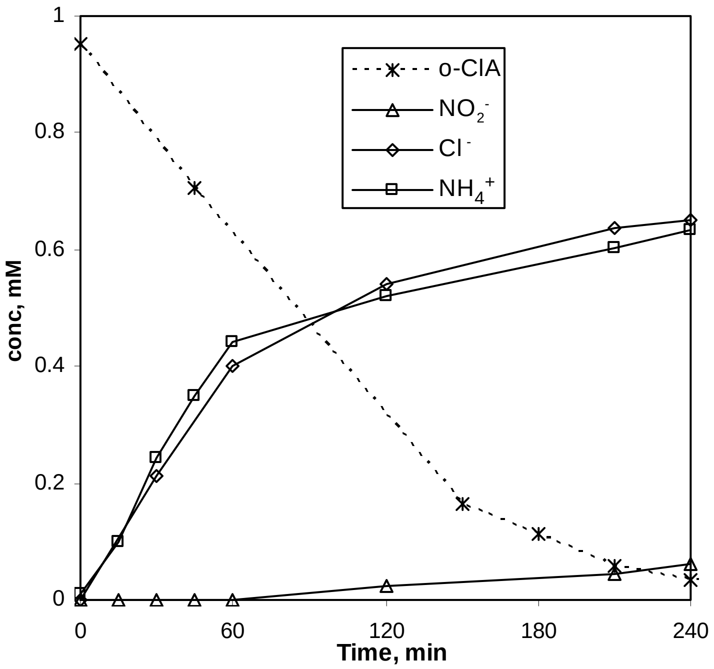

Figure 4C-2: Profile of ionic products.

At the initial stage of reaction, chloride and ammonium ions were detected and their levels kept increasing during the reaction. From the results of intermediate formation/decay as discussed previously, the generation of chloride ion is due to the •OH attack onto o-ClA. Similar observation was also reported by Winarno and Getoff (2002b). In addition, the formation of NH_4^+ and/or NH_3 is a pH dependent process as in the following (Eqn. 4C-1).

$$NH_3 + H_2O \rightleftharpoons NH_4^+ + OH^- \qquad (4C-1)$$

Since the pK_a of the above equation was reported as 9.24 (Hem, 1985), inadequate OH^- in low pH solution would favor the formation of ammonium ion. In our experimental condition, because the initial pH was set at 7 and it dropped gradually to 3.7 after 540 min of reaction. NH_4^+ is thus the dominate species in the solution. Meanwhile, very low level of nitrite (about 1/10 of NH_4^+) was identified at a later stage of the process. According to Stumm and Morgan (1996), ammonium ion can eventually be oxidized to nitrate (via the nitrite) in an oxidizing environment (Eqns. 4C-2 and 3).

$$NH_4^+ + 1.5\ O_2 \rightleftharpoons NO_2^- + H_2O + 2\ H^+ \qquad (4C\text{-}2)$$

$$NO_2^- + 0.5\ O_2 \rightleftharpoons NO_3^- \qquad (4C\text{-}3)$$

4C.1.3 Mineralization

Besides, the change of TOC is a good indicator of mineralization for the overall organic contents including parent and daughter compounds. Percentage of TOC in the solution was calculated and compared with the decay of o-ClA as shown in Figure 4C-3.

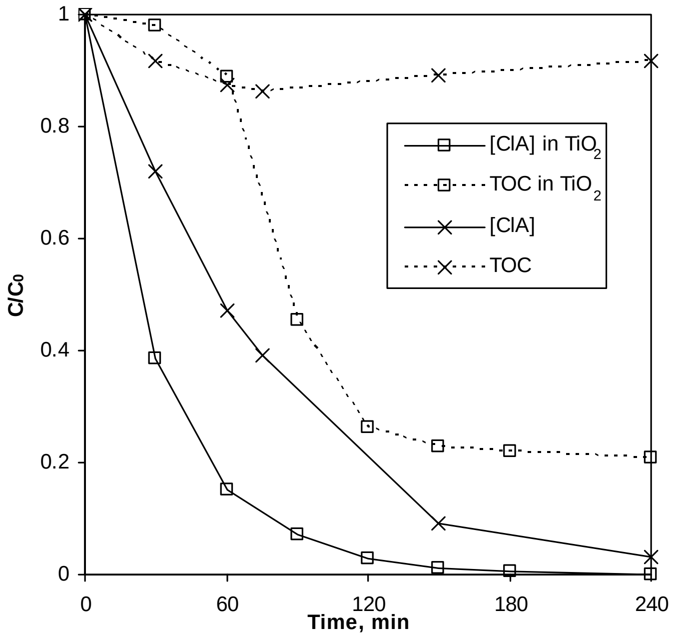

Figure 4C-3: Decay of o-ClA and change of TOC in UV/TiO_2 system (Notes: [o-ClA]$_0$ = 0.95 mM, TiO_2 was dosed at 0.1 gL^{-1}).

In sole UV process, the direct photolysis cannot remove TOC effectively, about 85% of TOC remain intact even though 95% of o-ClA was degraded after 240 min of reaction. In the presence of TiO_2, however, a concurrent removal of TOC along with o-ClA was observed in the solution. At the end of reaction (240 min), o-ClA was completely removed while only 20% of TOC was remained. Winarno and Getoff (2002b) have reported photodecay of o-ClA are able to be converted into non-toxic carbon dioxide, chloride ion, nitrate ion, etc followed by subsequent photoreaction (Augugliaro et al., 2000). The high removal of TOC is obviously due to the addition of TiO_2 that provide adequate $^\bullet OH$ for the conversion of intermediates. Because the TOC curve is leveled off even at an extended reaction time, the residual TOC is likely arising from the accumulation of non-oxidiziable intermediates in the solution. The tailing effect of TOC has proven to be the final products involved the breaking of C-C bonds and decarboxylation of intermediates such as maleic, acetic, oxalic or formic acid by further reaction with $^\bullet OH$ (Santos et al., 2002). Each bond breaking is accompanied by the formation of an acid with shorter chain and a CO_2 molecule.

4C.2 UV/TiO_2/IO_3^-

4C.2.1 Organic intermediates

Several organic intermediates degraded from o-ClA were identified in the UV/TiO_2/IO_3^- process. The profiles of six organic intermediates as shown in Figure 4C-4a matched with the NIST library. As indicated in Figure 4C-4b, the decay of o-ClA was quite fast in the first 10 min leading to the formation of intermediates at the early stage of the photoreaction.

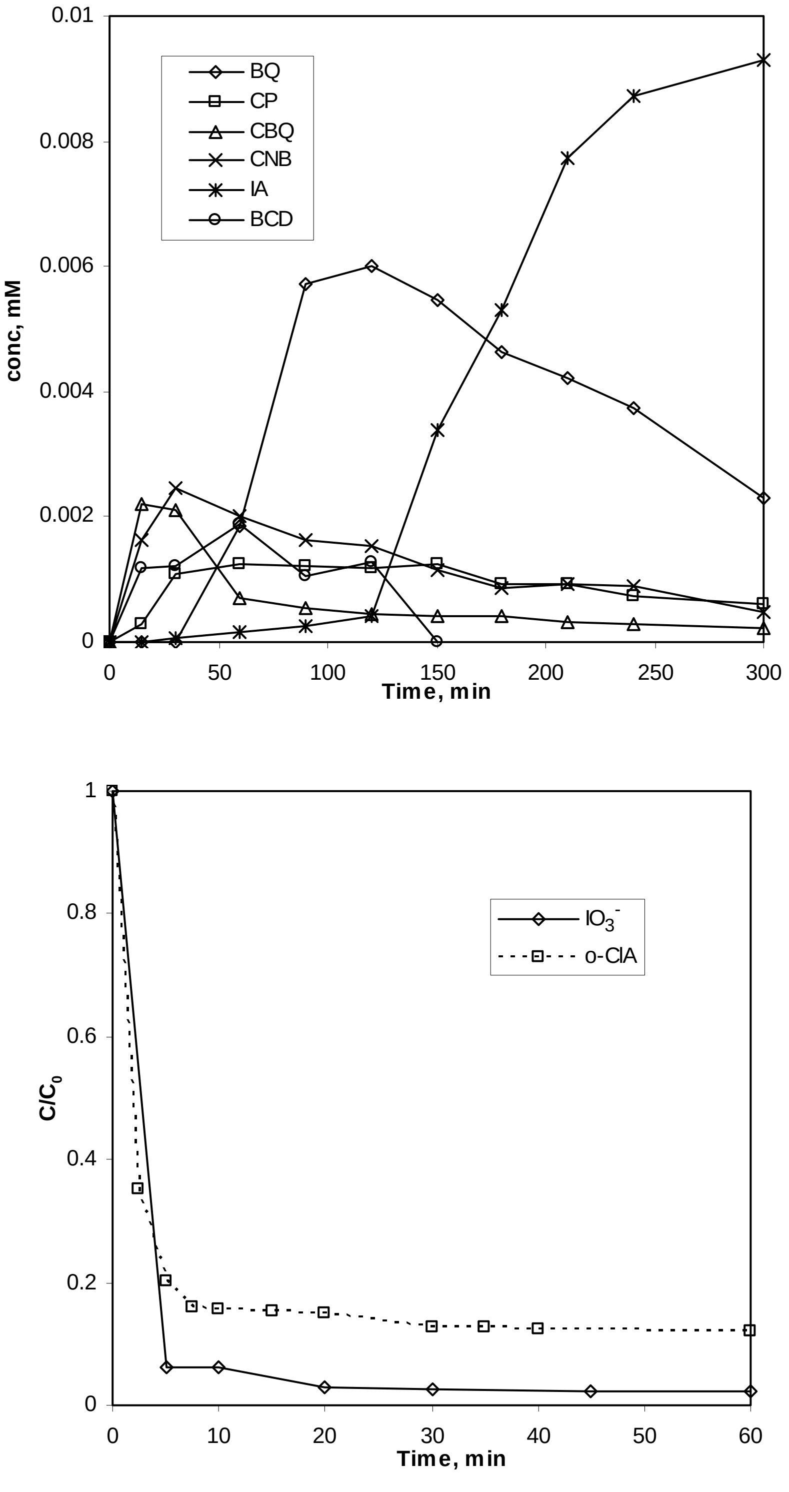

Figure 4C-4: (a) The intermediates profiles of UV/TiO_2/IO_3^-. (b) The consumption of IO_3^- and the o-ClA decay. (Note: [o-ClA] = 0.95 mM; [TiO_2] = 0.1 gL^{-1}; [IO_3^-] = 0.78 mM; initial pH = 7; irradiation time = 300 min)

Nevertheless, their increasing trend was maintained shortly and declined gradually. After 15 min of reaction time, four organic intermediates, 2-chlorophenol (CP), 2-chloronitrobenzene (CNB), 2-chloro-1,4-benzoquinone (CBQ) and bis(2-chlorophenyl)-diazene (BCD) were identified at low detection levels. For example, the CNB showed the highest level with a maximum at 0.0025 mM, which was only about 1/380 times of the original probe compound. Beside the CNB, other intermediates also presented at only ppb levels. It is reasonable that the concentration of intermediates was lower than the initial o-ClA level as they were degraded from the same source. Because the decay of o-ClA was fast, the exceptional low level and low accumulation of intermediates was due to the fast decay of themselves in the process and led to a fast mineralization. Side product 2-iodoaniline (IA) and a typical oxidative product 1,4-benzoquinone (BQ) were also identified at the later time of reaction. Among all the identified intermediates, IA was the only component that kept increasing in the process indicating a longer reaction time was required. In view of this, the photodegradation of IA was carried out separately in UV/TiO_2 (without using IO_3^- to minimize the interference).

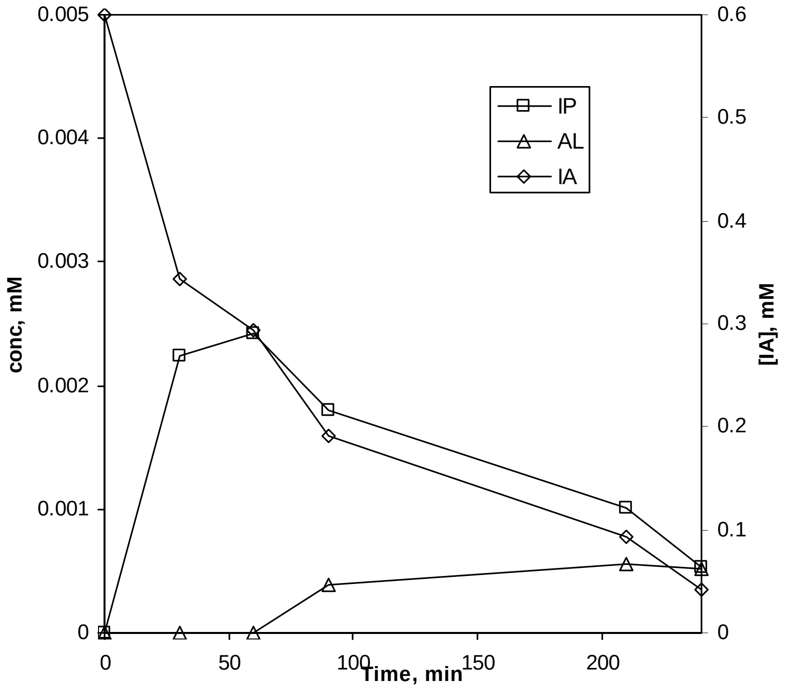

Figure 4C-5: Photodegradation of iodoaniline in UV/TiO$_2$ system. (Note: [IA] = 0.93 mM; [TiO$_2$] = 0.1 gL^{-1}; initial pH = 7)

As shown in Figure 4C-5, the decay of IA could be observed and about 92% of IA disappeared in 240 min. In addition, two organic compounds, 2-iodophenol (IP) and aniline (AL), were detected by the GC/MS analysis. To incorporating the profile of intermediates into Figure 4C-5, their levels were also found very low comparing with the initial [IA], where IP was found decreasing within the reaction time. Although the decay of aniline was not observed in this study, its degradation and mineralization were reported by Kumar and Mathur (2004) and Sauleda and Brillas (2001), respectively.

4C.2.2 Intermediates from second IO_3^- dosing

The second dose of IO_3^- at 5 and 20 min were selected for the intermediate examination. The o-ClA decay can be referred to Figure 4B-16 (symbols of Δ and *) while the examination of four selected intermediates were illustrated in Figures 4C-6.

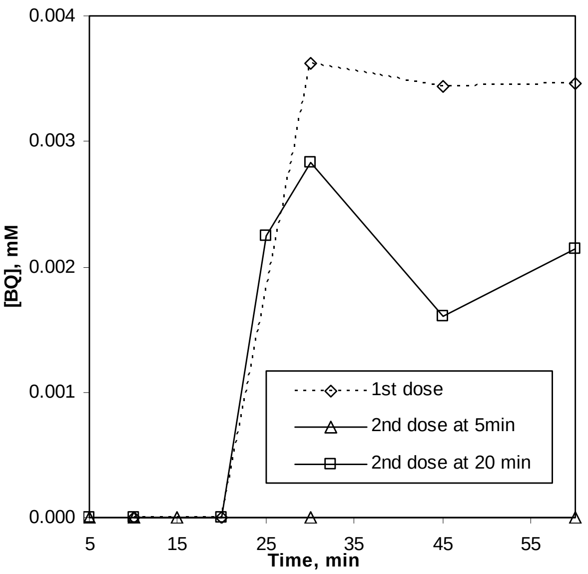

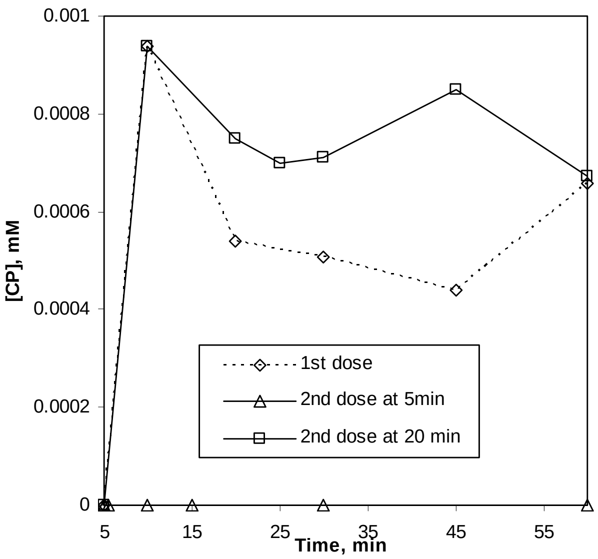

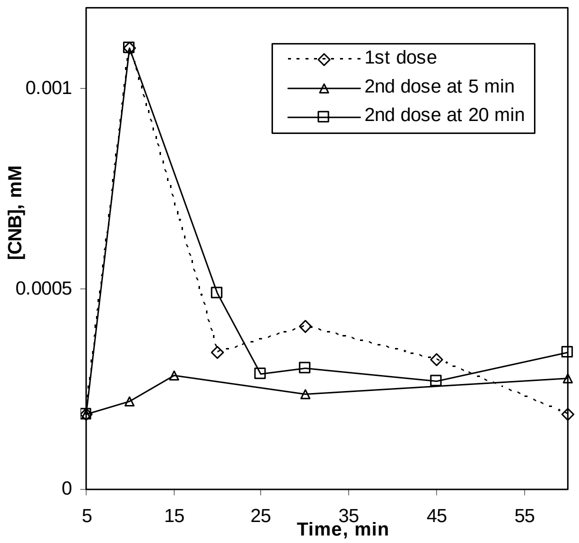

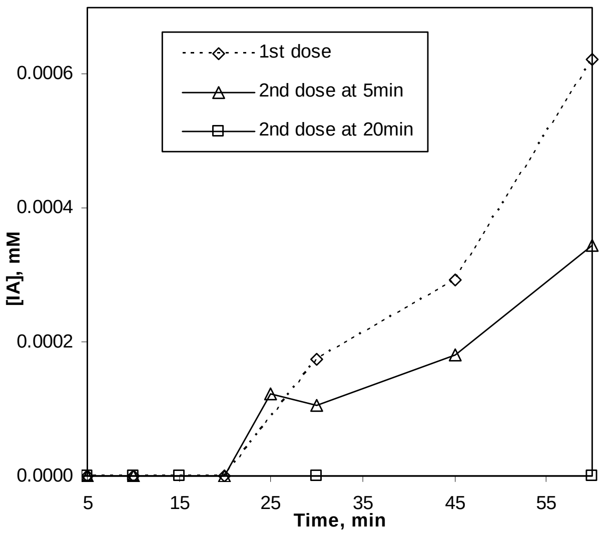

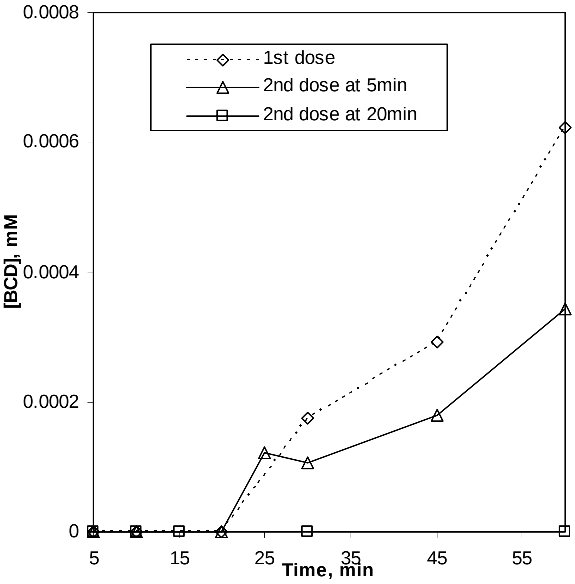

Figure 4C-6: Generation of intermediates at second iodate dosing. (a) 1,4-benzoqunione (BQ); (b) 2-chlorophenol (CP); (c) chloronitrobenzene (CNB); (d) 2-iodoaniline and (e) bis(2-chlorophenyl)-diazene (BCD).

During an 1-hr reaction, it was generally observed that the profile of intermediates was found to be similar between the single dose and the second dose at 20 min while the second dose at 5 min has given quite a different performance. In a shorter dosing interval, several major intermediates in UV/TiO_2/IO_3^- including BQ, CP and IA were not detected in all the samples while CNB and BCD were barely identified in relatively lower level than the other runs. To ensure a higher percentage removal of o-ClA and intermediates, successive dosing is encouraged at shorter time interval. The IO_3^- profile of second dosing has been monitored in Figure 4C-7.

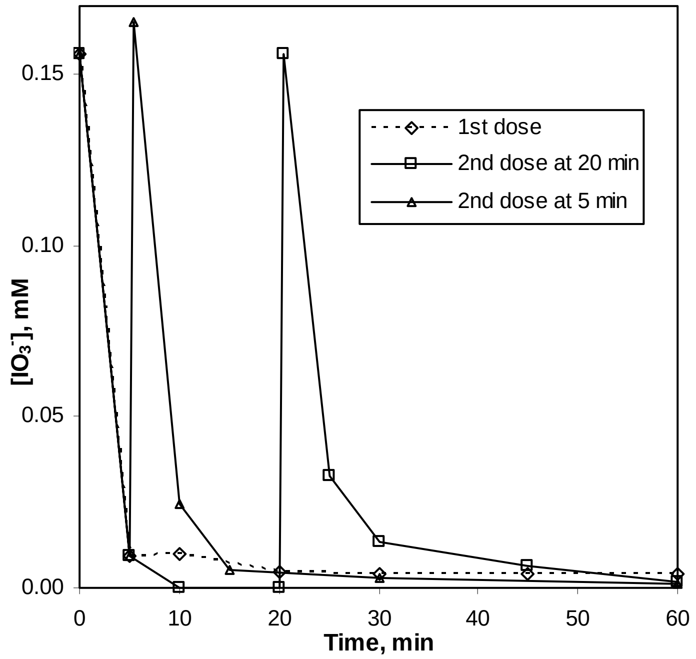

Figure 4C-7: Profile of iodate at second dosing.

When $[IO_3^-]$ was dropped to about 0.01 mM within 5 minutes' time, the second dosing could boost-up the system to ensure the source of oxidant was adequate for organic destruction. However it was surprised to note the second dose at 20 min did not significantly reduce the o-ClA and the generation of CP was even higher than the single dosing.

Weaver et al. (1997) have outlined the reduction pathway of IO_3^- under the UV illumination. During the process, it would generate other radical species such as $IO^{\bullet}_2$ and $HIO^{\bullet}_3{}^-$, yielding I^- as the end-product. Enhancing the photodecay is straightforward by the extra radicals, but the effect of I^- should not be overlooked. Ohtaki et al. (2000) have reported an inhibiting degradation in UV/TiO_2 process when halide ions existed in the system. The gradual increment of $[I^-]$ can significantly deteriorated the photodegradation. As indicated in Figure 4C-8, the slowest degradation was found in the solution containing iodide. The UV/TiO_2 was retarded by 25% when 0.15 mM iodide was added. It can be assumed that the generation of I^- as the reductive products of IO_3^- has functioned as a radical scavenger in the system. Such an effect is minimal at shorter time interval as large amount of radical species were still participating in the organic oxidation. However, after a longer reaction time, the accumulated I^- was dominant over the IO_3^- and the radical concentrations ($IO^{\bullet}_2$ and $HIO^{\bullet}{}_3^-$) which significantly retard the o-ClA decay even the source of IO_3^- was refilled.

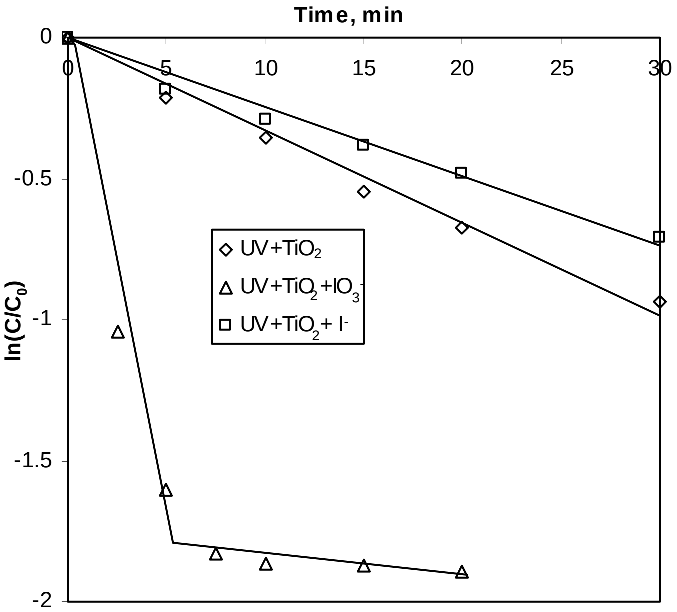

Figure 4C-8: Effect of iodide ion on the photodegradation of o-ClA. (Note: [o-ClA]$_0$ = 0.95 mM; [TiO_2] = 0.1 gL^{-1}; [IO_3^-] = 0.156 mM; [I^-] = 0.15 mM)

4C.2.3 Mechanistic Pathway

Based on the identification of intermediates as above, the degradation pathway of o-ClA was proposed in Figure 4C-9.

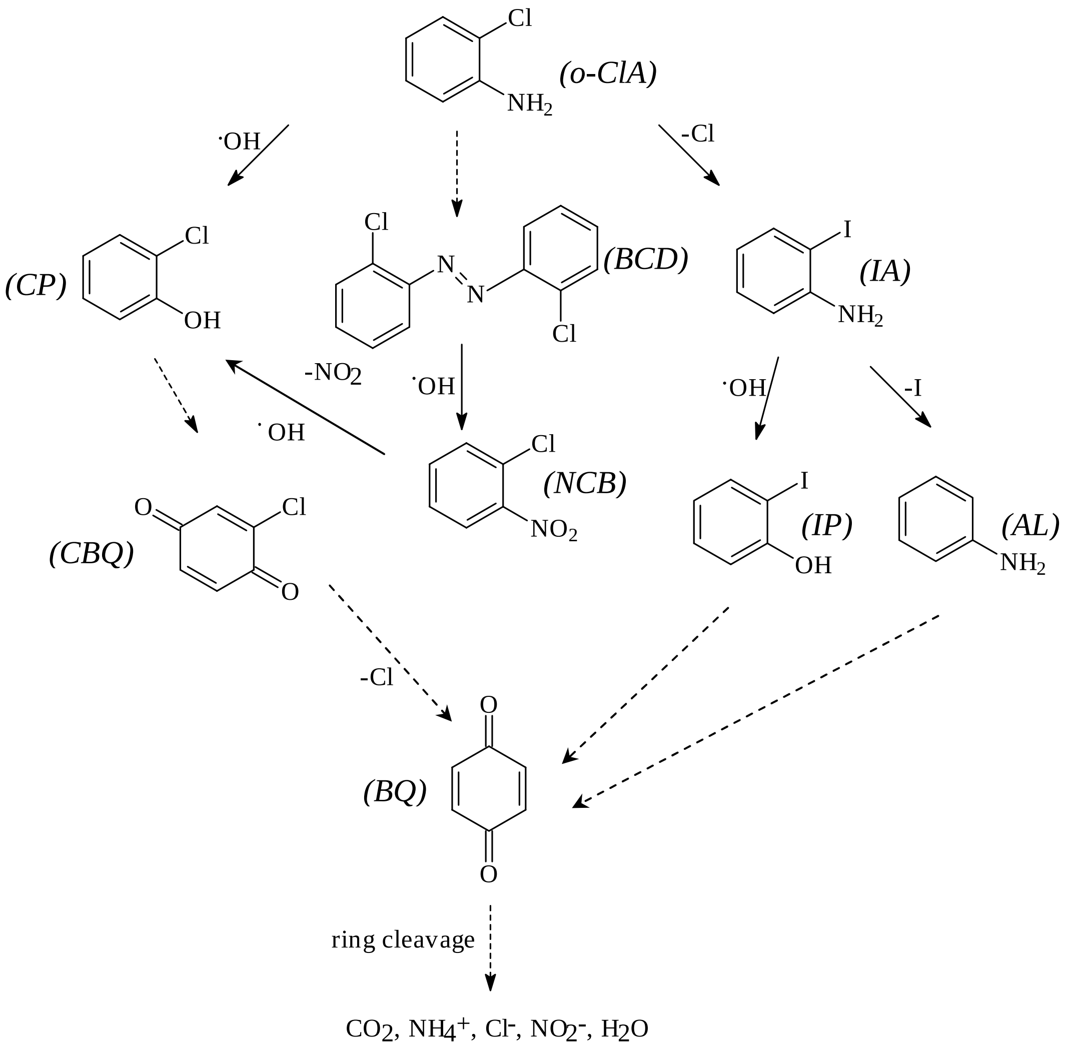

Figure 4C-9: The proposed degradation mechanism of o-ClA in the presence of UV/TiO_2/IO_3^- (Note: dashed arrow represents reactants could take more than one step to reach the products. Abbreviations were indicated as italic.).

Those organic intermediates were mainly degraded via the $^{\bullet}OH$ attack by the addition to the aromatic ring (Dorfman et al., 1962; Mathews and Sangster, 1967). Since the nature of $^{\bullet}OH$ is highly electrophilic, it preferentially attacks at the position with the highest electron density of the target molecule (Gottschalk and Libra, 2000; Serpone et al., 1992). Besides, H-abstraction and direct electron abstraction from the aromatic compound by $^{\bullet}OH$ to give a resonance-stabilized cation radical are also important mechanisms to participate the degradation pathway (Jakob et al., 1993; Snook and Hamilton, 1974).

The proposed scheme showed three possible products have been degraded from the primary oxidation of o-ClA in UV/TiO_2/IO_3^-. The $^{\bullet}OH$ could replace the amino group of o-ClA to form CP. Or alternatively, dimerization of o-ClA is possible via subsequent processes. Solar et al. (1986) have verified that $^{\bullet}OH$ attack to the amino-group could result in the aniline-radical formation (Eqn. 4C-4) by the pulse radiolysis. Kumar and Mathur (2004) have further discussed the combined of this radical could finally yield the dimer (BCD in our case) as shown in Eqn. 4C-5.

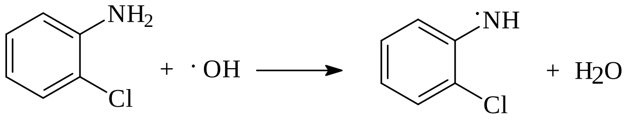

(4C-4)

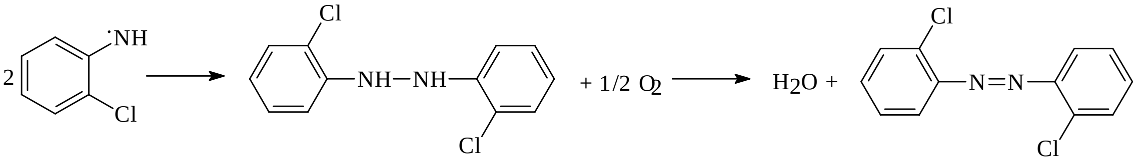

(4C-5)

As IO_3^- was used as an oxidant, an iodide related intermediate was identified. Chloride on o-ClA was found to be replaced by iodide and formed the IA. This product was identified at 30 min of reaction time. Such delay in IA formation may due to the less reactive substitution reaction comparing to the radical attack and the low level iodide in the solution at the beginning.

Since the primary intermediates were already in ppb level, further decay would lead to even lower level of secondary and tertiary products which are undetectable. Also, it is observed that BQ was accumulated and the amount was relatively higher than other intermediates. The generation of BQ was result from the decay of CP, BCD and IA. The degradation of CP has been proposed by Bandara et al. (2001) and Ma et al. (2001). Although ortho- and para-site in CP are both electron rich, they revealed that •OH attack is preferential at para-site. This is due to the steric strain is lower in para-site and the inductive electron-withdrawing effect of the chlorine atom might render attachment of the electrophilic •OH to the ortho- relative to the para-position. Ilisz et al. (2002) have reported chlorohydroquinone (CHQ) as the major product from the decay of CP while another minor product, catechol, (CHQ:catechol ~ 5:1) was also formed by the addition in ortho position followed by Cl abstraction (Eqns. 4C-6 and 7) (Alejandre et al., 1998; Duprez et al., 1996).

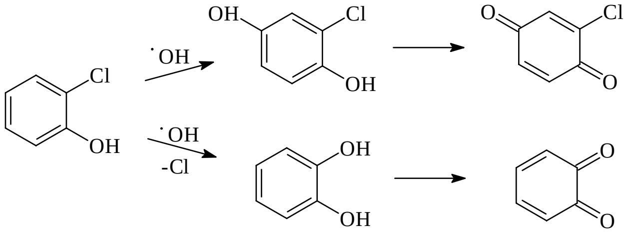

(4C-6)

(4C-7)

Subsequently, CHQ may dissociate two hydrogen atoms to give 2-chloro-1,4-benzoquinone (CBQ) which concurred with our observation. CBQ could further decay to BQ by dechlorination process.

Another primary photo-intermediate, BCD, was detected in the process but its concentration dropped to zero in 150 min. This compound is apparently not persistent in the photoreaction and can subsequently be oxidized to CNB. Although the direct formation of CNB from ClA photodegradation has been elsewhere reported (Mailhot et al., 2004); the formation of CNB via a two-step process involving the transformation of BCD is identified in this study. Canle et al. (2005) described the reaction of CNB via the addition of $^{\bullet}OH$ to the aromatic ring, followed by elimination of OH^{-} from the $^{\bullet}OH$ adduct and deprotonation of the radical cation. The $^{\bullet}OH$ can further attack the nitro group of CNB and transform CNB into CP. This mechanism has also been reported by Ishikawa et al. (1989).

As mentioned earlier, IP and AL have been detected as the primary products of IA and were also included in the degradation pathway. This suggested that IA could be decayed either through $^{\bullet}OH$ attack to the amino group or by the deiodination. The study of halogen compounds has revealed that the chemical properties within the halide group are similar except florine which has high electronegativity. Clark (2002) has stated that the bond enthalpies between H and halide are getting weaker from Cl to I. The increase in size has pulled the atoms further apart and weakens the attraction within. Therefore, it is feasible that IP undergoes analogous oxidation as CP and generates BQ as the product.

The profile of BQ in Figure 4C-3a has revealed a relatively higher concentration comparing to other intermediates. Although the decay of o-ClA could be routed to yield various species, the pathway would finally end up to the same products, BQ. The degradation of BQ has been examined by many researchers (Santos et al., 2002; Donlagic and Levec, 1998). It has been verified that further decay of BQ could initiate the ring cleavage leading to the formation of short chain organic acids such as oxalic acid, formic acid, maleic acid and malonic acid, etc. In addition, the ions formation (NH_4^+, NO_2^- and Cl^-) as the end-products has also been reported by other researchers (Winarno and Getoff, 2002b).

4D The Study of Photocatalytic Degradation of o-ClA on Supported TiO_2

4D.1 Effect on heat treatment

Although the photocatalysis by TiO_2 suspension have succeeded to degrade o-ClA in previous sections, additional post-treatment would complicate the process. Such disadvantage could be eradicated by the immobilization of TiO_2 onto substrate. The morphology of TiO_2 film annealed at different temperatures was shown in Figure 4D-1.

(a)

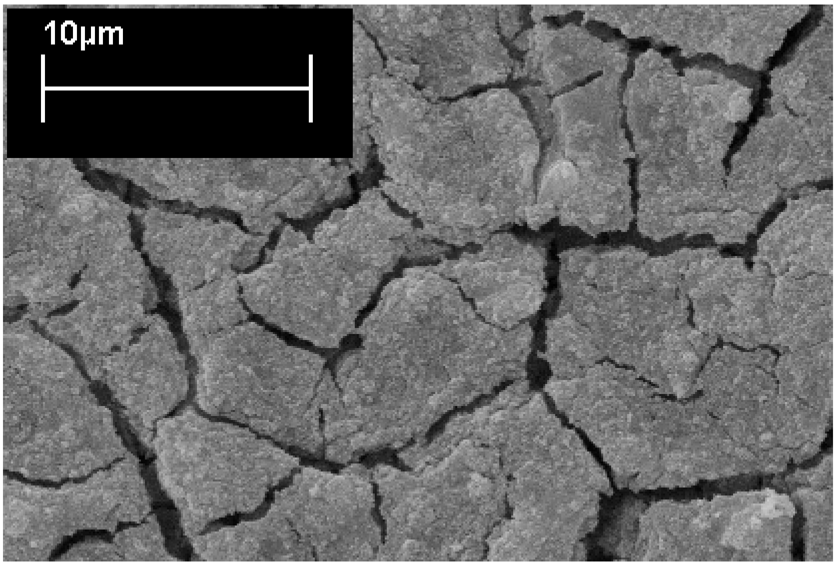

(b)

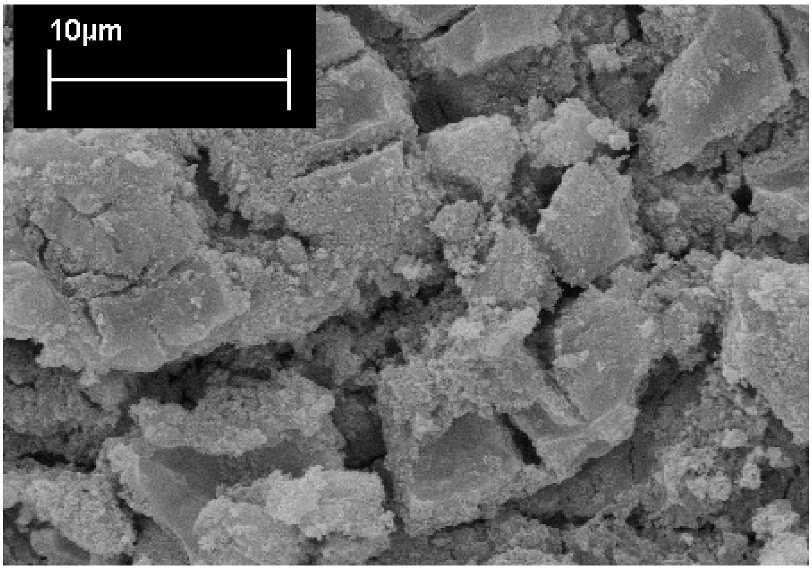

(c)

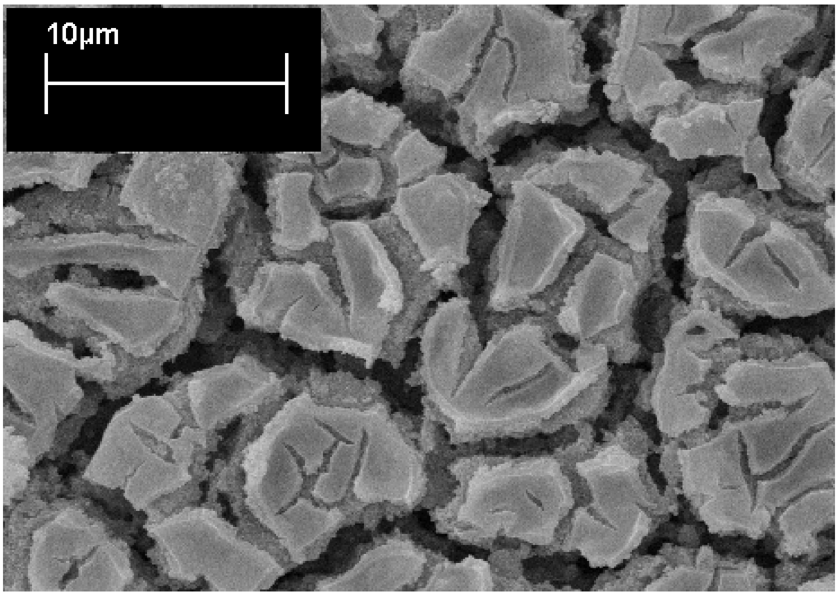

Figure 4D-1: Morphology of film surface annealed at (a) 250°C, (b) 450°C and (c) 700°C.

The diffraction profile of TiO_2 films at different annealing temperatures was illustrated in Figure 4D-2. The anatase (A) and the rutile (R) phases were recognized and marked in the same figure. From the heating condition at 450°C, anatase phase was most intensive at 25.35°. However, an increase of annealing temperature to 700°C has indicated a weaker response on anatase phase. In contrast, rutile peak identified at 27.5° showed a higher intensity at higher annealing temperature. The phase distribution was calculated from Eqn. 3-4 and summarized in Table 4D-1.

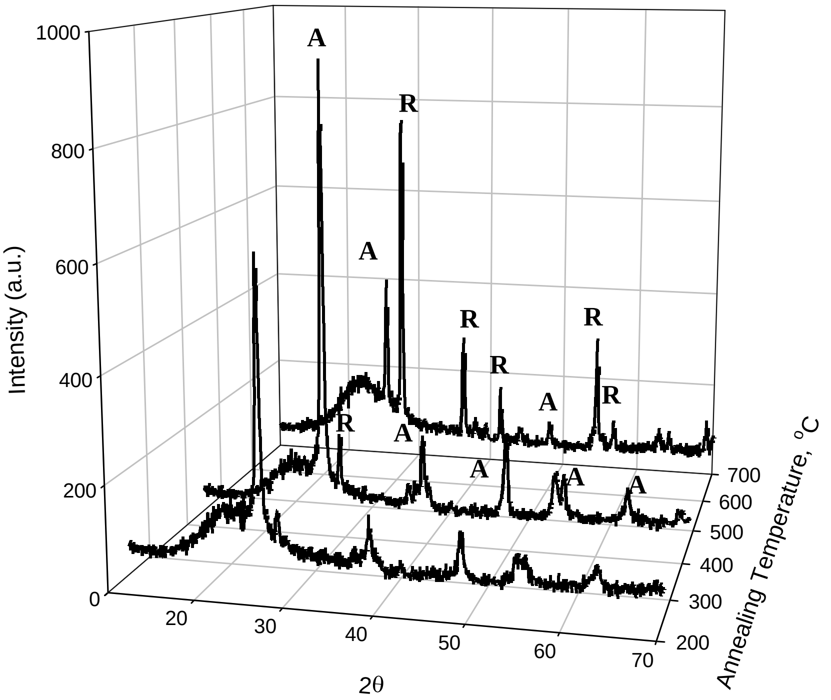

Figure 4D-2: XRD spectra of TiO_2 films at different annealing temperatures (Note: A = anatase; R = rutile).

Table 4D-1: Distribution of anatase and rutile phase at different annealing temperatures.

	Anatase phase		Rutile phase	
Annealing temperature, °C	%	size, nm	%	size, nm
250	76.38	9.86	23.62	20.65
450	80.29	10.93	19.71	19.06
700	29.74	16.94	70.26	14.16

From 450°C to 700°C, about 51% of anatase TiO_2 was converted to rutile. This suggests that the growth of TiO_2 has undergone phase transformation when heating condition was above 450°C. Residual anatase phase still existed in the samples up to 700°C, but the quantity was significantly reduced. Arroyo et al. (2002) has observed a complete transformation to the rutile phase at 900°C which may not be beneficial to the purpose of improving photodegradation process.

By the Scherrer formula in Eqn. 3-3, the crystallite size of anatase phase was also reported in Table 4D-1. It was generally increased with annealing temperature which could be attributed to the thermally promoted crystallite growth. The size of the anatase crystallites increased from 9.86 to 16.94 nm when the annealing temperature was raised from 250°C to 700°C.

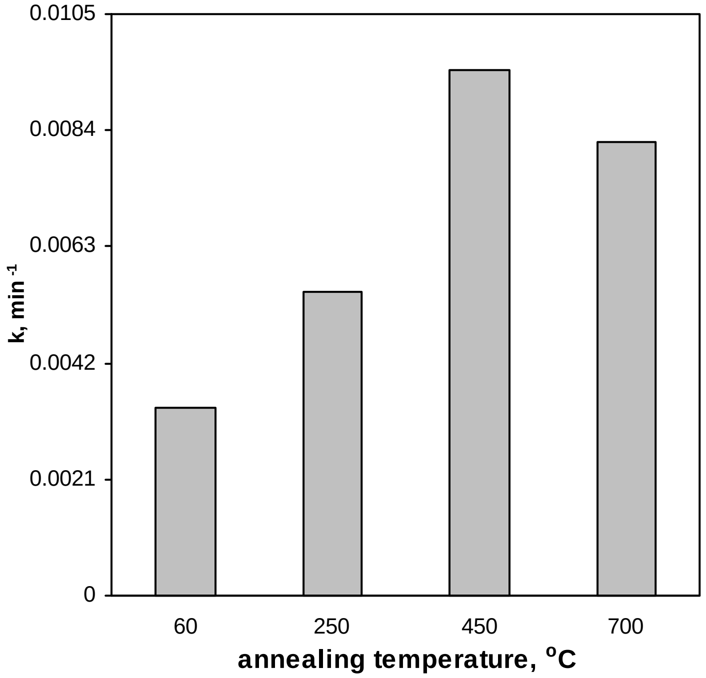

Figure 4D-3: Effect of annealing temperature on photodecay rates (Note: 9 layers were coated on the films).

The photoactivity of the TiO_2 film has been examined by the decay of o-ClA under a 350 nm illumination. As indicated in Figure 4D-3, the performance of photodecay depended very much on the annealing temperature. For a period of 1-hour photodegradation, the coated film was most efficient for the o-ClA photodecay under 450°C annealing which was about 1.5 times faster than that at 250°C. Incorporating with the phase transformation of TiO_2 that discussed beforehand, it can be summarized that the presence of anatase phase is more favorable for photocatalytic reaction which concurred the results reported by Tanaka et al. (1993) in TiO_2 suspension. Although, Yu et al. (2003) have recognized better crystallization could be achieved by the increase of annealing temperature, the weight increment through multi-coating of film was found minimal at 700°C in our test by comparing the weight of TiO_2 at different annealing temperatures (see Table 4D-2).

Table 4D-2: Record of film weights after coating.

Sample no.	Substrate	Annealing Temperature, ^{o}C	Weight of TiO_2, g			
			3 layers	6 layers	9 layers	12 layers
1	Quartz	700	0.0050	0.0068	0.0159	-
2	Quartz	250	0.0075	0.0156	0.0253	-
3	Quartz	450	0.0080	0.0200	0.0298	-
4	Glass	450	0.0063	-	-	-
5	Glass	450	0.0070	0.0151	-	-
6	Glass	450	0.0070	0.0171	0.0285	-
7	Glass	450	0.0073	0.0163	0.0256	0.0466

This is possibly due to the shrinkage of sol at elevated temperature which has been discussed extensively by Brinker and Scherer, (1990) and Scherer (1990). They suggested shrinkage accompanying weight loss is possibility attributed to change of structure and the removal of organics.

4D.2 Effect on substrate

From Figure 4D-4, the use of substrates obviously affected the photocatalytic activity. Quartz substrate exhibited a faster decay than the glass one under the same reaction conditions. Comparing to the direct photolysis (no TiO_2 involved), when TiO_2 was coated on glass substrate, the pseudo first-order reaction rate has been increased by 7 times, while the rate further increased to 9.8 times if the substrate was replaced by quartz. Referring to the weight increment in Table 4D-2, for 9 layers coating, the weight of TiO_2 on quartz and glass only differed by 4.5%.

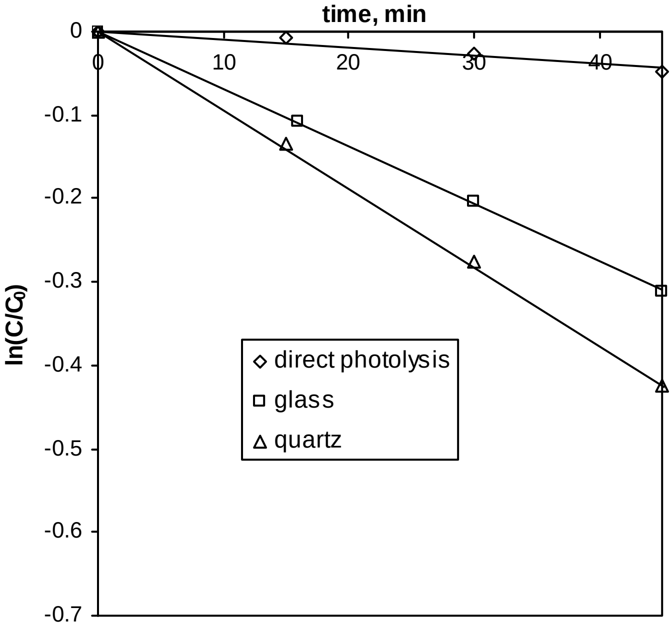

Figure 4D-4: Effect on substrate on the photocatalytic reaction.

In addition, by comparing the XRD pattern in Figure 4D-5, the peaks and intensities were almost the same on both substrates, indicating the adhesion on both substrates were similar. Therefore, the difference in reaction rates was reasonably attributed from the optical properties of substrates. It is known that quartz has excellent light transmission than glass for UV. The UV light illumination might be attenuated or blocked by the glass substrate more than that of quartz substrate. The former reduces the overall light absorbed by TiO_2 on both sides of the surface more significantly and a lower efficiency would be expected.

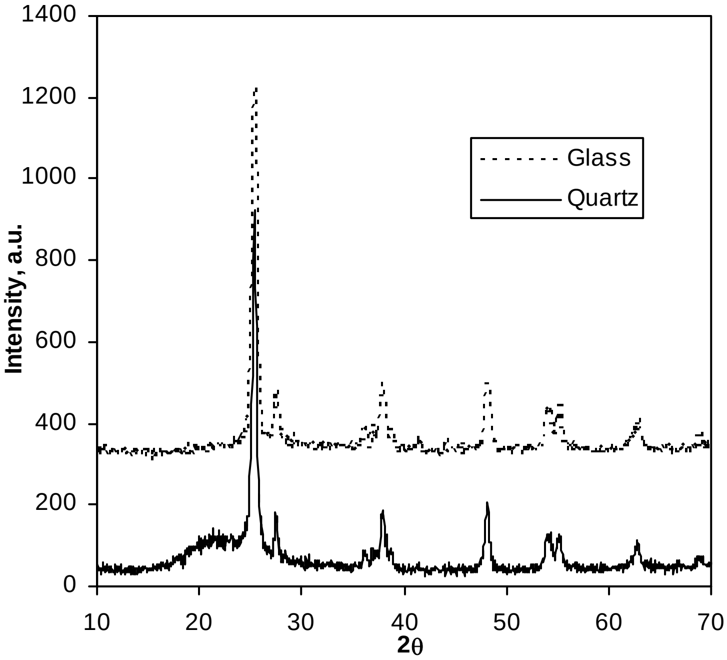

Figure 4D-5: XRD pattern of TiO_2 coating on glass and quartz.

4D.3 Effect on TiO_2 loading

To increase the performance of heterogeneous photocatalytic process, one common way is to increase the contact area of TiO_2 (i.e. size of slide) along the light path. Another possibility is to use multiple coating on the substrate. The latter was investigated in this study so that a better coating process can be realized. The number of coating layer was increased from three to fifteen (annealed for every three layers). After the coated film cooled down to room temperature, the increment of TiO_2 was carefully weighed and presented in Table 4D-2. The cross sectional view of TiO_2 film was shown in Figure 4D-6.

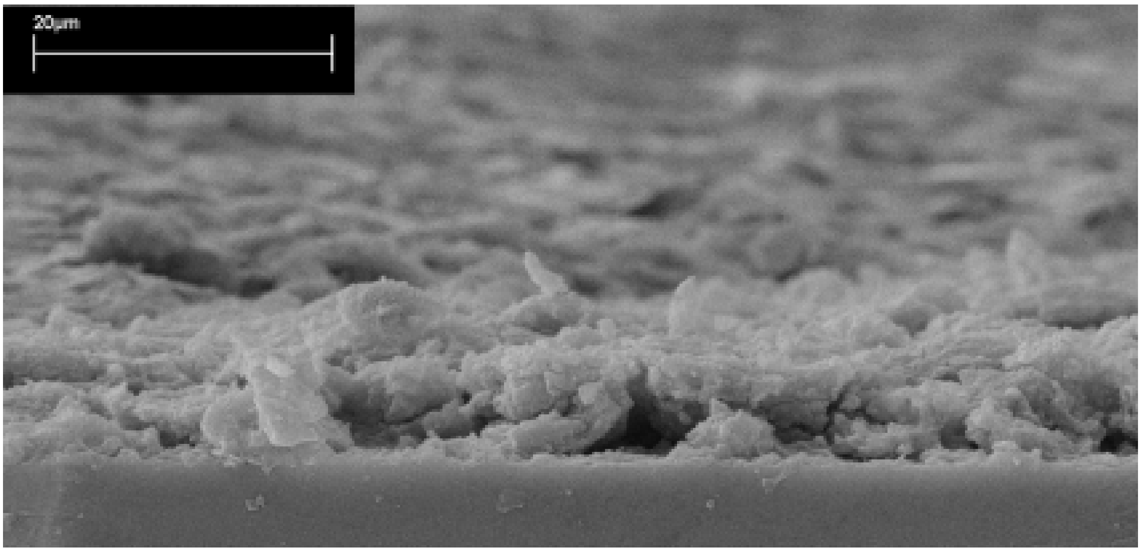

Figure 4D-6: Cross-sectional view of TiO_2 film by SEM. (Note: 9 layers of TiO_2 were coated and annealed at 450°C.

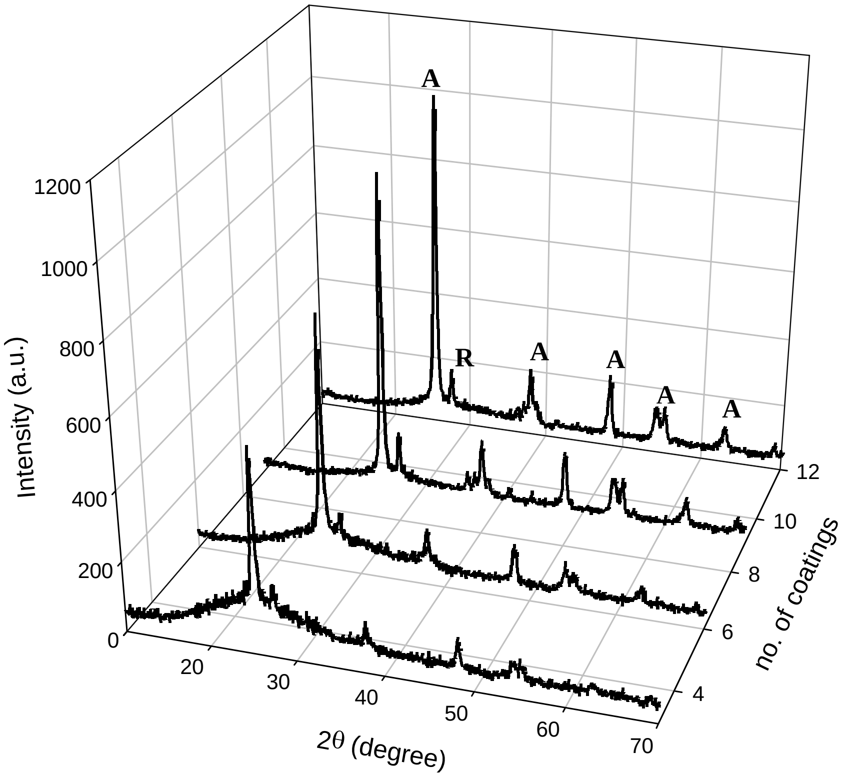

Figure 4D-7: XRD spectra of TiO_2 films with different layers of coating (Note: A = anatase; R = rutile).

The XRD pattern in Figure 4D-7 indicated phase transformation was not occurred on multi-coating, while stronger response was resulted when more TiO_2 was coated onto the substrate.

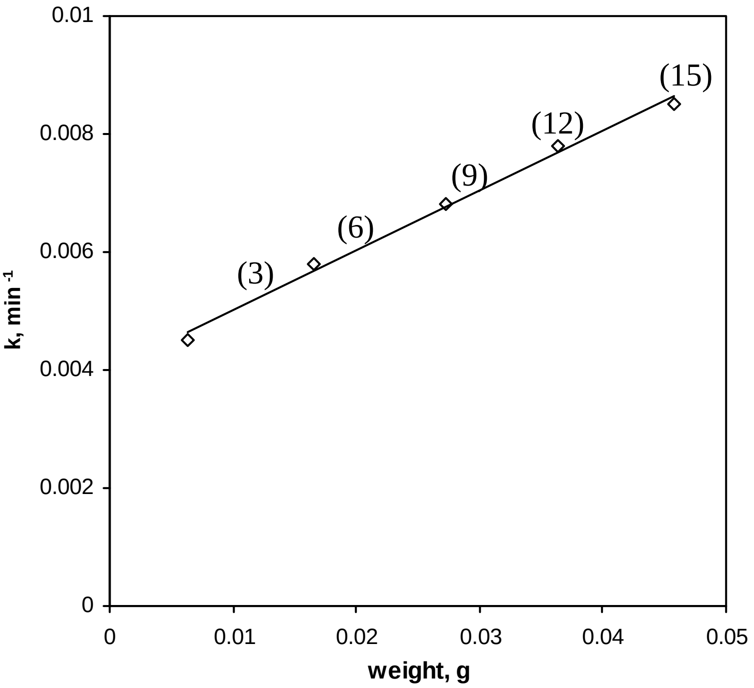

Figure 4D-8: Change of photodecay rate with the increase of TiO_2 coating (Note: numbers inside brackets represent the layer of coating).

The photocatalytic performance on the weight of TiO_2 was shown in Figure 4D-8 where coating layers were indicated in the brackets. A linear relationship ($r^2 = 0.993$) between the TiO_2 film weight and photodecay rate was observed up to fifteen coating layers. Recall the effect of dosage in TiO_2 suspension discussed in 4A.3, it has pointed out that enhancement of decay could be generally observed with increasing TiO_2 surface until excessive amount would retard the reaction by scattering the light penetration. Although no retardation was observed in Figure 4D-8, it should be noted that further coating could possibly increase the loading burden of TiO_2 film attached to the slide leading to a cracking problem. Atkinson and Guppy (1991) have examined the mechanic properties on coating, where the thick film was proven to carry higher tensile strength and would induce fracture of film structure. In order to reach the optimal dosage of TiO_2 on the photoreaction, insertion of more coated substrates is preferable than the increase of film thickness on a single substrate. By using two slides, the photodecay rate of o-ClA was 0.012 min^{-1} which was double to that by a single substrate (0.056 min^{-1}).

4D.4 Effect of light intensity

The photodecay of o-ClA on TiO_2 film was also found to be the function of light intensities. A series tests by increasing the light intensity from 6.5×10^{16} to 2.6×10^{17} (i.e., two to eight lamps) were conducted and pseudo first-order decay rates were presented in Figure 4D-9.

It was found that the photodecay rate was directly proportional to the light intensity applied. The increase of o-ClA decay was mainly due to the excitation of TiO_2 particles on the film. It is because: (1) additional photons could increase the photogenerated of electron-hole pairs which subsequently speed up the o-ClA decay. (2) the change of light intensity did not have much effect on direct photolysis and the decay rates were kept at about 0.001 min^{-1}. The result suggests that the excitation sites in TiO_2 have not been saturated, the increase of UV intensity can possibly further improve the decay rate.

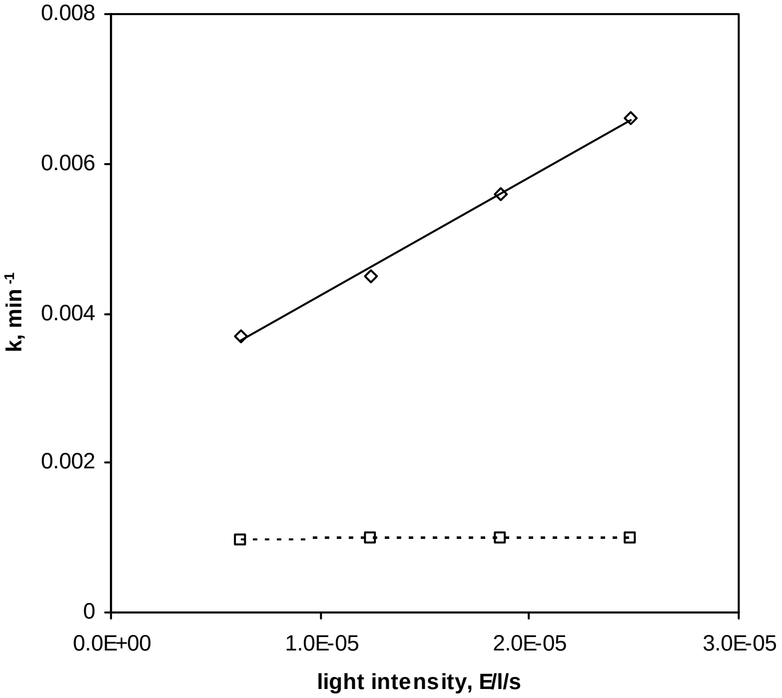

Figure 4D-9: Light intensity effect on the photocatalytic reaction of o-ClA (Note: dashed line was data from direct photolysis at different light intensities).

4D.5 Reuse of the film

TiO_2 film coated on heterogeneous phase is a practical approach for water and/or wastewater treatment as catalyst filtration or recycle is usually difficult or impossible. The reusability of the film is therefore another critical issue to be considered in the engineering application. It was found that an efficient regeneration of film could be achieved by heating the used film at 500°C to remove all the attached residuals of organics. However, the heating process was not convenient in real case and would complicate the on-site treatment. In this study, an alternative pretreatment of film was conducted by washing the used film with DDW followed by air drying. A nine-layer film was selected for a serial test under the same conditions. The pseudo first-order decay rates and the weight change of film during the nine sequential runs were reported in Figure 4D-10.

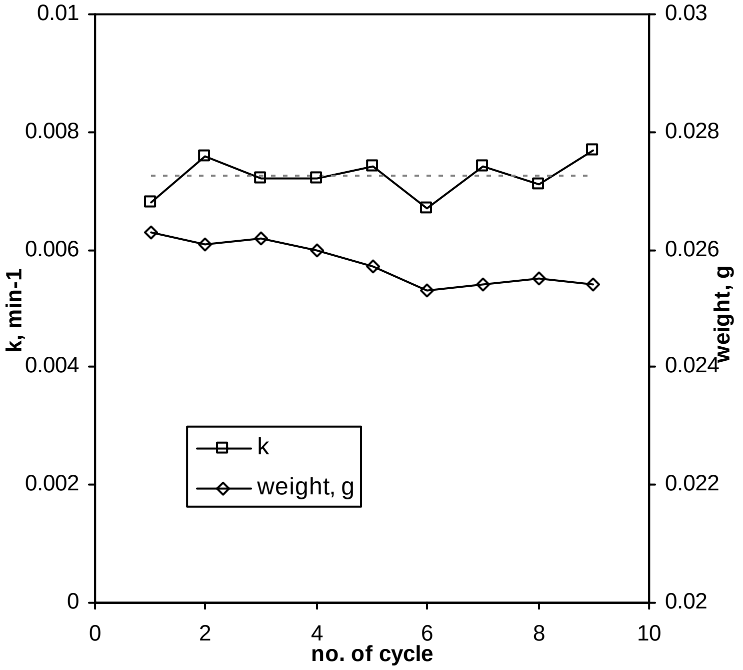

Figure 4D-10: Recycling performance of TiO_2 film.

It can be shown that the film performance with such a simple washing procedure was quite well. Results indicated that the decay of o-ClA was stable along the tests and only ±7% variation was observed. Also, only 3.4% of TiO_2 was lost after nine runs. Such loss was minimal and was believed attributing mostly to the fitting mechanism of the slide.

4D.6 Modeling of reaction kinetics

During the photocatalytic process, with respect to the results summarized in Figures 4D-8 and 9, the pseudo first-order reaction rates increase linearly with the increment of coating mass (M) and light intensity (I), indicating that the reaction rate of o-ClA photodecay is a function of the two design parameters. Therefore, the reaction rate can mathematically be defined as followed:

$$k = f(M, I) \tag{4D-1}$$

$$k = a_1[M] + a_2[I] + b \tag{4D-2}$$

where [M] is the mass of coated TiO_2 on the surface of slide (g); [I] is the light intensity being used (Einstein $\ell^{-1}s^{-1}$); a_1 and a_2 are the coefficient constant of M and I, respectively; and b is the corrector for the intercepts (min^{-1}).

Eqn. 4D-1 and 2 are valid when the input of M and I are within our test ranges. Base on the experimental data in Figures 4D-8 and 9, a_1, a_2, and b can be solved by multiple regressions with the results of 0.07982 $g^{-1}min^{-1}$, 105.3 $Einstein^{-1}\ell^{-1}s^{-1}$ min^{-1} and 0.002386 min^{-1}, respectively. The coefficient of determination (r^2) is 0.96. After the substitution of these coefficient constants into Eqn. 4D-2, the predicted and measured reaction rates could be compared. The predicted first order decay can be compared to the real decay data as illustrated in Figures 4D-11 and 12. In general, the predicted reaction rates are quite close to the measurements, less than 10% of differences are observed. For system design purpose, the removal percentage of o-ClA, R (%), can be estimated by the two measurable parameters of [M] and [I], as indicated in Eqn. 4D-3:

$$R = \{1 - \exp[(-0.07982[M] - 105.3[I] - 0.002386)t\}\} \times 100\% \tag{4D-3}$$

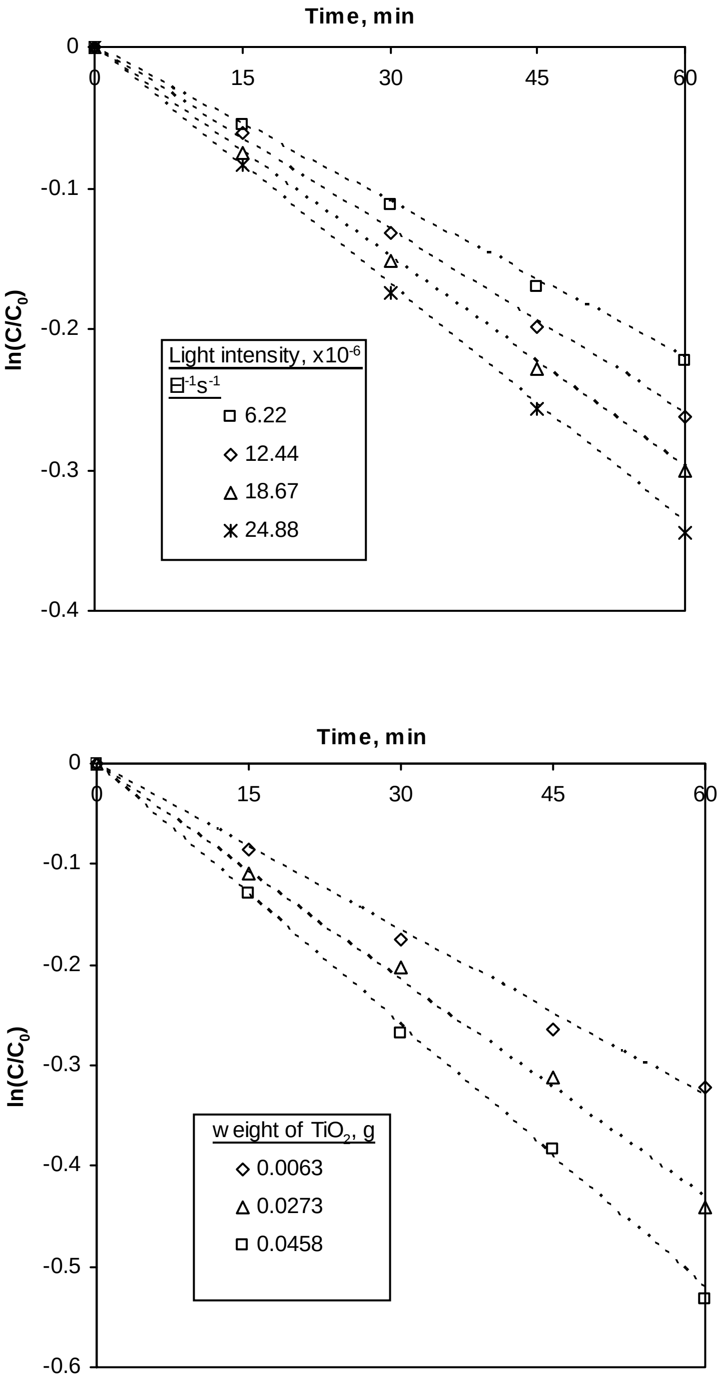

Figure 4D-11: Comparison of model and experimental data at (a) different light intensities and (b) different weights of TiO_2. (Note: dashed lines were calculated from model and marked data were real data from experiments.)

5 Conclusions and Recommendations

5.1 Conclusions

Through the processes applied in this study, it has been proven the photochemical method is an efficient means to remove organics in wastewater wherever appropriate photocatalysts and oxidants were chosen. A more detail conclusion can be drawn in the following sections.

In the study of kinetic properties in UV/TiO_2 system,

A-1 TiO_2 generally enhances the decay of o-ClA through the generation of powerful $^{\bullet}OH$. It is more effective for using together with UV wavelength above 300 nm. Although highest degradation was obtained at 254 nm, low quantum yield value indicates the decay was mainly contributed by the direct photolysis.

A-2 A continuous increment of [TiO_2] doses will scatter the light and slow down the photoreaction. An optimal dosage of TiO_2 at 0.1 g L^{-1} is recommended.

A-3 The photodegradation o-ClA is sensitive to the system pH. The reaction is obviously very much inhibited at strong acidic conditions (pH 2). It is attributed to the combined effect of o-ClA speciations and surface charge of TiO_2.

In the study of oxidants in UV/TiO_2 system,

B-1 The addition of oxidants including H_2O_2, RB and oxyhalogen in UV/TiO_2 led to totally different outcomes. Only H_2O_2 and IO_3^- could further enhance the degradation of o-ClA.

B-2 The decrease in TOC can be assisted by the use of TiO_2 through photocatalytic process, while no improvement of TOC removal was observed through direct photolysis.

B-3 The photodegradation of o-ClA in oxyhalogens or UV/ oxyhalogens was insignificant, but the decay was found to be efficient in the presence of TiO_2.

B-4 The oxidizing power of oxyhalogens in UV/TiO_2 process was in the order of $ClO_3^- < BrO_3^- < IO_3^-$. Oxyhalogen does not have overdosing problem.

B-5 o-ClA could be fully degraded within a minute when adequate IO_3^- was applied. The decay of o-ClA in UV/TiO_2/IO_3^- process is characterized by a two-stage pseudo kinetics, where a faster initial decay was followed by a retardation state. When the dosage of oxyhalogen is above a critical level, the second stage will be vanished.

B-6 The reduction of iodate is a pH dependent process, so the reactivity of radicals generated is a critical factor to the degradation process

B-7 Modeling of the two-stage o-ClA decay in UV/TiO2/IO_3^- system is successful for the predication of o-ClA decay with a designed IO_3^- dosage.

In the Photo-products study,

C-1 The photodegradation of o-ClA in the presence of TiO_2 has degraded to o-chlorophenol and p-benzoquinone.

C-2 The low level of photo-products has indicated the intermediates could undergo further decay and would not accumulate in the system.

C-3 The aromatic intermediates have been detected in UV/TiO_2/IO_3^-. The degradation was mainly initiated by radical attack and the mechanistic pathway was proposed accordingly.

C-4 Although different organics were formed, all of them can be eventually oxidized to BQ, which can be subsequently decayed into simple organic acids and ionic products through ring cleavage.

C-5 Second dosing of IO_3^- was proven useful in further improving the o-ClA decay, but the time interval for the second dosing was critical to the process. Experimental data has indicated the shorter time interval is beneficial to both o-ClA and product decay.

C-6 The final product from IO_3^- reduction, I^-, was believed to be the main species to scavenge the photo-oxidation in the system.

In the study of immobilizing TiO_2 onto substrate,

D-1 The photodecay of o-ClA at 350 nm showed about 20% faster then the film made solely by the sol gel solution.

D-2 The use of quartz has proven to be superior to glass in the photoreaction owing to the excellent optical property of quartz.

D-3 The performance of TiO_2 film was depending on the annealing temperature applied. The transformation of photoactive anatase phase to rutile was observed above 450°C. Such effect was accompanied by the photodecay which a slower reaction was resulted at higher fraction of rutile TiO_2.

D-4 The reuse of the TiO_2 film showed a promising performance with very low variation (±7%) of decay rate after nine consecutive usages. The findings have put forward to the investment of TiO_2 film on the advanced wastewater treatment where the filtration problem could be eliminated.

D-5 A practical model using two critical design parameters (film mass and light intensity) was also proposed in this study to predict the reaction rates, which will facilitate the design of the heterogeneous photocatalytic process.

5.2 Recommendations

Industrial manufacturing related to dye or chemical synthesis generates large amount of organic wastewater. High level of organics could possibly be toxic to the conventional wastewater treatment unit especially the biological treatment and the waste would eventually discharge directly into aquatic water without being treated. The photochemical process in this study could be installed at the discharge of industry which could significantly reduce the high level of organics exposure to the treatment plant and minimize human contact. Before the real application, this study should further extend basis on the suggestions below:

1 In this study, the destruction of single target organics was focused. For practical application, it is suggested to examine the effect of photocatalysis in the presence of multiple organics.

2 In the real treatment, influent are in flowing condition. Such a process can be simulated by the study of continuous flow reactor.

3 The oxidant study of IO_3^- can deepen to the investigation of its reductive species (e.g., IO_2^- and HOI, etc.). Those species could either take part in the photocatalysis or scavenge the organic decay.

4 The coating surface for TiO_2 can be expanded to other forms of substrates. For instances, glass beads and nano-tubes could provide much larger surface area for the photoreaction. Also, TiO_2 coated on the reactor is suggested.

5 In film coating, the enhancement of degradation could be carried out by the use of additional iodate to the solution which has proven to be effective in this study.

REFERENCES

Abdullah, M.; Low, C.; Matthews, R.W. Effects of common inorganic anions on rates of photocatalytic oxidation of organic carbon over illuminated titanium dioxide. *Journal of Physical Chemistry 94*, 6820-6825, 1990.

Alejandre, A.; Medina, F.; Fortuny, A.; Salagre, P.; Sueiras, J.E. Characterisation of copper catalysts and activity for the oxidation of phenol aqueous solutions. *Applied Catalysis B: Environment 16,* 53-67, 1998.

Arnold, S.M.; Hickey, W.J.; Harris, R.F. Degradation of atrazine by Fentons Reagent: Condition optimization and product quantification. *Environmental Science and Technology 29*, 2083–2089, 1995.

Arroyo, R.; Cordoba, G.; Padilla, J.; Lara, V.H. Influence of manganese ions on the anatase-rutile phase transition of TiO_2 prepared by the sol-gel process. *Materials Letters 54*, 397-402, 2002.

Atkinson, A.; Guppy, R.M. Mechanical stability of sol-gel films. *Journal of Materials Science 26*, 3869-3873, 1991.

Augugliaro, V.; Prevot, A.B.; Loddo, V.; Marci; Palmisano, L.; Pramauro, E.; Schiavello, M. Photodegradation kinetics of aniline, 4-ethylaniline, and 4-chloroaniline in aqueous suspension of polycrystalline titanium dioxide. *Research of Chemical Intermediates 26*, 5, 413-426, 2000.

Bandara, J.; Mielczarski, J.A.; Lopez, A.; Kiwi, J. 2. Sensitized degradation of chlorophenols on iron oxides induced by visible light: Comparison with titanium oxide. *Applied Catalysis B: Environmental 34*, 321-333, 2001.

Beydoun, D.; Tse, H; Amal, R.; Low, G.; McEvoy, S. Effect of copper(II) on the photocatalytic degradation of sucrose, *Journal of Molecular Catalysis A: Chemical 177*, 265-272, 2002.

Bickley, R.I.; Gonzalez-Carreno, T.; Lees, J.S.; Palmisano, L.; Tilley, R.J.D. A structrual investigation of titanium dioxide photocatalysts. *Journal of Solid State Chemistry 92*, 178-190, 1991.

Boreen, A.L.; Arnold, W.A.; Mcneill, K. Photochemical fat of sulfa drugs in the aquatic environment: Sulfa drugs containing five-membered heterocyclic groups. *Environmental Science and Technology 38*, 3933-3940, 2004.

Boreskov, G.K. Catalysis, In Great Soviet Encyclopedia, 3rd ed., vol. 2, Moscow, 1973.

Bouzaida, I.; Ferronato, C; Chovelon, J.M.; Rammah, M.E.; Herrmann, J.M. Heterogeneous photocatalytic degradation of the anthraquinonic dye, acid blue 25 (AB25): a kinetic approach. *Journal of Photochemistry and Photobiology A: Chemisty 168*, 23-30, 2004.

Brinker, C.J.; Scherer, G.W. *Sol-gel Science—The Physics and Chemistry of Sol-gel Processing*, Academic Press, 551, 1990.

BUA Report 153. p-chloroaniline. *Beratergremium fur Umweltrelevante Altstoffe* (BUA) der Gesellschaft Deutscher Chemiker. Weinheim, VCH, 171, 1995.

Canle M. L.; Santaballa, J.A.; Vulliet, E. On the mechanism of TiO_2-photocatalyzed degradation of aniline derivatives. Journal *of Photochemistry and Photobiology A: Chemistry 175*, 192-200, 2005.

Carp, O.; Huisman, C.L.; Reller, A. Photoinduced reactivity of titanium dioxide. *Progress in Solid State Chemistry 32*, 33-177, 2004.

Ceresa, E.M.; Burlamacchi, L.; Visca, M. An ESR study on the photoreactivity of titania pigments. *Journal of Material Science 18*, 289-294, 1983.

Cermola, F.; DellaGreca, M; Iesce, M.R.; Montella, S.; Pollio, A.; Temussi, F. A mild photochemical approach to the degradation of phenols from olive oil mill wastewater, *Chemosphere 55*, 1035-1041, 2004.

Chan, C.Y.; Tao, S.; Dawson, R.; Wong, P.K. Treatment of atrazine by integrating photocatalytic and biological processes. *Environmental Pollution 131*, 45-54, 2004.

Chen, J.; Eberlein, L.; Langford, C.H. Pathways of phenol and benzene photooxidation using TiO_2 supported on a zeolite. *Journal of Photochemistry and Photobiology A: Chemistry 148*, 183-189, 2002.

Chen, Y.; Sun, X.; Yang, Y. & Ke, Q. Heterogeneous photocatalytic oxidation of polyvinyl alcohol in water, *Journal of Photochemistry and Photobiology A: Chemistry 142*, 85-89, 2001.

Choudhry, G.G.; Webster, G.R. *Photochemistry of environmental aquatic system*. In: Cooper, W.J.; Zika, R.G., eds., In American Chemical Society: Washington DC, 61-73, 1987.

CICIS: 1977 production statistics for chemicals in the nonconfidential initial TSCA Chemical Substances inventory. U.S. Environmental Protection Agency, Office of Pesticides and oxic Substances, Washington, D.C., 1977.

Clark, J. Atomic and physical properties of the group 7 elements (the halogens), http://www.chemguide.co.uk/inorganic/group7/properties.html#top, 2002.

Cotton, F.A.; Wilkinson, G.; Gaus, P.L. The Halogens: Fluorine, Chlorine, Bromine, Iodine, and Astatine. In: *Basic Inorganic Chemistry*, 3rd Edition, John Wiley & Sons, Inc. p. 471, 1995.

Cullity, B.D. *Elements of x-ray diffraction*. 2nd ed., Addison-Wesley, Reading, MA, p.102, 1978.

D'Oliveira, J.; Minero, C.; Pelizzetti, E.; Pichat, P. Photodegradation of dichlorophenols and trichlorophenols in TiO_2 aqueous suspensions: kinetic effects of the positions of the Cl atoms and identification of the intermediates. *Journal of Photochemistry and Photobiology A: Chemistr, 72,* 261-267, 1993.

Donlagic, J.; Levec, J. Comparison of catalyzed and noncatalyzed oxidation of azo dye and effect on biodegradability. *Environmental Science and Technology 32*, 1294, 1998.

Dorfman, L.M.; Adams, G.E. *Reactivity of the hydroxyl radical in aqueous solutions,* U.S. Department of Commerce, National Bureau of Standards NSRDS-NS, 46, 1973.

Dorfman, L.M.; Taub, I.A.; Buhler, R.E. Pulse radiolysis studies. I. Transient spectra and reaction-rate constants in irradiated aqueous solutions of benzene *Journal of Chemical Physics 36,* 3051-3061, 1962.

Dunuwila, D.D.; Gagliardi, C.D.; Berglud, K.A. Application of controlled hydrolysis of titanium (IV) isopropoxide to produce sol-gel-derived thin films. *Chemistry of Materials 6*, 1556-1562, 1994.

Duprez, D.; Delanoë, J.; Barbier, J.; Isnard, Jr., P.; Blanchard, G. Catalytic oxidation of organic compounds in aqueous media. *Catalysis Today 29,* 317-322, 1996.

Ekaterina, A.K.; Panagiotis, G.S.; Alexandre, V.V. Comparative study on photocatalytic oxidation of four organophosphorus simulants of chemical warfare agents in aqueous suspension of titanium dioxide. *Journal of Photochemistry and Photobiology A: Chemistry 162*, 503-511, 2001.

Environmental Health and Safety Division of Environment Agency Japan. *Report on Environmental Survey and Wildlife Monitoring of Chemicals in Fiscal Year, September* 2000.

European Union, 76/464/EEC. Council directive of 4 May 1976 on pollution caused by certain dangerous substances discharged into the aquatic environment of the community. Official journal no. L129, 18/05/1976, p.23, 1976.

Formenti M; Juillet F; Meriaudeau P; Teichner SJ. Heterogeneous photocatalysis for partial oxidation of paraffins. *Chemical Technology*, 680-681, 1971.

Fox, M.A.; Dulay, M.T. Heterogeneous Photocatalysis. *Chemical Review 93*, 341-357, 1993.

Fox, M.A.; Kim, Y.; Wahab, A.; Dulay, M.T. Photocatalytic decontamination of sulfur containing alkyl halides on irradiated semiconductor suspensions, *Catalysis Letters 5*, 369, 1990.

Fujishima, A.; Honda, K. Electrochemical photolysis of water at a semiconductor electrode. *Nature 238***,** 37–38, 1972.

Fujishima, A.; Rao, T.N.; Tryk, D.A. Titanium dioxide photocatalysis. *Journal of Photochemistry and Photobiology C: Photochemistry Reviews 1*, 1-21, 2000.

Gao, R.; Stark, J.; Bahnemann, D.W.; Rabani, J. Quantum yields of hydroxyl radicals in illuminated TiO_2 nanocrystallite layers. *Journal of Photochemistry and Photobiology A: Chemistry 148*, 387-391, 2002.

Gottschalk, C. J.A.; Libra, A. S. *Ozonation of Water and Waste Water: A Practical Guide to Understanding Ozone and its Application*, Wiley-VCH Verlage GmbH, Germany, 2000.

Goutailler, G.; Valette, G.C.; Guillard, C.; Païssé, O.; Faure, R. Photocatalysed degradation of cyromazine in aqueous titanium dioxide suspensions: comparison with photolysis. *Journal of Photochemistry and Photobiology A: Chemistry,* vol 141,79-84, 2001.

Greenwood, N.N.; Earnshaw, A. *Chemistry of the elements*. Oxford: Butterworth-Heinemann, 1997.

Hague, D.C.; Mayo, M.J. The effect of crystallization and a phase transformation on the grain growth of nanocrystalline titania. *Nanostructured Materials 3*, 61, 1993.

Hargesheimer, E.E.; Couttis, R.T.; Pasutto, F.M. Gas-liquid chromatographic determination of aniline metabolites of substituted urea and carbamate herbicides in aqueous solution. *Journal of Association of Analytical Chemists 64*, 833-840, 1981.

Hem, J .D. Study and interpretation of the chemical characteristics of natural waters. US Geological Survey Water Supply Paper 2254, p. 263, 1985.

Herrmann, J.M. Heterogeneous photocatalysis: fundamentals and applications to the removal of various types of aqueous pollutants. *Catalysis Today 53*, 115-129, 1999.

Hinshelwood, C.N. The Kinetics of Chemical Change in Gaseous Systems. Clarendon Press: Oxford, 1926.

Hommel, D. Handbuch der gefahrlichen Guter. Berlin, Springer-Verlag, 1985.

HSDB/Hazardous Substances Data Bank. In: Tomes plus. *Environmental Health and Safety Series* I. vol 26. National Library of Medicine, 1995

Ian, M. T. Multicomponent glasses from the sol-gel process. In: ed. Lisa C.K., Sol-gel technology for thin films, fibers, performs, electronics, and specialty shapes. Noyes Publications, p.2, 1988.

IARC, Lyon. *Hawley's Condensed Chemical Dictionary*, 11th ed. Sax, N.I.; Lewis, R.J. Sr., Eds., p. 262. Van Nostrand Reinhold, New York, 1987.

IARC, International Agency for Research on Cancer. Aniline and aniline hydrochloride. In some aromatic amines, anthraquinones and nitroso compounds, and inorganic fluorides used in drinking-water and dental preparations. IARC Monographs on the Evaluation of the Carcinogenic Risk of Chemicals to Humans, 27, 39-61, 1982.

IAWR, Rheinbericht 1996-1998. Julich, Internationale Arbeitsgemeinschaft der Wasserwerke im Rheineinzugsgebiet, 1998.

Ilisz, I.; Dombi, A.; Mogyorósi, K.; Farkas, A.; Dékány, I. Removal of 2-chlorophenol from water by adsorption combined with TiO_2 photocatalysis, *Applied Catalysis B: Environment, 39*, 247-256, 2002.

Inel, Y.; Okte, A. Photocatalytic degradation of malonic acid in aqueous suspensions of titanium dioxide: an initial kinetic investigation of CO_2 photogeneration. *Journal of Photochemistry and Photobiology A: Chemistry*, *96*, 175-180, 1996.

Irmak, S.; Kusvuran; E., Erbatur; O. Degradation of 4-chloro-2-methylphenol in aqueous solution by UV irradiation in presence of titanium dioxide. *Applied Catalysis B: Environmental 54*, 85-91, 2004.

Ishikawa, S; Baba, K; Hanada, Y; Uchimura, Y; Kido, K. Photodecomposition of o-chloroaniline in aqueous solution with low pressure mercury lamp, *Bulletin of Environmental Contamination and Toxicology 42*, 65-70, 1989.

Jaeger, C.D.; Bard, A.J. Spin trapping and electron spin resonance detection of radical intermediates in the photodecompoisition of water at TiO_2 particle systems. *Journal of Physical Chemistry 83*, 3146-3152, 1979.

Jakob, L.; Hashem, T.L.; Burki, S.; Guindz, N.M.; Braun, A.M. Vacuum-ultraviolet (VUV) photolysis of water: oxidative degradation of 4-chlorophenol. *Journal of Photochemistry and Photobiology A: Chemistry 75*, 97-103, 1993.

Jen, J.F.; Chang, C.T.; Yang, C. On-line Microdialysis-high-performance liquid chromatographic determination of aniline and 2-chloroiline in polymer industrial wastewater. *Journal of Chromatography A 930*, 119-125, 2001.

Kagan, J. *Organic Photochemistry – Principles and Applications*. Academic Press, p.10, 1993.

Kalyanasundaram, K.; Gratzel, M. *Photosensitization and Photoctalysis using Inorganic and Organometallic Compounds*, vol. 14, Catalysis by Metal Complexes. Kluwer Academic Publisher, 1993.

Kavan, L.; Gratzel, M. Highly efficient semiconducting TiO_2 photoelectrodes prepared by aerosol pyrolysis. *Electrochimica Acta 40*, 643-652, 1995.

Kavan, L.; Ray, O.A.; Gratzel, M. Preparation of TiO_2 (anatase) films on electrodes by anodic oxidative hydrolysis of $TiCl_3$. *Journal of Electroanalytical Chemistry 346*, 291-307, 1993.

Klessinger, M.; Michel, J. *Excited States and Photochemistry of Organic Molecules*, VCH Publishers, p. 247, 1995.

Klug, H.P.; Alexander, L.E. *X-Ray Diffraction Procedures*, Wiley, New York, 1954.

Kuhn, R.; Pattard, M.; Pernak, K.D.; Winter, A. Results of the harmful effects of selected water pollutants (anilines, phenols, aliphatic compounds) to Daphnia magna. *Water Research 23*, 495-499, 1989.

Kumar, A.; Mathur, N. Photocatalytic oxidation of aniline using Ag^+ loaded TiO_2 suspensions, *Applied Catalysis A: General 275*, 189-197, 2004.

Kwan, C.Y.; Chu, W. Photodegradation of 2,4-dichlorophenoxyacetic Acid in Various Iron-mediated Oxidation Systems. *Water Research 37*, 4405-4412, 2003.

Laha, S.; Luthy, R.G. Oxidation of aniline and other primary aromatic amines by manganese dioxide. *Environmental Science and Technology 24*, 363-373, 1990.

Landau, L.D.; Levich, B.G. Dragging of a liquid by a moving plate. *Acta Physiochimica* U.R.S.S., 17, 42-54, 1942.

Langford, J.I.; Wilson, A.J.C. Scherrer after sixty years: A survey and some new results in the determination of crystallite size. *Journal of Applied Crystallography 11*, 102-113, 1978.

Leng, W.H.; Cheng, S.A.; Zhang, J.Q. Cau, C.N. Kinetics of photocatalytic degradation of aniline in water over TiO_2 supported on porous nickel. *Journal of Photochemistry and Photobiology A: Chemistry 69*, 241-249, 1992.

Linsebigler, A.L.; Lu, G.; Yates, J.T., Jr. Photocatalysis on TiO_2 surfaces: principles, mechanisms, and selected results. *Chemical Review 95*, 735-758, 1995.

Linstrom, P.J.; Mallard, W.G. Eds., NIST Chemistry WebBook, NIST Standard Reference Database Number 69, *National Institute of Standards and Technology*, Gaithersburg MD, 20899 (http://webbook.nist.gov), 2005.

Livage, J.; Henry, M.; Sanchez, C. Sol-gel chemistry of transition metal oxides. *Progress of Solid State Chemistry 18*, 259-341, 1988.

Lyman, W.J.; Reehl, W.F.; Rosenblatt, D.H. Handbook of chemical property estimation methods. Environmental behavior of organic compounds, pp.15-21 to 15-29. McGraw-Hill Book Company, New York, 1982.

Ma, H.M.; Wohlers, J.; Meierhenrich, U.; Bernecker, A.; Suling, V.; Thiemann, W. Analysis of oxidative degradation products of 2,4,6-trichlorophenol treated with air ions, *Analytical Chemistry 73*, 3506–3510, 2001.

Mailhot, G.; Hykrdová, L.; Jirkovský, J.; Lemr, K.; Grabner, G.; Bolte, G. Iron(III)-photoinduced degradation of 4-chloroaniline in aqueous solution. *Applied Catalysis B: Environmental 50*, 25-35, 2004.

Martin, S.T.; Lee, A.T.; Hoffmann, M.R. Chemical mechanism of inorganic oxidants in the TiO_2/UV process: increased rates of degradation of chlorinated hydrocarbons. *Environmental Science and Technology 29***,** 2567–2573, 1995.

Mathews, R.W.; Sangster, D.F. Production of isomeric nitrophenols in radiolysis of aqueous nitrobenzene solution. *Journal of Physical Chemistry 71*, 4056-4062, 1967.

Merck Index, 10th ed. (M. Windholz, Ed), p.297. Merck and Company, Rahway, N.J. 1983.

Mezyk, S.P.; Elliot, A.J. Pulse Radiolysis of Iodate in Aqueous Solution. *Journal of the Chemical Society. Faraday transactions 90*, 831-836, 1994.

Miller, G.C.; Crosby, D.G. Photoxidation of 4-chloroanilne and N-(4-chlorophenyl)-benzenesulfonamide to nitroso- and nitro- products. *Chemosphere 12*, 1217-1228, 1983.

Mills, A.; Morris, S.; Davis, R. Photomineralization of 4-Chlorophenol sensitized by titanium dioxide: a study of the intermediates, *Journal of Photochemistry and Photobiology A: Chemistry 70*, 183-191, 1993.

MSDS from Physical Chemistry at Oxford University. http://physchem.ox.ac.uk/MSDS/, 2007.

Naomi, L.S.; Peller, J.; Vinodgopal, K.; Kamat, P.V. Combinative sonolysis and photocatalysis for textile dye degradation. *Environmental Science Technology 34*, 1747-1750, 2000.

Natarajan, C.; Ogami, G. *Jouranl of Electrochemical Society 146*, p.1547, 1996.

Neamtu, M.; Siminiceanu, I.; Yediler, A.; Kettrup, A. kinetics of decolorization and mineralization of reactive azo dyes in aqueous solution by the UV/H_2O_2 oxidation. *Dyes and Pigments* 53, 93-99, 2002.

NIOSH. National Occupational Exposure Survey (1981-83). Unpublished provisional data as of 7/1/90. Cincinnati, OH: U.S. Department of Health and Human Services, 1990.

Ohtaki, M.; Sato, H.; Fujii, H.; Eguchi, K. Intramolecularly selective decomposition of surfactant molecules on photocatalytic oxidative degradation over TiO_2 photocatalyst. *Journal of Molecular Catalysis A: Chemical 155*, 121-129, 2000.

Okudera, H.; Yokogawa, Y. Fabrication of titania-coated silica filbers and effect of substrate shape on coating growth rate. *Thin Solid Films 423*, 119-124, 2003.

Ollis, D.F.; Ekabi, H. A. *Photocatalytic Purification and Treatment of Water and Air*, Elsevier, Amsterdam, 1993.

Ollis, D.F.; Hsiao, C.; Budiman, L.; Lee, C. Heterogeneous photoassisted catalysis: Conversions of perchloroethylene, dichloroethane, chloroacetic acids, and chlorobenzenes. *Journal of Catalysis 88*, 89–95, 1984.

Pelizzetti, E.; Carlin, V.; Minero, C.; Gratzel, M.. Enhancement of the rate of photocatalytic degradation on TiO_2 of 2-chlorophenol, 2,7-dichlorodibenzodioxin and atrazine by inorganic oxidizing species. *New Journal of Chemistry 15*, 351-359, 1990.

Pierre, A.C. Introduction to sol-gel processing, Kluwer Academic Publishers, 1998.

Pruden, A.L.; Ollis, D.F. Photoassisted heterogeneous catalysis: the degradation trichloroethylene in water. *Journal of Catalysis 82*, 404-417, 1983.

Rabek, J.F. *Experimental Methods in Photochemistry and Photophysics Part 2*, Chapter 24, John Wiley & Songs Ltd., p.854, 1982.

Richard, C.; Benagana, S. pH effect in the photocatalytic transformation of a phenyl-urea herbicide. *Chemosphere 33*, 635, 1996.

Rothenberger, G.; Moser, J.; Gratzel, M.; Serpone, N.; Sharma, D.K. Charge carrier trapping and recombination dynamics in small seciconductor particles. *Journal of American Chemical Society 107*, 8054-8059, 1985.

San, N.; Hatipoglu, A.; Koçtürk, G.; Çınar, Z. Prediction of primary intermediates and the photodegradation kinetics of 3-aminophenol in aqueous TiO_2 Suspensions. *Journal of Photochemistry and Photobiology A: Chemistry 139*, 225-232, 2001.

Sanchez, M.; Wolfger, H.; Getoff, N. Raidation-induced degradation of 4-chloroaniline in aqueous solution. *Radiation Physics and Chemistry 65*, 611-620, 2002.

Santos, A.; Yustos, P.; Quintanilla, A.; Rodriguez, S.; Garcia-Ochoa, F. Route of the catalytic oxidation of phenol in aqueous phase. *Applied Catalysis B: Environmental 39*, 97-113, 2002.

Sauleda, R.; Brillas, E. Mineralization of aniline and 4-chlorophenol in acidic solution by ozonation catalyzed with Fe^{2+} and UVA light. *Applied Catalysis B: Environmental 29*, 135-145, 2001.

Scalfani, A.; Palmisano, L.; Davi, E. Photocatalytic degradation of aniline in UV-illuminated aqueous TiO_2 suspensions. *Electroquimica Acta 42*, 1877, 1997.

Scherer, G.W. Theory of Drying. *Journal of American Ceramic Society 73*, 3-14, 1990.

Schindler, K.M.; Kunst, M. Charge–carrier dynamics in TiO_2 powders. *Journal of Physical Chemistry 94*, 8222–8226, 1990.

Scriven, L.E. Physics and applications of dip coating and spin coating. *Material Research Society Symposium Proceedings 121*, in Better Ceramics through Chemistry III, 717-729, 1988.

Serpone, N. Relative photonic efficiencies and quantum yields in heterogeneous photocatalysis. *Journal of Photochemistry and Photobiology A: Chemistry* 104, 1-12, 1997.

Serpone, N.; Lawless, D.; Disdier, J.; Herrmann, J.M. Spectroscopic, photoconductivity and photocatalytic studies of TiO_2 Colloids: Naked and with the lattice doped with Cr^{3+}, Fe^{3+} and V^{5+} cations. *Langmuir 10*, 643-652, 1994.

Serpone, N.; Lawless, D.; Terzian, R.; Meisel, D. In: Mackay, R.A.; Texter, J. (Eds), Electrochemistry in Colloids and Dispersions, VCH, New York, N.T., p. 399, 1992.

Singh, R.S.; Grimes, C.A.; Dickey, E.C. Fabrication of nonoporous TiO_2 films through Benard-Marangoni convection. *Material Resources Innovation 5,* 178-184, 2002.

Sivakumar, S.; Krishna Pillai, P.; Mukundan, P.; Warrier, K.G.K. Sol-gel synthesis of nanosized anatase from titanyl sulfate. *Material Letters 57*, 330-335, 2002.

Snook, M.E.; Hamilton, G.A. Oxidation and fragmentation of some phenyl-substituted alcohols and ethers by peroxydisulfate and Fenton's reagent. *Journal of American Chemical Society 96*, 860, 1974.

Solar, S.; Solar, W.; Getoff, N. Resolved multiple OH-attack on aqueous aniline studied by pulse radiolysis. *Radiation Physics and Chemistry 28*, 229–234, 1986.

Stir, M.; Traykova, T.; Nicula, R.; Burkel, E.; Baethtz, C.; Knapp, M.; Lathe, C. In situ high-pressure and high-temperature diffraction experiments on pure and Ag-doped TiO_2 nanpowders. *Nuclear Instruments and Methods in Physics Research Section B 199*, 59-63, 2003.

Sturini, M.; Fasani, E.; Prandi, C.; Casaschi, A.; Albini, A. Titanium dioxide photocatalysed decomposition of some thiocarbamates in water. *Journal of Photochemistry and Photobiology A: Chemistry* 101, 251, 1996.

Tanaka, K.; Hisanaga, T.; Riviera, A.P.In: Ollis, D.F.; Al-Ekabi, H. (Eds.). *Photocatalytic purification and treatment of water and air*. Elsevier, Amsterdam, 169-178, 1993.

Tang, W.Z. Chapter 9 - UV/Titanium Dioxide, In: *Physicochemical Treatment of Hazardous Wastes*, Lewis Publishers, 321-377, 2004.

Turchi, C.S.; Ollis, D. Photocatalytic degradation of organic water contaminants: mechanism involving hydroxyl radical attack. *Journal of Catalysis 122*, 178-192, 1990.

USEPA. Health and Environmental Effects Document for Chloroanilines ECAO-CIN-G003 (Final Draft), pp. 7, 12-3, 15, 1987.

USEPA, Background Information Document: Procedures Approved for Demonstrating Compliance with 40 CFR, Part 61. National Emission Standard for Hazardous Air Pollutants, 1985.

Voyksner, R.D.; Straub, R.; Keever, J.T.; Freeman, H.S.; Hsu, W.N. Determination of aromatic amines originating from azo dyes by chemical reduction combined with liquid chromatography/mass spectrometry. *Environmental Science and Technology 27*, 1665, 1993.

Wagner, I.; Strehlow, H. Flash photolysis in aqueous periodate-solutions. *Ber. Bunsenges. Phys. Chem.*, **86**, 297, 1982.

Wang, Y.B.; Hong, C.S. Effect of hydrogen peroxide, periodate and persulfate on photocatalysis of 2-chlorobiphenyl in aqueous TiO_2 suspensions. *Water Research 33*, 2031-2036, 1999.

Watanabe, N.; Horikoshi, S.; Kawabe, H.; Sugie, Y.; Zhao, J.; Hidaka, H. Photodegradation mechanism for bisphenol A at the TiO_2/H_2O interfaces. *Chemosphere 52*, 851-859, 2003.

Watson, S.S.; Beydoun, D.; Scott, J.A.; Amal, R. The effect of preparation method on the photoactivity of crystalline titanium dioxide particles. *Chemical Engineering Journal 95*, 213-220, 2003.

Weavers, L.K.; Hua, I.; Hoffmann, M.R. Degradation of triethanolamine and chemical oxygen demand reduction in wastewater by photoactivated periodate. *Water Environment Research 69*, 1112, 1997.

Wei, Y.T.; Wan, C. Kinetics of Photocatalytic oxidation of Phenol on TiO_2 Surface, *Journal of Photochemistry and Photobiology A: Chemistry 69*, 241-249, 1992.

Wen, S.; Zhao, J.; Sheng, G.; Fu, J.; Peng, P. Photocatalytic reactions of phenanthrene at TiO_2/water interfaces, *Chemosphere 46*, 871-877, 2002.

Wilkinson, F.; Helman, W.P.; Ross, A.B. Quantum yields for the photosensitized formation of the lowest electrochemically excited singlet state of molecular oxygen in solution. *Journal of Physical and Chemical Reference Data, 22,* 113-262, 1993.

Winarno, E.K.; Getoff, N. Comparative studies on the degradation of aqueous 2-chloroanilne by O_3 as well as by UV-light and γ–rays in the presence of ozone. *Radiation Physics and Chemistry 65*, 387-395, 2002a.

Winarno, E.K.; Getoff, N. Photo-induced decomposition of 2-chloroaniline in aqueous solution. Journal of Biosciences , 57c, 512-515, 2002b.

Wold, A. Photocatalytic Properties of TiO_2. *Chemistry of Materials 5*, 280-283, 1993.

Wong, C. C.; Chu, W. The hydrogen peroxide-Assisted photocatalytic degradation of alachlor in TiO_2 suspensions. *Environmental Science and Technology 37*, 2310-2316, 2003.

Woolfrey, J.L.; Bartlett, J.R. Processing colloidal powders, sols and gels. In: *Sol-gel Processing of Advanced Materials*, ed. Klein, L.C.; Pope, E.J.A.; Sakka, S.; Woolfrey, J.L., The American Ceramic Society, Westerville, OH, 3-20, 1998.

Wright, J.D.; Sommerdijk, N.A.J.M. Sol-gel materials chemistry and applications. Chapter 2 Silica Sol-Gels: Reaction mechanisms, Gordon and Breach Science Publishers, p.21, 2001.

Yasumori, A.; Shinoda, H.; Kameshima, Y.; Hayashi, S.; Okada, K. Photocatalytic and photoelectrochemical properties of TiO_2-based multiple layer thin film prepared by sol–gel and reactive-sputtering methods *Journal of Materials Chemistry 11*, 1253-1257, 2001

Young, S.K. *Overview of Sol-gel Science and Technology. Army Research Laboratory*, p.1, 2002.

Yu, J.G.; Yu, H.G.; Cheng, B.; Zhao, H.J.; Yu, J.C.; Ho, W.K. The effect of calcination temperature on the surface microstructure and photocatalytic activity of TiO_2 thin films prepared by liquid phase deposition. *Journal of Physical Chemistry B 107*, 13871 – 13879, 2003.

Zhang, F.; Zhao, J.; Shen, T.; Hidaka, H.; Pelizzetti, E.; Serpone, N. TiO_2-assisted photodegradation of dye pollutants II. Adsorption and degradation kinetics of eosin in TiO_2 dispersions under visible light irradiation. *Applied Catalysis B: Environmental 15*, 147-156, 1998.

APPENDIX I

MSDS for o-chloroaniline, 98+%
**** MATERIAL SAFETY DATA SHEET ****

o-chloroaniline, 98+%

** SECTION 1 - CHEMICAL PRODUCT AND COMPANY IDENTIFICATION **

MSDS Name: o-chloroaniline, 98+%
Catalog Numbers:
10857-0000, 10857-0010, 10857-2500
Synonyms:
o-chlorobenzenamine
Company Identification (Europe): Acros Organics BVBA
Janssen Pharmaceuticalaan 3a
2440 Geel, Belgium
Company Identification (USA): Acros Organics
One Reagent Lane
Fairlawn, NJ 07410
For information in North America, call: 800-ACROS-01
For information in Europe, call: 0032(0) 14575211
For emergencies in the US, call CHEMTREC: 800-424-9300
For emergencies in Europe, call: 0032(0) 14575299

**** SECTION 2 - COMPOSITION, INFORMATION ON INGREDIENTS ****

CAS#	Chemical Name	%	EINECS#
95-51-2	o-chloroaniline	98+%	202-426-4

Hazard Symbols: T N
Risk Phrases: 23/24/25 33 50/53

**** SECTION 3 - HAZARDS IDENTIFICATION ****

EMERGENCY OVERVIEW

Toxic by inhalation, in contact with skin and if swallowed. Danger of cumulative effects. Very toxic to aquatic organisms; may cause long-term adverse effects in the aquatic environment.Light sensitive.Air sensitive.

Potential Health Effects
Eye:
May cause eye irritation. Causes redness and pain.

Skin:

May cause skin irritation. May cause skin sensitization, an allergic reaction, which becomes evident upon re-exposure to this material. Causes symptoms similar to those of inhalation. Toxic in contact with skin. Substance is readily absorbed through the skin.

Ingestion:

May cause irritation of the digestive tract. Poison by ingestion. May cause effects similar to those for inhalation exposure.

Inhalation:

May cause cyanosis (bluish discoloration of skin due to deficient oxygenation of the blood). May cause respiratory tract irritation. Toxic if inhaled. Methemoglobinemia is characterized by dizziness, drowsiness, headache, breath shortness, cyanosis with bluish skin, rapid heart rate and chocolate-brown blood. May cause headache. May cause nausea and possible vomiting.

Chronic:

May cause liver and kidney damage.

**** SECTION 4 - FIRST AID MEASURES ****

Eyes:

Immediately flush eyes with plenty of water for at least 15 minutes, occasionally lifting the upper and lower eyelids. Get medical aid immediately.

Skin:

Get medical aid immediately. Immediately flush skin with plenty of soap and water for at least 15 minutes while removing contaminated clothing and shoes.

Ingestion:

Get medical aid immediately. Wash mouth out with water.

Inhalation:

Get medical aid immediately. Remove from exposure to fresh air immediately. If not breathing, give artificial respiration. If breathing is difficult, give oxygen.

Notes to Physician:

Treat symptomatically and supportively.

**** SECTION 5 - FIRE FIGHTING MEASURES ****

General Information:

As in any fire, wear a self-contained breathing apparatus in pressure-demand, MSHA/NIOSH (approved or equivalent), and full protective gear. During a fire, irritating and highly toxic gases may be generated by thermal decomposition or combustion. Containers may explode in the heat of a fire.

Extinguishing Media:

Use water spray, dry chemical, carbon dioxide, or chemical foam.

**** SECTION 6 - ACCIDENTAL RELEASE MEASURES ****

General Information: Use proper personal protective equipment as indicated in Section 8.

Spills/Leaks:

Absorb spill with inert material (e.g. vermiculite, sand or earth), then place in suitable container. Do not flush into a sewer.

**** SECTION 7 - HANDLING and STORAGE ****

Handling:

Do not breathe dust, vapor, mist, or gas. Do not get in eyes, on skin, or on clothing. Take precautionary measures against static discharges. Use only in a chemical fume hood.

Storage:

Keep away from sources of ignition. Store in a cool, dry place. Do not store in direct sunlight. Store in a tightly closed container.

**** SECTION 8 - EXPOSURE CONTROLS, PERSONAL PROTECTION ****

Engineering Controls:

Use adequate ventilation to keep airborne concentrations low.

Personal Protective Equipment

Eyes:

Wear chemical goggles.

Skin:

Wear appropriate protective gloves to prevent skin exposure.

Clothing:

Wear appropriate protective clothing to prevent skin exposure.

Respirators:

Follow the OSHA respirator regulations found in 29CFR 1910.134 or European Standard EN 149. Always use a NIOSH or European Standard EN 149 approved respirator when necessary.

**** SECTION 9 - PHYSICAL AND CHEMICAL PROPERTIES ****

Physical State:	Liquid
Appearance:	clear pale yellow - brown
Odor:	characteristic odor
pH:	Not available.
Vapor Pressure:	0.13 mbar @ 20 deg C
Viscosity:	Not available.
Boiling Point:	209 deg C @760mmHg

Freezing/Melting Point: -3 deg C
Autoignition Temperature: > 500 deg C (> 932.00 deg F)
Flash Point: 98 deg C (208.40 deg F)
Explosion Limits, lower: 2.4 Vol%
Explosion Limits, upper: 14.2 Vol%
Decomposition Temperature: >300 deg C
Solubility in water: 5.13g/l in water (20°C)
Specific Gravity/Density: 1.2130g/cm3
Molecular Formula: C_6H_6ClN
Molecular Weight: 127.57

**** SECTION 10 - STABILITY AND REACTIVITY ****

Chemical Stability:
Stable. Darkens on exposure to light and air.
Conditions to Avoid:
Incompatible materials, light, exposure to air.
Incompatibilities with Other Materials:
Strong oxidizing agents, acids, acid chlorides, acid anhydrides, chloroformates.
Hazardous Decomposition Products:
Hydrogen chloride, nitrogen oxides, carbon monoxide, carbon dioxide, nitrogen.
Hazardous Polymerization: Will not occur.

**** SECTION 11 - TOXICOLOGICAL INFORMATION ****

RTECS#:
CAS# 95-51-2: BX0525000
LD50/LC50:
CAS# 95-51-2: Inhalation, rat: LC50 = 797 ppm/4H; Oral, mouse: LD50 = 256 mg/kg.
Carcinogenicity:
o-chloroaniline -
Not listed by ACGIH, IARC, NIOSH, NTP, or OSHA.
See actual entry in RTECS for complete information.

**** SECTION 12 - ECOLOGICAL INFORMATION ****

Ecotoxicity:
Fish: Leuciscus idus: LC0 = 2mg/l; 48H; .log POW = 1.9
Other
Avoid entering into waters or underground water. Do not empty into drains.

**** SECTION 13 - DISPOSAL CONSIDERATIONS ****

Dispose of in a manner consistent with federal, state, and local regulations.

**** SECTION 14 - TRANSPORT INFORMATION ****

IATA
Shipping Name: CHLOROANILINES, LIQUID
Hazard Class: 6.1
UN Number: 2019
Packing Group: II
IMO
Shipping Name: CHLOROANILINES, LIQUID
Hazard Class: 6.1
UN Number: 2019
Packing Group: II
RID/ADR
Shipping Name: CHLOROANILINES, LIQUID
Hazard Class: 6.1
UN Number: 2019
Packing group: II

**** SECTION 15 - REGULATORY INFORMATION ****

European/International Regulations
European Labeling in Accordance with EC Directives
Hazard Symbols: T N
Risk Phrases:

R 23/24/25 Toxic by inhalation, in contact with skin and if swallowed.

R 33 Danger of cumulative effects.

R 50/53 Very toxic to aquatic organisms; may cause long-term adverse effects in the aquatic environment.

Safety Phrases:

S 28A After contact with skin, wash immediately with plenty of water.

S 36/37 Wear suitable protective clothing and gloves.

S 45 In case of accident or if you feel unwell, seek medical advice immediately (show the label where possible).

S 60 This material and/or its container must be disposed of as hazardous waste.

S 61 Avoid release to the environment. Refer to special instructions/Safety data sheets.

WGK (Water Danger/Protection)
CAS# 95-51-2: 2
United Kingdom Occupational Exposure Limits

Canada
CAS# 95-51-2 is listed on Canada's DSL List.

CAS# 95-51-2 is not listed on Canada's Ingredient Disclosure List.

Exposure Limits

CAS# 95-51-2: Not available.

US FEDERAL

TSCA

CAS# 95-51-2 is listed on the TSCA inventory.

**** SECTION 16 - ADDITIONAL INFORMATION ****

MSDS Creation Date: 7/16/1996 Revision #1 Date: 2/02/2001

The information above is believed to be accurate and represents the best information currently available to us. However, we make no warranty of merchantability or any other warranty, express or implied, with respect to such information, and we assume no liability resulting from its use. Users should make their own investigations to determine the suitability of the information for their particular purposes. In no way shall the company be liable for any claims, losses, or damages of any third party or for lost profits or any special, indirect, incidental, consequential or exemplary damages, howsoever arising, even if the company has been advised of the possibility of such damages.

APPENDIX II: Experimental runs

	Run	wavelength, nm	[o-ClA], mM	[TiO_2] (P25), gL^{-1}	Oxidants		pH
					compound	conc, mM	
Dark reaction	A-1	-	0.57	0.1	-	-	2
	A-2	-	0.28	0.1	-	-	2
	A-3	-	0.095	0.1	-	-	2
	A-4	-	0.019	0.1	-	-	2
	A-5	-	0.57	0.1	-	-	4
	A-6	-	0.28	0.1	-	-	4
	A-7	-	0.095	0.1	-	-	4
	A-8	-	0.019	0.1	-	-	4
	A-9	-	0.57	0.1	-	-	7
	A-10	-	0.28	0.1	-	-	7
	A-11	-	0.095	0.1	-	-	7
	A-12	-	0.019	0.1	-	-	7
	A-13	-	0.57	0.1	-	-	11
	A-14	-	0.28	0.1	-	-	11
	A-15	-	0.095	0.1	-	-	11
	A-16	-	0.019	0.1	-	-	11
TiO_2 suspension	A-17	300	0.095	0	-	-	7
	A-18	300	0.095	0.1	-	-	7
	A-19	300	0.19	0.1	-	-	7
	A-20	300	0.285	0.1	-	-	7
	A-21	300	0.57	0.1	-	-	7
	A-22	300	0.095	0.017	-	-	7
	A-23	300	0.095	0.05	-	-	7
	A-24	300	0.095	0.5	-	-	7
	A-25	300	0.095	1	-	-	7
	A-26	300	0.095	1.6	-	-	7
	A-27	300	0.095	0.1	-	-	2
	A-28	300	0.095	0.1	-	-	5
	A-29	300	0.095	0.1	-	-	9
	A-30	300	0.095	0.1	-	-	11
	A-31	254	0.095	0.1	-	-	7
	A-32	350	0.095	0.1	-	-	7
	A-33	300	0.095	-	-	-	7
	A-34	254	0.095	-	-	-	7
	A-35	350	0.095	-	-	-	7

(Cont’d)

Effect of oxidants	B-1	300	0.095	0.1	H_2O_2	0.01	7
	B-2	300	0.095	0.1	H_2O_2	0.01	2
	B-3	300	0.095	0.1	H_2O_2	0.01	4
	B-4	300	0.095	0.1	H_2O_2	0.01	9
	B-5	300	0.095	0.1	H_2O_2	0.01	12
	B-6	300	0.095	0.1	H_2O_2	100	7
	B-7	300	0.095	0.1	H_2O_2	200	7
	B-8	300	0.095	0.1	H_2O_2	300	7
	B-9	300	0.095	0.1	H_2O_2	400	7
	B-10	300	0.095	0.1	RB	0.5	7
	B-11	300	0.095	0.1	RB	1	7
	B-12	300	0.095	0.1	RB	5	7
	B-13	300	0.095	0.1	RB	10	7
	B-14	300	0.095	-	ClO_3^-	0.195	7
	B-15	300	0.095	-	BrO_3^-	0.195	7
	B-16	300	0.095	-	IO_3^-	0.195	7
	B-17	300	0.095	0.1	ClO_3^-	0.195	7
	B-18	300	0.095	0.1	BrO_3^-	0.195	7
	B-19	300	0.095	0.1	IO_3^-	0.039	
	B-20	300	0.095	0.1	IO_3^-	0.078	
	B-21	300	0.095	0.1	IO_3^-	0.137	7
	B-22	300	0.095	0.1	IO_3^-	0.175	7
	B-23	300	0.095	0.1	IO_3^-	0.078	2.5
	B-24	300	0.095	0.1	IO_3^-	0.078	5
	B-25	300	0.095	0.1	IO_3^-	0.078	9
	B-26	300	0.095	0.1	IO_3^-	0.078	11
	B-27	300	0.095	0.1	IO_3^-	0.039	2.5
	B-28	300	0.095	0.1	IO_3^-	0.195	2.5
	B-29	300	0.095	0.1	IO_3^-	0.039	11
	B-30	300	0.095	0.1	IO_3^-	0.195	11
	B-31	300	0.095	0.1	2nd IO_3^- at 5 min	0.156×2	7
	B-32	300	0.285	0.1	2nd IO_3^- at 7.5 min	0.156×2	7
	B-33	300	0.285	0.1	2nd IO_3^- at 10 min	0.156×2	7
	B-34	300	0.285	0.1	2nd IO_3^- at 15 min	0.156×2	7
	B-35	300	0.285	0.1	2nd IO_3^- at 20 min	0.156×2	7

(cont’d)

Photo-products	C-1	300	0.95	0.1	-	-	7
	C-2	300	0.95	0.1	IO_3^-	0.78	7
	C-3	300	0.93 [IA]	0.1	-	-	7

	Run	Wavelength, nm	$[o\text{-}ClA]_0$, mM	Weight of coating, g	Annealing temp, °C	substrate	pH
TiO_2 film	D-1	350	0.095	0.0159	700	Quartz	7
	D-2	350	0.095	0.0298	450	Quartz	7
	D-3	350	0.095	0.0253	250	Quartz	7
	D-4	350	0.095	0.0063	450	Glass	7
	D-5	350	0.095	0.0151	450	Glass	7
	D-6	350	0.095	0.0285	450	Glass	7
	D-7	350	0.095	0.0466	450	Glass	7

APPENDIX III: Mass spectrums of o-ClA and identified intermediates

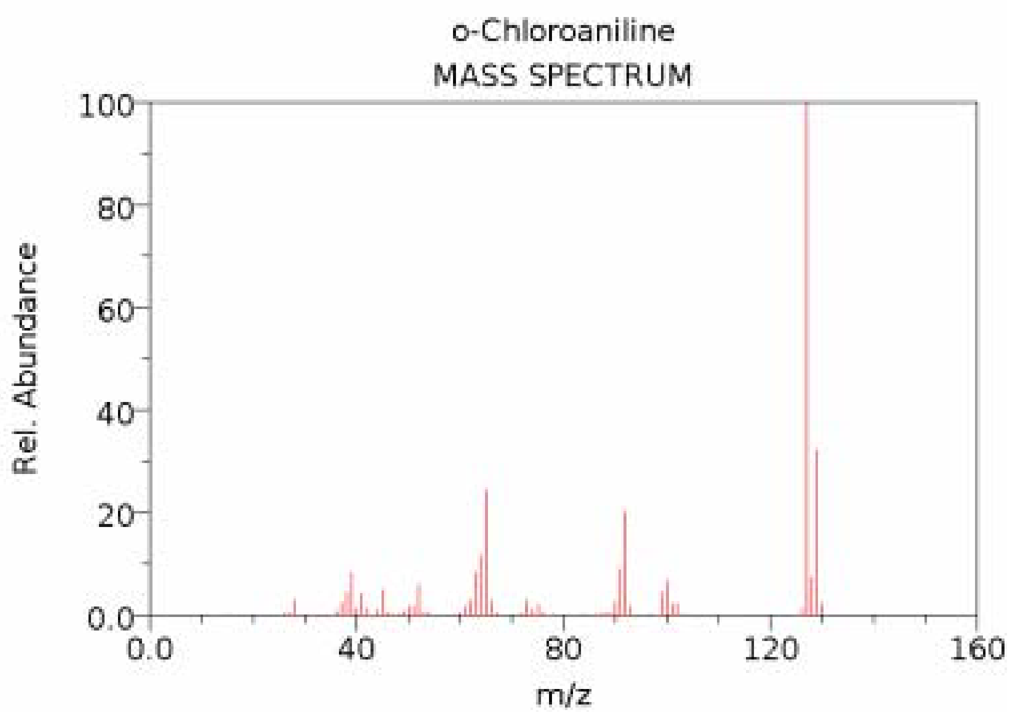

NIST Chemistry WebBook (http://webbook.nist.gov/chemistry)

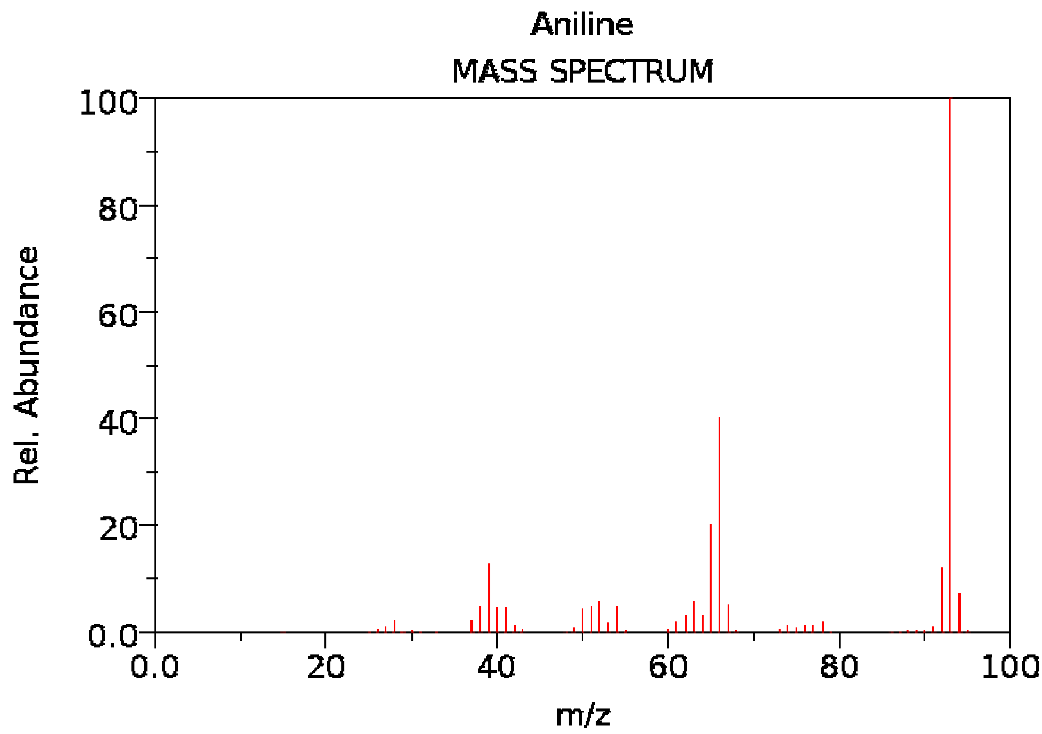

NIST Chemistry WebBook (http://webbook.nist.gov/chemistry)

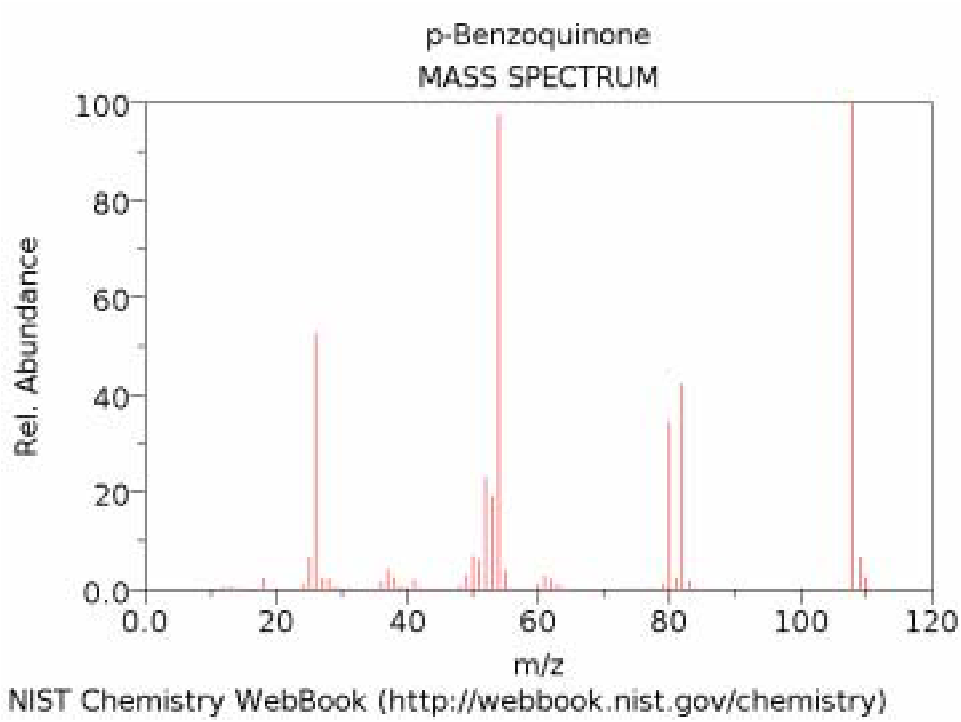
p-Benzoquinone
MASS SPECTRUM
Rel. Abundance
100
80
60
40
20
0.0
0.0
20
40
60
80
100
120
m/z
NIST Chemistry WebBook (http://webbook.nist.gov/chemistry)

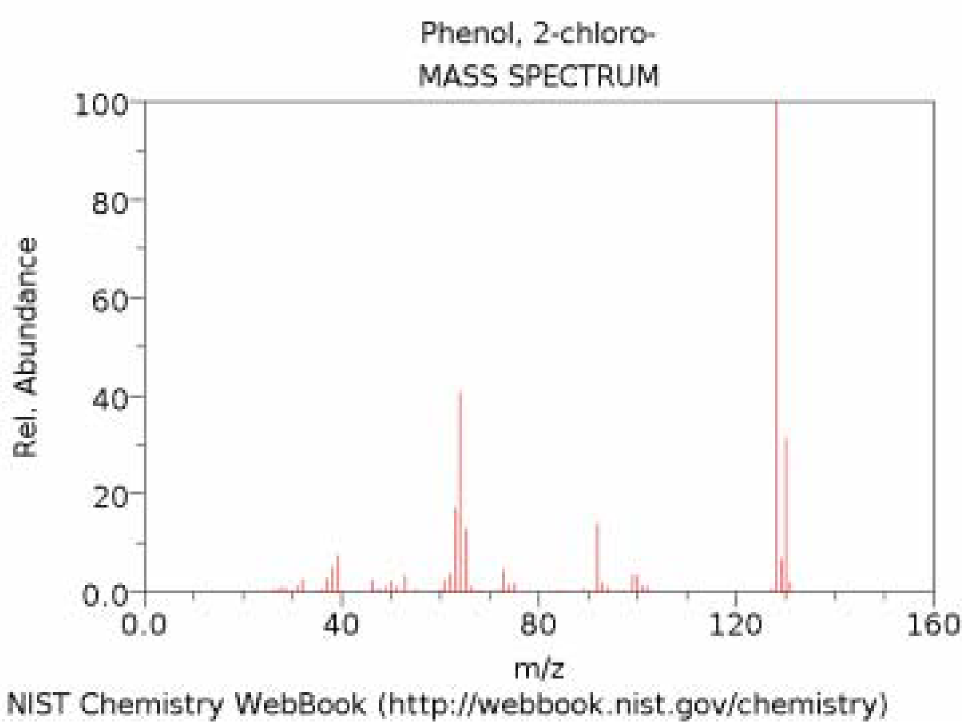
Phenol, 2-chloro-
MASS SPECTRUM
Rel. Abundance
100
80
60
40
20
0.0
0.0
40
80
120
160
m/z
NIST Chemistry WebBook (http://webbook.nist.gov/chemistry)

1,4-Benzenediol, 2-chloro-
MASS SPECTRUM

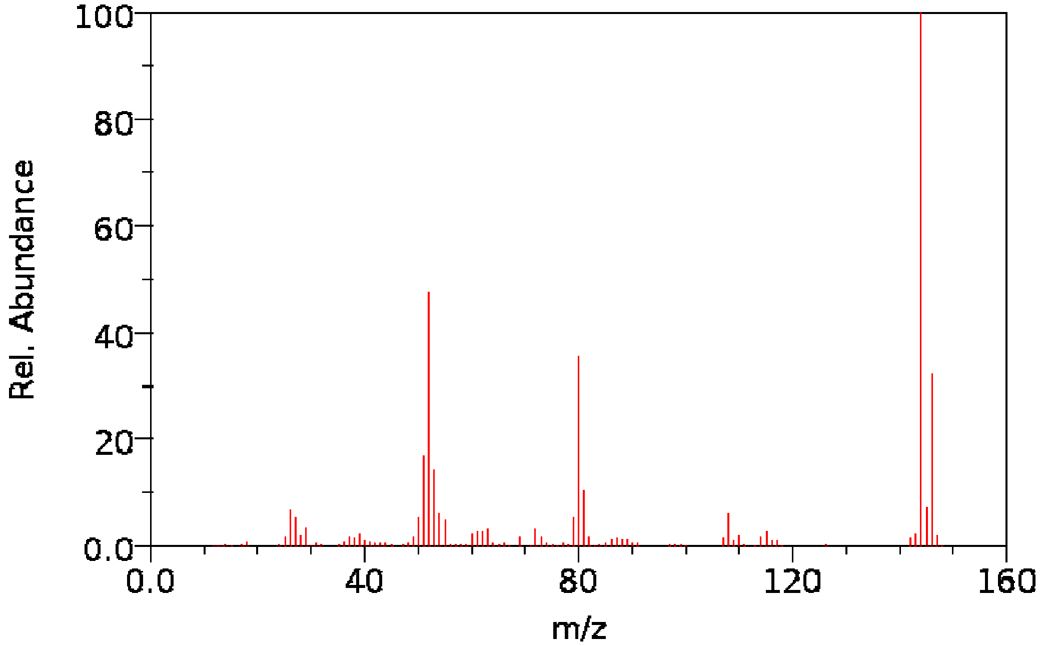

NIST Chemistry WebBook (http://webbook.nist.gov/chemistry)

Benzene, 1-chloro-2-nitro-
MASS SPECTRUM

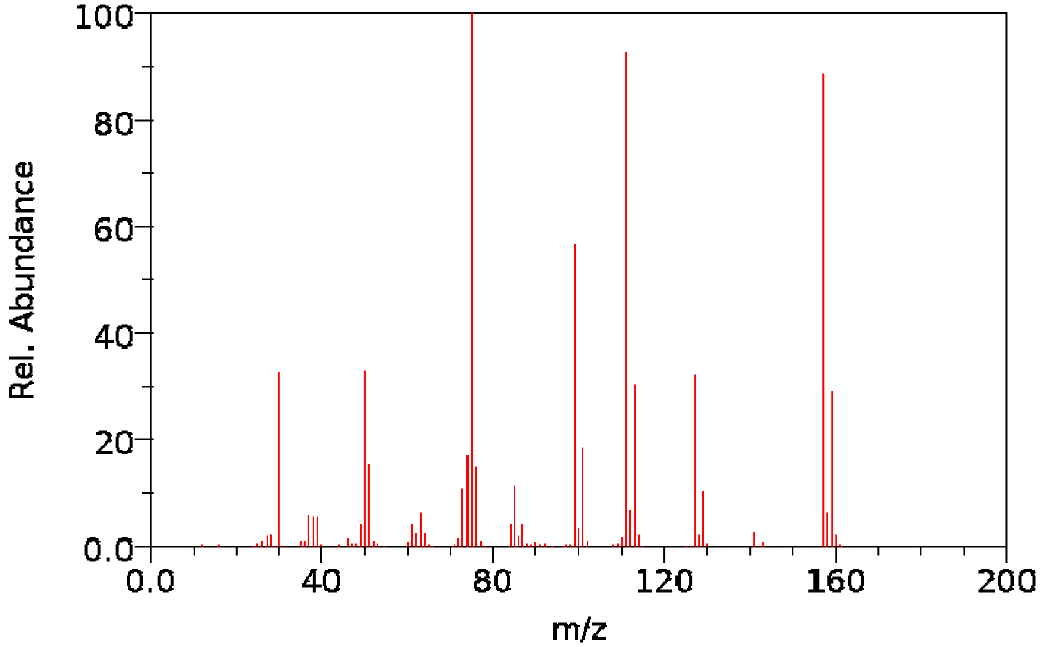

NIST Chemistry WebBook (http://webbook.nist.gov/chemistry)

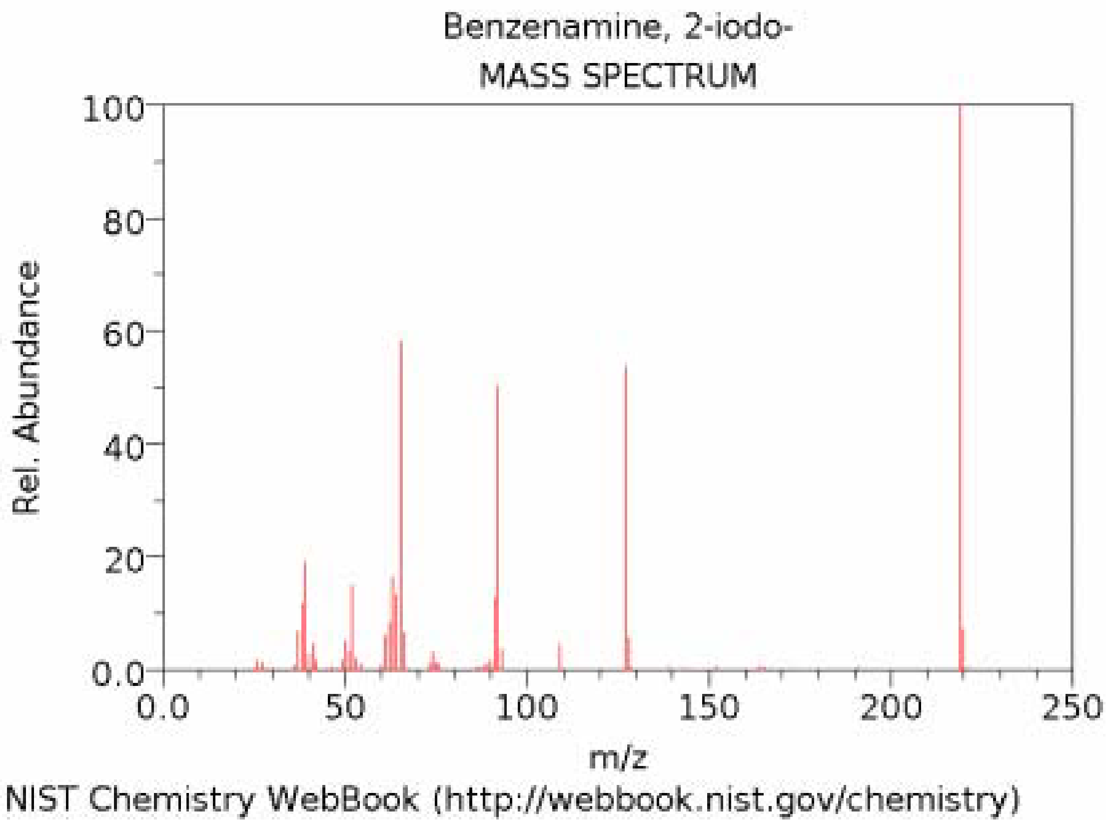
Benzenamine, 2-iodo-
MASS SPECTRUM

NIST Chemistry WebBook (http://webbook.nist.gov/chemistry)

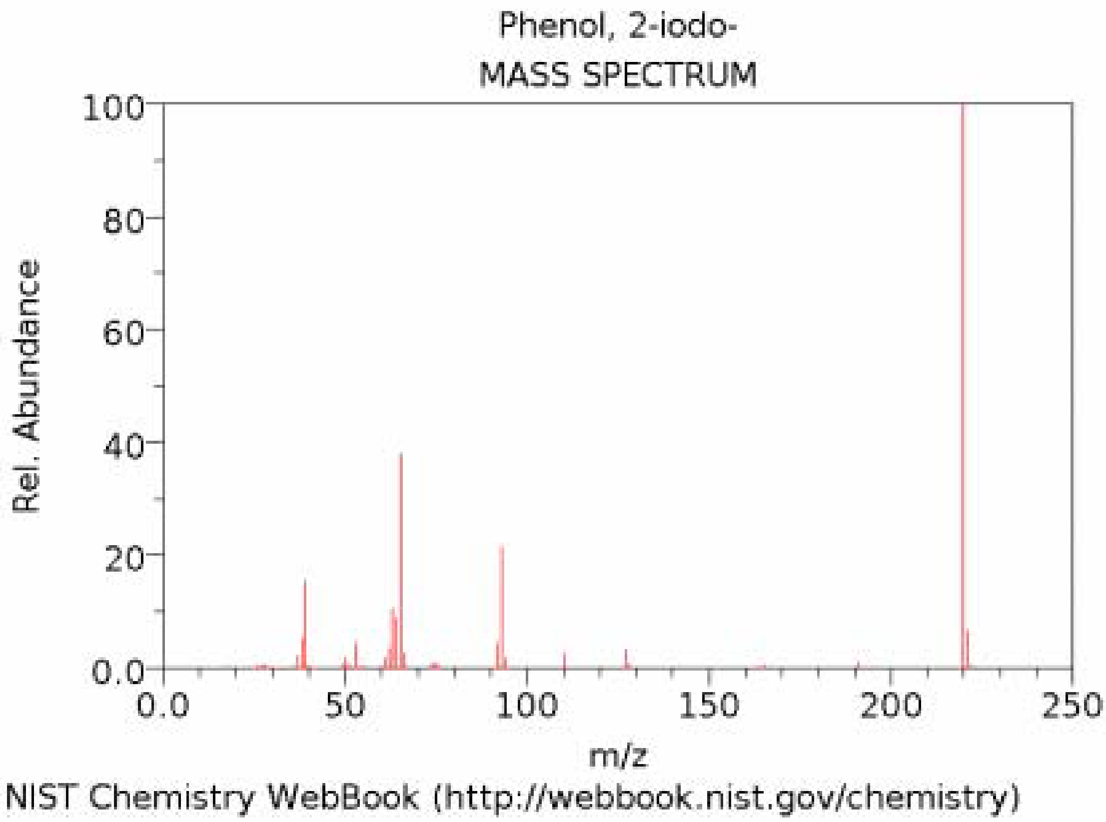
Phenol, 2-iodo-
MASS SPECTRUM

NIST Chemistry WebBook (http://webbook.nist.gov/chemistry)

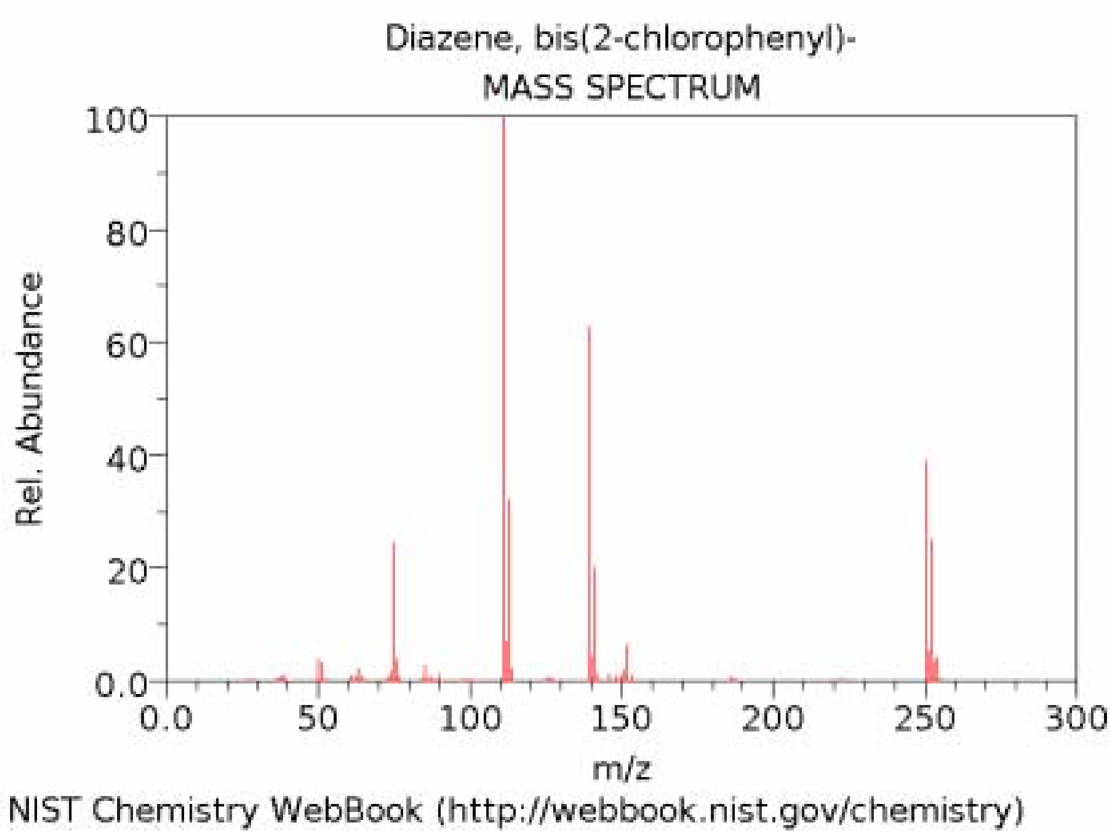
Diazene, bis(2-chlorophenyl)-
MASS SPECTRUM
Rel. Abundance
100
80
60
40
20
0.0
0.0
50
100
150
200
250
300
m/z
NIST Chemistry WebBook (http://webbook.nist.gov/chemistry)

APPENDIX IV: Absorption spectrum of o-ClA and RB

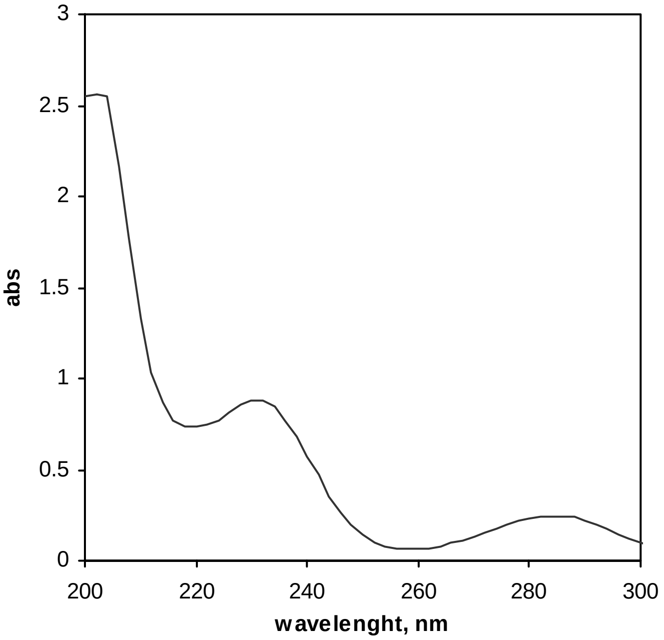

Figure A-1: Absorption spectrum of o-ClA at 0.095 mM.

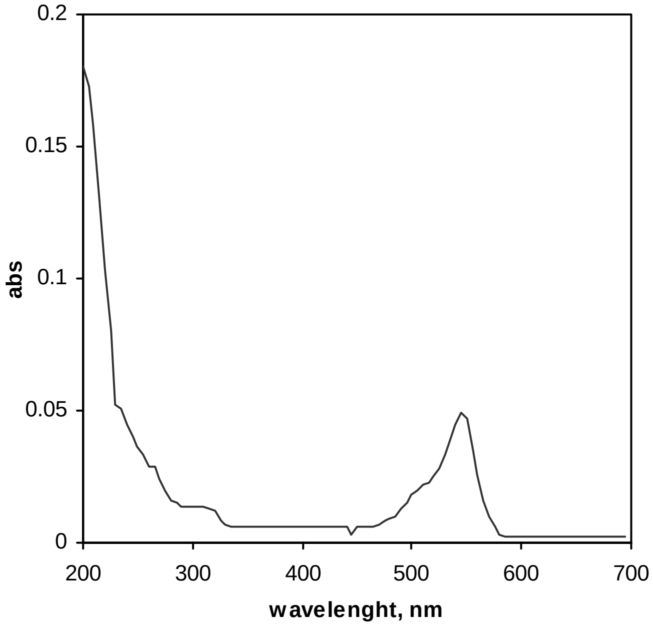

Figure A-2: Absorption spectrum of rose bengal at 1 mgL^{-1}.

APPENDIX V: Experimental data

$[ClA]_0$=0.095 mM $[TiO_2]$=0.1g/L 2 lamps at 254nm

t	R.T.	Area	ppm	C/C_0	$\ln(C/C_0)$
0	5.162	1113256	10.1252	1	0
9	5.162	722496	6.571192	0.6489936	-0.43233
18	5.147	567267	5.159365	0.5095567	-0.67421
27	5.147	374164	3.403069	0.3360988	-1.09035
36	5.127	288830	2.626945	0.2594462	-1.34921
45	5.134	220027	2.001173	0.1976428	-1.62129

$[ClA]_0$=0.095 mM no TiO_2 2 lamps at 254nm

t	R.T.	Area	ppm	C/C_0	$\ln(C/C_0)$
0	5.163	1302252	11.84415	1	0
9	5.168	1095531	9.963992	0.8412588	-0.17286
18	5.161	939240	8.542506	0.7212429	-0.32678
27	5.163	810750	7.373873	0.6225754	-0.47389
36	5.163	790885	7.193199	0.607321	-0.4987
45	5.152	599401	5.451628	0.4602803	-0.77592

$[ClA]_0$=0.095 mM $[TiO_2]$=0.1g/L 2 lamps at 300nm

t	R.T.	Area	ppm	C/C_0	$\ln(C/C_0)$
0	5.033	1082437	10.08081	1	0
9	5.035	785795	7.318162	0.7259499	-0.32027
18	5.046	617371	5.749618	0.5703528	-0.5615
28	5.034	460052	4.284496	0.425015	-0.85563
36	5.049	367846	3.425775	0.3398313	-1.07931
45	5.043	273808.8	2.55	0.2529559	-1.37454

$[ClA]_0$=0.095 mM no TiO_2 2 lamps at 300nm

t	R.T.	Area	ppm	C/C_0	$\ln(C/C_0)$
0	5.05	1260868	11.74255	1	0
9	5.049	1203850	11.21154	0.9547788	-0.04628
18	5.046	1140669	10.62313	0.9046696	-0.10019
25	5.042	1088775	10.13984	0.8635123	-0.14675
30	5.038	1051406	9.791816	0.8338748	-0.18167
45	5.042	965653.84	8.9932	0.7658643	-0.26675

$[ClA]_0$=0.095 mM $[TiO_2]$=0.1g/L   2 lamps at 350nm

t	R.T.	Area	ppm	C/C_0	$\ln(C/C_0)$
0	5.144	1255476	11.41871	1	0
9	5.145	990219	9.006166	0.78872	-0.23734
18	5.133	818871	7.447735	0.6522395	-0.42734
27	5.137	701627	6.381386	0.5588534	-0.58187
36	5.133	587378.88	5.342285	0.4678535	-0.7596
45	5.129	485786.91	4.418293	0.3869344	-0.9495

$[ClA]_0$=0.095 mM   no TiO_2 2 lamps at 350nm

t	R.T.	Area	ppm	C/C_0	$\ln(C/C_0)$
0	5.129	1315948	11.96871	1	0
9	5.114	1301812.2	11.84015	0.9892581	-0.0108
18	5.132	1287427	11.70931	0.9783267	-0.02191
27	5.124	1273994.6	11.58714	0.9681193	-0.0324
36	5.13	1260309.5	11.46267	0.9577198	-0.0432
45	5.128	1246506	11.33713	0.9472304	-0.05421

$[ClA]_0$=0.095 mM   [TiO2]=0.1g/L

time	R.T	area	ppm	C/C_0	$\ln(C/C_0)$
0	5.075	1475327	9.887455	1	0
5	5.088	656774	4.401616	0.4451718	-0.80929
10	5.08	405218	2.71572	0.2746632	-1.29221
15	5.092	203989	1.367109	0.138267	-1.97857
20	5.089	99625	0.667674	0.0675274	-2.69522
25	5.078	60782	0.407353	0.041199	-3.18934
30	5.087	30392	0.203683	0.0206002	-3.88246
40	5.076	9018	0.060437	0.0061125	-5.09741

$[ClA]_0$=0.19 mM $[TiO_2]$=0.1g/L   97286.585

time	R.T., min	area	ppm	C/C_0	$\ln(C/C_0)$
0	5.19	2393250	24.5999	1	0
10	5.19	1315353	13.52034	0.5496095	-0.59855
20	5.181	823018	8.459691	0.3438914	-1.06743
30	5.161	525622	5.402798	0.2196269	-1.51583
40	5.168	324673	3.33727	0.135662	-1.99759

$[ClA]_0$=0.28 mM $[TiO_2]$=0.1g/L 101618.24

time	R.T	area	ppm	C/C_0	$\ln(C/C_0)$
0	5.197	3688742	36.30008	1	0
10	4.966	2187560	21.52729	0.5930369	-0.5225
20	4.968	1563330	15.38438	0.4238112	-0.85847
30	4.966	1113290	10.95564	0.3018075	-1.19797
40	4.966	886870	8.727489	0.2404261	-1.42534

$[ClA]_0$=0.57 mM $[TiO_2]$=0.1g/L 101533.64

time	R.T	area	ppm	C/C_0	$\ln(C/C_0)$
0	5.181	7371342	72.59974	1	0
11	5.175	5719773	56.33357	0.7759473	-0.25367
20	5.184	4992530	49.17102	0.6772892	-0.38966
30	5.179	4236266	41.72263	0.574694	-0.55392
40	5.158	4002326	39.41858	0.5429576	-0.61072

Adsorption

t	ppm	C/C_0	% loss
0	12.1304139	1	0
10	11.3213507	0.9333029	6.669708
30	11.28440503	0.9302572	6.974279
50	11.27515706	0.9294948	7.050517
90	11.33502402	0.9344301	6.556989
120	11.26811715	0.9289145	7.108552
150	10.91239837	0.8995899	10.04101
180	11.20705839	0.923881	7.611904
1080	10.42017738	0.8590125	14.09875

$[ClA]_0$=0.095 mM no TiO_2

t	R.T	area	ppm	C/C_0	$\ln(C/C_0)$
0	5.501	580962	8.73325	1	0
15	5.25	360975	5.426319	0.6213401	-0.47588
30	5.02	235298	3.537092	0.4050144	-0.90383
45	4.92	164248	2.469041	0.2827173	-1.26331
70	4.849	60573	0.910557	0.1042633	-2.26084
90	4.841	49363	0.742044	0.0849677	-2.46548
120	4.834	17528	0.263488	0.0301706	-3.50089
150	4.891	3870	0.058175	0.0066614	-5.01143

$[ClA]_0$=0.095 mM TiO_2=0.017g/L

t	R.T.	Area	ppm	C/C_0	$\ln(C/C_0)$
0	5.069	1143540	12.10992	1	0
7	5.087	477309	5.054633	0.417396	-0.87372
12	5.166	272575	2.88653	0.2383607	-1.43397
18	5.121	145804	1.544043	0.1275023	-2.05962
30	5.192	35238	0.373165	0.0308148	-3.47976
36		17375	0.184	0.0151942	-4.1868

$[ClA]_0$=0.095 mM TiO_2=1.6g/L

t	R.T.	Area	ppm	C/C_0	$\ln(C/C_0)$
0	4.952	1199041	12.11924	1	0
6	4.945	469927	4.74976	0.391919	-0.9367
12	4.937	192166	1.942307	0.1602664	-1.83092
18.5	5.039	52333	0.528953	0.0436457	-3.13165
24		22315	0.225552	0.018611	-3.984
30		8242	0.083308	0.006874	-4.98

$[ClA]_0$=0.095 mM $[TiO_2]$=0.1g/L

time	R.T	area	ppm	C/C_0	$\ln(C/C_0)$
0	5.092	1545257	11.85258	1	0
5	5.093	855944	6.565347	0.5539169	-0.59074
10	5.075	529045	4.057934	0.342367	-1.07187
15	5075	323570	2.481879	0.2093956	-1.56353
20	5.088	201952	1.549032	0.1306915	-2.03492
30	5.078	71236	0.546401	0.0460998	-3.07695

$[ClA]_0$=0.095 mM $[TiO_2]$=0.1g/L

time	R.T	area	ppm	C/C_0	$\ln(C/C_0)$
0	5.081	1533010	11.75865	1	0
5	5.079	735038	5.637962	0.4794737	-0.73507
10	5.077	482959	3.70444	0.3150397	-1.15506
15	5.075	341593	2.620121	0.222825	-1.50137
20	5.067	204431	1.568047	0.1333527	-2.01476
30		72379	0.555169	0.0472137	-3.05307

$[ClA]_0$=0.095 mM $[TiO_2]$=0.1g/L

time	R.T	area	ppm	C/C_0	$\ln(C/C_0)$
0	5.102	1576633	12.09325	1	0
5	5.143	1006308	7.718684	0.6382639	-0.449
10	5.131	683083	5.239451	0.4332543	-0.83643
15	5.116	484158	3.713637	0.3070835	-1.18064
20	5.117	339248	2.602134	0.2151725	-1.53632
25	5.11	244165	1.872819	0.1548648	-1.8652
30	5.108	181077	1.388915	0.1148504	-2.16412

$[ClA]_0$=0.095 mM $[TiO_2]$=0.1g/L

t	R.T	area	ppm	C/C_0	$\ln(C/C_0)$
0	5.03	824261	12.39062	1	0
6	5.074	545059	8.193542	0.6612699	-0.41359
12	5.086	442446	6.651023	0.536779	-0.62217
18	5.083	436789	6.565985	0.5299159	-0.63504
24	5.109	433182	6.511763	0.5255398	-0.64333
30	5.162	430660	6.473851	0.5224801	-0.64917

$[ClA]_0$=0.095 mM $[TiO_2]$=0.1g/L H_2O_2=0.6 M

time	R.T	area	ppm	C/C_0	$\ln(C/C_0)$
0	5.089	1769778	11.86083	1	0
4	5	1197856	8.02788	0.6768397	-0.39032
8	5.049	864168	5.791545	0.4882918	-0.71684
12	5.072	638994	4.282457	0.3610588	-1.01871
16	5.027	428540	2.872021	0.2421434	-1.41823
20	5.041	300044	2.010857	0.1695376	-1.77468

$[ClA]_0$=0.095 mM $[TiO_2]$=0.1g/L H_2O_2=0.4 M

time	R.T	area	ppm	C/C_0	$\ln(C/C_0)$
0	5.017	1817708	12.18205	1	0
5	5	1076618	7.215358	0.5922943	-0.52375
10	5.087	730974	4.898896	0.4021405	-0.91095
15	5.108	460894	3.088853	0.2535578	-1.37216
20	5.119	281942	1.88954	0.1551085	-1.86363

$[ClA]_0$=0.095 mM $[TiO_2]$=0.1g/L H_2O_2=0.3 M

time	R.T	area	ppm	C/C_0	$\ln(C/C_0)$
0	5.071	1813832	12.15607	1	0
4	5.024	1058656	7.094979	0.5836571	-0.53844
8	5.059	759616	5.090851	0.4187907	-0.87038
12	5.052	528542	3.542222	0.2913952	-1.23307
16	5.086	352546	2.362719	0.1943653	-1.63802

$[ClA]_0$=0.095 mM $[TiO_2]$=0.1g/L H_2O_2=0.2 M

time	R.T	area	ppm	C/C_0	$\ln(C/C_0)$
0	5.1	1739292	11.65652	1	0
5	5.089	1009378	6.764724	0.5803384	-0.54414
10	5.101	615946	4.127992	0.3541361	-1.03807
15	5.106	370744	2.48468	0.213158	-1.54572
20	5.101	194560	1.303917	0.1118616	-2.19049

$[ClA]_0$=0.095 mM $[TiO_2]$=0.1g/L H_2O_2=0.1 M

time	R.T	area	ppm	C/C_0	$\ln(C/C_0)$
0	5.079	1819938	12.19699	1	0
5	4.959	791972	5.307696	0.4351643	-0.83203
10	4.992	384144	2.574485	0.2110753	-1.55554
15	5.029	157684	1.056778	0.0866425	-2.44596
20	4.976	37284	0.249873	0.0204864	-3.88799
25	5.078	7898	0.052931	0.0043397	-5.43995

$[ClA]_0$=0.095 mM $[TiO_2]$=0.1g/L H_2O_2=0.0 M

time	R.T	area	ppm	C/C_0	$\ln(C/C_0)$
0	5.089	1747144	11.70914	1	0
5	5.042	1134972	7.606439	0.6496156	-0.43137
10	5.1	696984	4.671099	0.3989276	-0.91898
15	5.112	495636	3.32169	0.2836835	-1.2599
20	5.052	305098	2.044728	0.1746267	-1.7451

$[ClA]_0$=0.095 mM $[TiO_2]$=0.1g/L H_2O_2=0.01 M

time	R.T	area	ppm	C/C_0	$\ln(C/C_0)$
0	5.045	1809412	12.12645	1	0
4	5.013	1066688	7.148808	0.5895219	-0.52844
8	5.009	662350	4.438986	0.3660581	-1.00496
12	5.024	354074	2.372959	0.1956846	-1.63125
16	5.025	193552	1.297161	0.1069696	-2.23521
20	5.028	84876	0.568828	0.0469081	-3.05957

$[ClA]_0$=0.095 mM $[TiO_2]$=0.1g/L H_2O_2=0.003 M

time	R.T	area	ppm	C/C_0	$\ln(C/C_0)$
0	5.079	1756782	11.77373	1	0
5	5.025	784278	5.256132	0.4464288	-0.80648
10	5.038	448214	3.003874	0.2551335	-1.36597
15	5.034	206968	1.387073	0.1178109	-2.13867
21	5.039	94376	0.632496	0.053721	-2.92395
25	5.034	49856	0.334129	0.0283792	-3.5621

$[ClA]_0$=0.095 mM $[TiO_2]$=0.1g/L H_2O_2=0.00088 M

time	R.T	area	ppm	C/C_0	$\ln(C/C_0)$
0	5.107	1316080	12.18762	1	0
6	5.099	568160	5.261472	0.4317063	-0.84001
12	5.113	294622	2.72836	0.2238633	-1.49672
16	5.105	707680.22	1.85971	0.1525901	-1.88
20	5.118	137774	1.275862	0.1046851	-2.2568

$[ClA]_0$=0.095 mM $[TiO_2]$=0.1g/L H_2O_2=0.00044 M

time	R.T	area	ppm	C/C_0	ln(C/C0)
0	5.084	1384886	12.8248	1	0
6	5.098	611370	5.66162	0.4414587	-0.81767
12	5.098	343352	3.179627	0.247928	-1.39462
16	5.0865	611791.98	2.263655	0.1765061	-1.7344
20.5	5.112	166462	1.541529	0.1201991	-2.11861

$[ClA]_0$=0.095 mM $[TiO_2]$=0.1g/L   RB=10 mg/L

time	R.T	area	ppm	C/C_0	$\ln(C/C_0)$
0	5.104	1708286	11.44872	1	0
5.5	5.095	1438864	9.643085	0.8422852	-0.17164
10	5.094	1395046	9.349422	0.8166349	-0.20256
20	5.137	1230570	8.247125	0.7203536	-0.32801
30	5.138	1018070	6.822977	0.5959599	-0.51758

$[ClA]_0$=0.095 mM $[TiO_2]$=0.1g/L   RB=5mg/L

time	R.T	area	ppm	C/C_0	$\ln(C/C_0)$
0	5.097	1695698	11.36435	1	0
5	5.084	1457584	9.768544	0.8595776	-0.15131
10	5.125	1305554	8.749658	0.7699213	-0.26147
15	5.088	1211300	8.11798	0.7143371	-0.3364
20	5.079	1010454	6.771935	0.5958927	-0.51769
30	5.057	70487	0.4724	0.0415686	-0.75

$[ClA]_0$=0.095 mM $[TiO_2]$=0.1g/L RB=1mg/L

time	R.T	area	ppm	C/C_0	$\ln(C/C_0)$
0	5.149	1658272	11.11353	1	0
5	5.151	1371444	9.191245	0.827032	-0.18991
10	5.163	1053034	7.057301	0.6350189	-0.4541
16.5	5.14	744318	4.988325	0.4488516	-0.80106
20	5.132	583310	3.90927	0.3517577	-1.04481
30	5.127	326278	2.186674	0.1967578	-1.62578

$[ClA]_0$=0.095 mM $[TiO_2]$=0.1g/L RB=0.5mg/L

time	R.T	area	ppm	C/C_0	$\ln(C/C_0)$
0	5.072	1684870	11.29179	1	0
5	5.073	1080080	7.23856	0.6410465	-0.44465
10	5.076	776598	5.204662	0.4609246	-0.77452
15	5.08	573682	3.844744	0.3404904	-1.07737
20	5.086	413134	2.768772	0.2452023	-1.40567
30	5.076	247260.74	1.65711	0.1467536	-1.919

$[ClA]_0$=0.095 mM $[ClO_3^-]$=0.195 mM

t	R.T.	area	ppm	C/C_0	$\ln(C/C_0)$
0	5.022	1250833	11.64909	1	0
15	5.046	760428	7.081918	0.6079373	-0.49768
30	5.033	472484	4.400276	0.3777355	-0.97356
45	5.028	267603	2.492205	0.2139398	-1.54206
60	5.029	160196	1.491916	0.1280715	-2.05517

$[ClA]_0$=0.095 mM $[BrO_3^-]$=0.195 mM

t	R.T.	area	ppm	C/C_0	$\ln(C/C_0)$
0	5.024	1258193	11.71764	1	0
15	5.022	806374	7.509816	0.6408985	-0.43902
30	5.026	521840	4.859931	0.4147535	-0.8742
45	4.785	321074	2.990184	0.2551866	-1.35989
60	4.783	211822	1.972713	0.1683541	-1.77582

$[ClA]_0$=0.095 mM $[IO_3^-]$=0.195 mM

t	R.T.	area	ppm	C/C_0	$\ln(C/C_0)$
0	5.031	1245519	11.5996	1	0
15	5.022	824515	7.678764	0.6619851	-0.41677
30	5.026	574727	5.352472	0.4614358	-0.77767
45	4.785	409257	3.811438	0.3285835	-1.11722
60	4.783	320799	2.987623	0.2575625	-1.36075

$[ClA]_0$=0.095 mM $[TiO_2]$=0.1g/L $[ClO_3^-]$=0.195 mM

time	R.T.	Area	ppm	C/C_0	$\ln(C/C_0)$
0	5.01	1132094	12.10006	1	0
5	4.989	534250	5.710178	0.4719131	-0.75096
10.5	4.931	285065	3.046836	0.2518033	-1.37911
15	4.912	129664	1.385877	0.1145347	-2.16688
20	5.001	68093	0.727793	0.0601478	-2.81095
30	4.985	13763	0.147102	0.0121571	-4.40984

$[ClA]_0$=0.095 mM $[TiO_2]$=0.1g/L $[BrO_3^-]$ =0.195 mM

time	R.T.	Area	ppm	C/C_0	$\ln(C/C_0)$
0	5.026	1050050	10.38143	1	0
3	5.021	570064	5.635995	0.5428922	-0.61084
6	5.016	409145	4.045053	0.3896434	-0.94252
10	5.017	286249	2.83003	0.2726051	-1.29973
15	5.08	195715	1.934956	0.1863864	-1.67993
20	5.083	121221	1.198464	0.1154431	-2.15898
30	5.095	37861	0.374317	0.0360564	-3.32267

$[ClA]_0$=0.095 mM $[TiO_2]$=0.1g/L $[IO_3^-]$=0.195 mM

t	R.T.	Area	ppm	C/C_0	$\ln(C/C_0)$
0	5.178	1166969	10.86806	1	0
1.5	5.18	303810	2.829403	0.2603411	-1.34576
3	5.192	50285	0.468308	0.0430903	-3.14446
5	5.172	9758	0.090877	0.0083618	-4.78408

$[ClA]_0$=0.095 mM $[TiO_2]$=0.1g/L $[IO_3^-]$=0.175 mM

time	R.T	area	ppm	$\ln(C/C_0)$	C/C_0
0	4.95	1183215	11.01936	1	0
2.5	4.94	129527	1.206294	0.1094704	-2.2121
5	4.933	17565	0.163584	0.0148451	-4.21008
8	4.939	7411	0.069019	0.0062634	-5.07303
12.5	4.939	7302	0.068004	0.0061713	-5.08784
16	4.982	8236	0.076702	0.0069607	-4.96748
20	4.937	7912	0.073685	0.0066869	-5.00761

[ClA]$_0$=0.095 mM [TiO$_2$]=0.1g/L [IO$_3^-$]=0.156 mM

t	R.T.	Area	ppm	C/C$_0$	ln(C/C$_0$)
0	5.185	1240076	11.54891	1	0
1.5	5.18	327984	3.054537	0.264487	-1.32996
3	5.154	92029	0.857072	0.0742124	-2.60082
5	5.172	23980	0.223327	0.0193375	-3.94571
7.5	5.181	6506	0.060591	0.0052465	-5.2502
10	5.179	5162	0.048074	0.0041626	-5.4816
15	5.149	4892	0.04556	0.0039449	-5.53533
20	5.149	4134	0.0385	0.0033337	-5.70368
60	5.018	1223	0.01139	0.0009862	-6.92162

[ClA]$_0$=0.095 mM [TiO$_2$]=0.1g/L [IO$_3^-$]=0.137 mM

time	R.T.	Area	ppm	C/C$_0$	ln(C/C$_0$)
0	5.02	1159790	12.10005	1	0
1.5	4.92	351038	3.662368	0.3026738	-1.1951
2.5	4.849	209809	2.188931	0.1809026	-1.7098
3.5	4.841	110340	1.151174	0.0951379	-2.35243
5	4.834	96125	1.002869	0.0828814	-2.49034
10.5	4.891	87675	0.91471	0.0755956	-2.58236
15	4.912	83631	0.87252	0.0721087	-2.62958
20	4.949	79066	0.824893	0.0681727	-2.68571

[ClA]$_0$=0.095 mM [TiO$_2$]=0.1g/L [IO$_3^-$]=0.078 mM

time	R.T.	Area	ppm	C/C$_0$	ln(C/C$_0$)
0	4.917	1191256	11.51996	0	1
1	4.998	501184	4.846666	-0.86579	0.420719
2	4.87	348931	3.374313	-1.227889	0.29291
4	4.95	280090	2.708591	-1.447653	0.235122
6	4.965	265579	2.568264	-1.500851	0.22294
8.5	4.899	243364	2.353435	-1.588205	0.204292
12	4.923	211678	2.047018	-1.727697	0.177693
15	4.943	206680	1.998685	-1.751592	0.173498
20	4.91	172117	1.664446	-1.934589	0.144484

$[ClA]_0$=0.095 mM $[TiO_2]$=0.1g/L $[IO_3^-]$=0.039 mM

time	R.T.	Area	ppm	C/C_0	$\ln(C/C_0)$
0	4.875	1097856	10.61674	1	0
1.5	4.896	491076	4.748917	0.4473046	-0.80452
3.5	4.913	388896	3.760792	0.3542322	-1.0378
6	4.936	360773	3.488831	0.328616	-1.11287
8	4.923	320802	3.102294	0.2922077	-1.23029
12	4.894	268826	2.599663	0.2448645	-1.40705
15	4.904	234791	2.27053	0.2138632	-1.54242
20	4.938	201701	1.950536	0.1837226	-1.69433
30	4.921	120597	1.166225	0.1098477	-2.20866
40	4.876	62138	0.600901	0.0565994	-2.87176
50	4.888	22595	0.218503	0.020581	-3.88339
60	4.901	1718	0.016614	0.0015649	-6.45995

$[ClA]_0$=0.095 mM $[TiO_2]$=0.1g/L $[IO_3^-]$=0.078 mM

t	R.T.	area	ppm	C/C_0	$\ln(C/C_0)$
0	5.146	1309277	12.09907	1	0
5	5.165	361483	3.340477	0.2760936	-1.28702
10	5.187	133024	1.229279	0.1016011	-2.2867
15	5.184	73944	0.683319	0.056477	-2.87392
20	5.205	52014	0.480663	0.0397273	-3.22572

$[ClA]_0$=0.095 mM $[TiO_2]$=0.1g/L $[IO_3^-]$=0.078 mM

t	R.T.	area	ppm	C/C_0	$\ln(C/C_0)$
0	5.012	1273192	12.05537	1	0
5	5.015	453713	4.296036	0.3563587	-1.03182
11	5.009	197052	1.865811	0.1547701	-1.86581
15	5.008	102873	0.974065	0.0807993	-2.51579
20	5.017	65579	0.620943	0.0515075	-2.96603

$[ClA]_0$=0.095 mM $[TiO_2]$=0.1g/L $[IO_3^-]$=0.078 mM

t	R.T.	area	ppm	C/C_0	$\ln(C/C_0)$
0	5.01	1288088	12.19642	1	0
2.5	5.099	84934	0.804208	0.065938	-2.71904
5	5.006	27013	0.255776	0.0209714	-3.8646
10	5.099	24926	0.236015	0.0193512	-3.945
15	5.009	17873	0.169233	0.0138756	-4.27762
20	5.017	18655	0.176637	0.0144827	-4.2348

$[ClA]_0$=0.095 mM $[TiO_2]$=0.1g/L $[IO_3^-]$ =0.078 mM

t	R.T.	area	ppm	C/C_0	$\ln(C/C_0)$
0	5.226	1216426	12.09784	1	0
5.5	5.226	148283	1.474734	0.1219006	-2.10455
11.5	5.216	108468	1.078758	0.0891694	-2.41722
15	5.219	93808	0.932958	0.0771177	-2.56242
20	5.22	95270	0.947498	0.0783196	-2.54696

$[ClA]_0$=0.095 mM $[TiO_2]$=0.1g/L $[IO_3^-]$ =0.195 mM

t	R.T.	area	ppm	C/C_0	$\ln(C/C_0)$
0	4.912	1216426	12.09784	1	0
5	4.934	414990	4.127241	0.3411552	-1.07542
10.5	4.837	194270	1.932093	0.1597056	-1.83442
15	4.854	89487	0.889984	0.0735655	-2.60958
20	4.901	48087	0.478244	0.0395314	-3.23066

$[ClA]_0$=0.095 mM $[TiO_2]$=0.1g/L $[IO_3^-]$ =0.195 mM

t	R.T.	area	ppm	C/C_0	$\ln(C/C_0)$
0	5.226	1260082	12.05843	1	0
5	5.226	518490	4.961722	0.4114732	-0.88801
10	5.216	233728	2.236674	0.1854863	-1.68477
15	5.219	120834	1.156328	0.0958938	-2.34451
20	5.22	58349	0.558374	0.0463057	-3.07249

$[ClA]_0$=0.095 mM $[TiO_2]$=0.1g/L $[IO_3^-]$ =0.039 mM

t	R.T.	area	ppm	C/C_0	$\ln(C/C_0)$
0	4.91	1260082	12.53202	1	0
5.5	4.881	569116	5.660086	0.45165	-0.79485
10	4.912	298022	2.963948	0.23651	-1.44176
15	4.801	125191	1.245075	0.0993515	-2.30909
20	4.923	57687	0.57372	0.0457804	-3.0839

$[ClA]_0$=0.28 mM $[TiO_2]$=0.1g/L

t	R.T.	area	ppm	C/C_0	$\ln(C/C_0)$
0	5.029	3998735	36.15852	1	0
15	5.043	803114	5.187251	0.1434586	-1.94171
20	5.043	848623	5.48119	0.1515878	-1.88659
23	5.037	735718	4.751945	0.1314198	-2.02936
26	5.036	654734	4.228876	0.1169538	-2.14598
29	5.033	488939	3.158019	0.0873382	-2.43797
32	5.01	331626	2.498938	0.0691106	-2.67205
35	5.03	344608	2.596762	0.071816	-2.63365
40	5.001	357298	2.692387	0.0744606	-2.59748

$[ClA]_0$=0.28 mM $[TiO_2]$=0.1g/L

t	R.T.	area	ppm	C/C_0	$\ln(C/C_0)$
0	5.047	3907360	36.65819	1	0
5	5.047	980247	9.196512	0.2508719	-1.38281
10	5.05	574913	5.393737	0.1471359	-1.9164
15	5.057	608115	5.705232	0.1556332	-1.86025
17.5	5.058	513205	4.814803	0.1313432	-2.02994
20	5.056	420551	3.945538	0.1076305	-2.22905
22.5	5.057	376778	3.534868	0.0964278	-2.33896
25	5.033	292805	2.747047	0.0749368	-2.59111
27.5	5.03	235852	2.212724	0.060361	-2.80741
30	5.043	235727	2.211551	0.060329	-2.80794
40	5.017	233967	2.195039	0.0598785	-2.81544

$[ClA]_0$=0.28 mM $[TiO_2]$=0.1g/L

t	R.T.	area	ppm	C/C_0	$\ln(C/C_0)$
0	5.054	4107322	37.14042	1	0
5	5.056	775078	7.008636	0.1887064	-1.66756
10	5.057	642209	5.807169	0.1563571	-1.85561
12.5	5.081	524001	4.738274	0.1275773	-2.05903
15	5.109	351892	3.18198	0.0856743	-2.4572
17.5	5.058	256239	2.317039	0.0623859	-2.77442
20	5.012	186829	1.689399	0.0454868	-3.09033
30	5.002	171391	1.549802	0.0417282	-3.17658
40	5.031	153971	1.392281	0.037487	-3.28376

$[ClA]_0$=0.28 mM $[TiO_2]$=0.1g/L

t	R.T.	area	ppm	C/C_0	$\ln(C/C_0)$
0	4.947	3911686	36.69878	1	0
2.5	4.931	1643177	11.85847	0.3231298	-1.1297
5	4.929	976060	7.044023	0.1919416	-1.65056
7.5	4.926	768122	6.005326	0.1636383	-1.8101
10	4.935	586471	4.585143	0.1249399	-2.07992
15	4.939	265045	2.072173	0.0564644	-2.87415
18	4.983	234408	0.999626	0.0272387	-3.60312
21	4.912	239708	1.022227	0.0278545	-3.58076
25	4.963	253784	1.082254	0.0294902	-3.5237
30	4.976	234327	0.99928	0.0272292	-3.60346
40	4.973	217737	0.928533	0.0253015	-3.67689

[ClA]$_0$=0.28 mM [TiO$_2$]=0.1g/L

t	R.T.	area	ppm	C/C$_0$	ln(C/C$_0$)
0	4.92	4051543	36.63604	1	0
5	4.849	799423	7.228775	0.1973132	-1.62296
8	4.841	222915	2.015707	0.0550198	-2.90006
12	4.834	30053	0.271754	0.0074177	-4.90389
16	4.921	24983	0.225909	0.0061663	-5.08866
20	4.872	34372	0.310808	0.0084837	-4.76961
30	4.932	28921	0.261518	0.0071383	-4.94229

[ClA]$_0$=0.095 mM 9 coatings at 250°C (Quartz) 8 lamps at 350nm

t	R.T.	area	ppm	C/C$_0$	ln(C/C$_0$)
0	5.056	1315092	12.14215	1	0
15	5.057	1209228	11.16472	0.9195007	-0.08392
30	5.033	1113286	10.27889	0.8465461	-0.16659
45	5.03	1025063	9.464333	0.7794611	-0.24915
60	5.043	947349	8.746805	0.7203671	-0.32799

[ClA]$_0$=0.095 mM 9 coatings at 450°C (Quartz) 8 lamps at 350nm

t	R.T.	area	ppm	C/C$_0$	ln(C/C$_0$)
0	5.051	1315574	12.10402	1	0
15	5.046	1149225	10.57352	0.8735541	-0.13519
30	5.059	998815	9.18966	0.7592237	-0.27546
45	5.059	860947	7.921197	0.6544269	-0.424
60	5.062	742740	6.833626	0.5645749	-0.57168

[ClA]$_0$=0.095 mM 9 coatings at 700°C (Quartz) 8 lamps at 350nm

t	R.T.	area	ppm	C/C$_0$	ln(C/C$_0$)
0	5.064	1320525	12.10303	1	0
15	5.052	1169125	10.7154	0.8853486	-0.12177
30	5.048	1032974	9.467532	0.7822449	-0.24559
46	5.046	907773	8.320025	0.6874334	-0.37479
60	5.052	809314	7.417618	0.6128729	-0.4896

$[ClA]_0$=0.095 mM 9 coatings at 60°C (Quartz) 8 lamps at 350nm

time	R.T.	Area	ppm	C/C_0	$\ln(C/C_0)$
0	5.012	1286044	12.10839	1	0
16	5.001	1214694	11.43661	0.9445198	-0.05708
30	5.078	1161868	10.93924	0.9034434	-0.10154
45	5.002	1108132	10.43331	0.8616595	-0.1489

$[ClA]_0$=0.095 mM 8 lamps at 350nm 15 layers coating

t	R.T.	area	ppm	C/C_0	$\ln(C/C_0)$
0	4.863	1299398	12.09564	1	0
10	4.934	1196056	11.13366	0.9204693	-0.08287
20	4.935	1101781	10.25609	0.8479165	-0.16497
30	4.937	1009041	9.392806	0.776545	-0.2529
45	4.937	882126	8.211399	0.6788728	-0.38732

$[ClA]_0$=0.095 mM 8 lamps at 350nm 12 layers coating

t	R.T.	area	ppm	C/C_0	$\ln(C/C_0)$
0	4.967	1299484	12.1173	1	0
15	4.988	1152764	10.74918	0.8870936	-0.1198
30	4.973	1014662	9.461424	0.7808192	-0.24741
45	4.917	921655	8.594161	0.7092469	-0.34355

$[ClA]_0$=0.095 mM 8 lamps at 350nm 6 layers coating

t	R.T.	area	ppm	C/C_0	$\ln(C/C_0)$
0	5.012	1311602	12.19052	1	0
15	5.078	1204604	11.19604	0.9184219	-0.0851
30	5.098	1105480	10.27474	0.8428471	-0.17097
45	5.027	1010262	9.38975	0.7702504	-0.26104

$[ClA]_0$=0.095 mM 8 lamps at 350nm 9 layers coating

t	R.T.	area	ppm	C/C_0	$\ln(C/C_0)$
0	5.038	1296494	12.08942	1	0
16	5.014	1163061	10.8452	0.8970817	-0.10861
30	5.087	1058707	9.87213	0.8165923	-0.20262
45	5.069	949135	8.850404	0.7320782	-0.31187

$[ClA]_0$=0.095 mM 8 lamps at 350nm 3 layers coating

t	R.T.	area	ppm	C/C_0	$\ln(C/C_0)$
0	5.163	1296494	12.08942	1	0
15	5.153	1211868.9	11.30032	0.9347277	-0.0675
30	5166	1132767.4	10.56272	0.8737159	-0.135
45	5.165	1058829.1	9.873269	0.8166865	-0.2025

Cycle 1 9 layers

time	R.T.	Area	ppm	C/C_0	$\ln(C/C_0)$
0	5.161	1319818	12.15795	1	0
15	5.168	1200814	11.0617	0.909833	-0.09449
30	5.129	1084612	9.991267	0.8217891	-0.19627
45	5.166	990160	9.121191	0.7502247	-0.28738

Cycle 2 9 layers

time	R.T.	Area	ppm	C/C_0	$\ln(C/C_0)$
0	5.107	1321415	12.17266	1	0
15	5.12	1175222	10.82595	0.8893663	-0.11725
30	5.122	1052330	9.693891	0.796366	-0.2277
45	5.131	942237	8.679732	0.7130515	-0.3382

Cycle 3 9 layers

time	R.T.	Area	ppm	C/C_0	$\ln(C/C_0)$
0	5.157	1304725	12.09692	1	0
15	5.166	1171152	10.85848	0.8976236	-0.108
30	5.165	1055811	9.78908	0.8092211	-0.21168
45	5.165	940697	8.721786	0.7209925	-0.32713

Cycle 4 9 layers

time	R.T.	Area	ppm	C/C_0	$\ln(C/C_0)$
0	5.154	1327371	12.11591	1	0
15	5.149	1185362	10.81969	0.8930148	-0.11315
30	5.15	1071074	9.776498	0.8069138	-0.21454
45	5.149	962943	8.789505	0.7254513	-0.32096

Cycle 5

time	R.T.	Area	ppm	C/C_0	$\ln(C/C_0)$
0	5.149	1314400	12.10804	1	0
15	5.151	1176560	10.83828	0.8951309	-0.11079
30	5.154	1058454	9.750304	0.8052754	-0.21657
45	5.152	939998	8.659107	0.7151537	-0.33526

Cycle 6

time	R.T.	Area	ppm	C/C_0	$\ln(C/C_0)$
0	5.153	1316638	12.12865	1	0
15.5	5.153	1182188	10.89012	0.8978839	-0.10771
30	5.138	1076894.6	9.920176	0.8179124	-0.201
45	5.183	975583	8.98691	0.7409652	-0.2998

Cycle 7

t, min	R.T.	area	ppm	C/C_0	$\ln(C/C_0)$
0	5.165	1314747	12.19063	1	0
15	5.17	1169258	10.84162	0.8893407	-0.11727
30	5.201	991679.06	9.19507	0.7542737	-0.282
40	5.183	980787	9.094076	0.7459892	-0.29304

Cycle 8

t, min	R.T.	area	ppm	C/C_0	$\ln(C/C_0)$
0	5.186	1290618	12.10075	1	0
15	5.17	1156757	10.84568	0.8962815	-0.1095
30	5.163	1041299	9.763154	0.806822	-0.21465
45	5.163	939341	8.807203	0.7278226	-0.3177

Cycle 9

t, min	R.T	area	ppm	C/C_0	$\ln(C/C_0)$
0	5.163	1293782	12.13042	1	0
15	5.153	1150976	10.79148	0.8896213	-0.11696
30	5166	1030641	9.663226	0.796611	-0.22739
45	5.165	915905	8.587468	0.7079284	-0.34541

Intermediates of o-ClA in UV/TiO_2

	o-ClA			Chlorophenol			p-benzoquinone		
t, min	R.T.	area	conc, M	R.T	area1	conc, M	R.T.	area1	conc, M
0	12.086	3.24E+10	0.952756	-	-	-	-	-	-
45	12.104	2.72E+10	0.704846	8.115	2.55E+08	1.77E-05	-	-	-
150	12.06	6.86E+09	0.162705	8.108	1.29E+08	8.93E-06	-	-	-
180	12.086	4.6E+09	0.112277	8.111	1.2E+08	8.34E-06	-	-	-
210	12.081	2.08E+09	0.057167	8.139	1.17E+08	8.14E-06	-	-	-
240	12.078	1.17E+09	0.034853	8.115	94800000	6.57E-06	-	-	-
360	12.071	6.88E+08	0.017478	8.131	68200000	4.73E-06	6.451	27780000	2.62E-06
420	12.082	4.69E+08	0.011079	8.137	29350000	2.04E-06	6.458	30360000	5.59E-06
480	12.044	1.47E+08	0.003752	-	-	-	6.422	12830000	2.42E-06
540	12.052	35150000	0.000972	-	-	-	0	0	0

Intermediates of o-ClA in UV/TiO_2/IO_3^-

	o-ClA			p-benzoquinone (60%)			o-chlorophenol		
t, min	RT.	area	con, M	R.T.	area	conc, M	R.T	area	conc, M
0		0	0.00089	-	-	-	-	-	-
15	12.094	5.01E+09	0.000108	-	-	-	8.132	2896000	2.79E-07
30	12.094	1.82E+09	5.17E-05	-	-	-	8.153	15000000	1.08E-06
60	12.074	1.25E+09	3.26E-05	6.452	10380000	1.84E-06	8.131	17940000	1.25E-06
90	12.084	9.19E+08	2.44E-05	6.445	30640000	5.73E-06	8.139	17640000	1.2E-06
120	12.102	7.98E+08	2.17E-05	6.465	33210000	6.02E-06	8.159	16980000	1.18E-06
150	12.088	8.11E+08	2.33E-05	6.49	29110000	5.46E-06	8.153	19210000	1.24E-06
180	12.042	7.75E+08	2.1E-05	6.458	22120000	4.64E-06	8.113	15230000	9.35E-07
210	12.079	7.03E+08	2.13E-05	6.405	24050000	4.22E-06	8.149	14480000	9.25E-07
240	12.059	7.05E+08	1.86E-05	6.473	22800000	3.73E-06	8.129	9380000	7.23E-07
300	12.071	6.38E+08	1.68E-05	6.477	13330000	2.29E-06	8.126	8628000	5.92E-07

Intermediates of o-ClA in UV/TiO_2/IO_3^- (cont'd)

Monochlorobenzoquinone			2-chloronitrobenzene (79.91%)			Benzenamin,3-iodo- (67.52%)			Bis-(3-chlorophenyl)-diazene		
R.T	area	conc, M	R.T	area	conc, M	R.T	area	conc, M	R.T	area	conc, M
-	-	-	-	-	-	-	-	-		0	0
10.955	86790000	2.21E-06	15.361	22490000	1.63E-06	-	-	-	33.566	97980000	1.19E-06
10.962	87340000	2.11E-06	15.377	36890000	2.46E-06	17.63	4128000	6.25E-08	33.573	92490000	1.22E-06
10.984	22020000	5.98E-07	15.352	31260000	2.03E-06	17.589	10020000	1.64E-07	33.548	1.37E+08	1.88E-06
10.993	18100000	4.51E-07	15.37	24440000	1.62E-06	17.595	15820000	2.54E-07	33.558	73360000	1.04E-06
11.017	17100000	4.23E-07	15.389	24730000	1.52E-06	17.611	25200000	4.09E-07	33.568	98090000	1.27E-06
-	-	-	15.354	18150000	1.16E-06	17.583	2.34E+08	3.53E-06	-	-	-
-	-	-	15.311	13690000	8.78E-07	17.541	3.63E+08	5.5E-06	-	-	-
-	-	-	15.347	14500000	9.29E-07	17.577	4.53E+08	7.42E-06	-	-	-
-	-	-	15.337	14070000	9.02E-07	17.561	5.2E+08	8.45E-06	-	-	-
-	-	-	15.348	7302000	4.68E-07	17.583	5.46E+08	8.94E-06	-	-	-